University of Ljubljana
Faculty of Mathematics and Physics
Department of Physics

Boštjan Markun

Casimir effect in smectic liquid crystals

Doctoral thesis

Adviser: prof. dr. Slobodan Žumer

Ljubljana, 2007

Univerza v Ljubljani
Fakulteta za matematiko in fiziko
Oddelek za fiziko

Boštjan Markun

Casimirjev pojav v smektičnih tekočih kristalih

Doktorska disertacija

Mentor: prof. dr. Slobodan Žumer

Ljubljana, 2007

Zahvaljujem se prof. Slobodanu Žumru za mentorsko vodstvo od samega začetka moje raziskovalne poti, katere rezultat je pričujoče delo. Sodelavcem Andreji, Brini, Danielu, Gregorju, Mateju in Mihu hvala za zelo prijetno delovno vzdušje in pomoč pri reševanju takšnih in drugačnih težav. Še posebej sem hvaležen Primožu za vse pordečele verzije mojih besedil ter za vse pametne in "pametne" nasvete.

Disertacijo posvečam vsem svojim bližnjim, ki so mi vsa ta leta stali ob strani.

Abstract

The thesis deals with various aspects of the Casimir effect in smectic liquid crystals. The Casimir interaction in planar smectic-A systems is studied, considering both types of smectic ordering – positional and orientational – including the coupling between them. This provides a complete picture of the phenomenon in smectic-A systems with homogeneous equilibrium order. The behavior of the Casimir interaction in vicinity of the smectic-A to smectic-C phase transition is considered. The presence of this transition results in some special features of the interaction. A special attention is devoted to confined systems with non-trivial equilibrium order. The Casimir interaction in a homeotropic smectic cell with surface enhanced positional order is studied; an exponential decay of the Casimir force is predicted, contrary to the long-range interaction in homogeneous smectic systems. In a homeotropic nematic cell with surface induced presmectic order a faster decay of the Casimir force than in normal nematics is discovered. In addition, a few systems where inhomogeneity of equilibrium ordering does not affect the Casimir interaction are presented.

Keywords: Casimir effect, smectic liquid crystals, fluctuations, confinement, phase transition

PACS: 61.30.Dk, 61.30.Hn, 64.70.Md, 68.60.Dv

Povzetek

Delo je posvečeno različnim vidikom Casimirjevega pojava v smektičnih tekočih kristalih. Obravnavamo Casimirjevo interakcijo v planarnih smektičnih A sistemih. Pri tem zajamemo oba vidika smektične ureditve - pozicijskega in orientacijskega - ter sklopitev med njima. S tem podamo popoln opis Casimirjevega pojava v smektičnih A sistemih s homogeno ravnovesno ureditvijo. Nadalje raziščemo obnašanje Casimirjeve sile v bližini prehoda iz smektične A v smektično C fazo. Bližina tega faznega prehoda se odraža v nekaterih posebnih lastnostih sile. Posebno pozornost v disertaciji posvetimo ograjenim sistemom z netrivialno ravnovesno ureditvijo. Obravnavamo homeotropno smektično celico s povečanim površinskim pozicijskim redom. Ugotovimo, da je Casimirjeva sila v takem sistemu kratkega dosega, v nasprotju s homogenimi smektičnimi sistemi, kjer je sila dolgega dosega. Izračunali smo Casimirjevo silo v nematski homeotropni celici s površinsko vsiljenim predsmektičnim redom. V tem primeru sila upada precej hitreje kot v običajnem nematiku. Predstavili smo tudi nekaj sistemov, kjer nehomogena ravnovesna struktura ne vpliva na Casimirjevo interakcijo.

Ključne besede: Casimirjev pojav, smektični tekoči kristali, fluktuacije, ograditev, fazni prehod

PACS: 61.30.Dk, 61.30.Hn, 64.70.Md, 68.60.Dv

Contents

1

Introduction

The history of the Casimir effect dates back into 1948 when the Dutch physicist H. B. G. Casimir predicted that even two uncharged parallel conducting plates should experience mutual attraction [1]. This attraction, seemingly stemming "from nowhere", originates from a modified spectrum of zero-point fluctuations (and hence a modified energy density) of electromagnetic field in confined volume as compared to free space. The pioneering work of Casimir has inspired a large number of theoretical and also experimental studies of the Casimir force [2]. The interest in the subject is on the one hand purely fundamental as the Casimir interaction represents one of a few macroscopic manifestations of quantum phenomena and zero-point fluctuations. On the other hand, with recent prosperity of nanotechnology a lengthscale has been reached where the Casimir force can by no means be considered a marginal effect.

The rationale behind the Casimir interaction can be most easily demonstrated with the following calculation [3]. Let us consider two perfectly conducting plates parallel to x-y plane and separated by a distance h (Fig. 1.1). Even if the plates are uncharged and at zero temperature ($T = 0$ K) the electromagnetic (EM) field exists in terms of zero-point fluctuations with energy $E = 1/2 \sum_n \hbar\omega_n$, where $\hbar$ is the reduced Planck constant and ω_n are frequencies of fluctuation modes. In confined space the modes of EM field adjust to the boundary conditions dictated by the conducting plates and can be written as:

$$\boldsymbol{E}(\boldsymbol{q}, n) = \boldsymbol{E}_0 \exp(i\boldsymbol{q}\boldsymbol{\rho}) \sin\left(\frac{n\pi z}{h}\right) , \tag{1.1}$$

where $\boldsymbol{q} = (q_x, q_y)$ is a wave-vector in x-y plane and n the number of standing wave modes in z direction (there are actually two different types of EM modes present in such a wave-guide, but for the sake of simplicity we omit this detail). The corresponding frequency is

$$\omega(\boldsymbol{q}, n) = c\sqrt{q_x^2 + q_y^2 + \frac{n^2\pi^2}{h^2}} , \tag{1.2}$$

where c is the speed of light. Now in the confined space the wave-number n is limited to integer values ($n = 0, 1, 2, \ldots$) whereas in an open space the wave-spectrum is

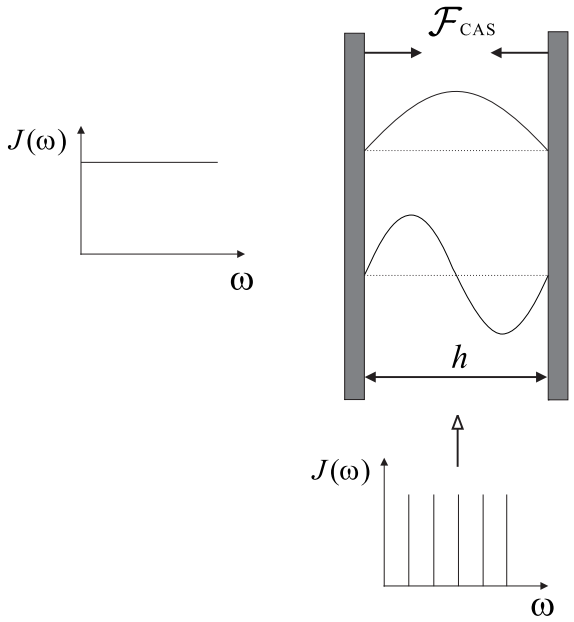

Figure 1.1 Casimir force between uncharged parallel conducting plates. The difference between the discrete spectrum of electromagnetic modes in the confined volume and continuous spectrum in the open space leads to an attractive interaction between the plates.

continuous and n can be any real number. The interaction energy can thus be defined as the difference between the energy of fluctuations in confined space and the energy of fluctuations in free space

$$\begin{aligned} E(h) &= \frac{\hbar}{2}\sum_{\boldsymbol{q},n}\left[\omega(\boldsymbol{q},n) - \lim_{h\to\infty}\omega(\boldsymbol{q},n)\right] \\ &= \frac{\hbar}{2}\sum_{\boldsymbol{q}}\left[\sum_{n}\omega(\boldsymbol{q},n) - \int_0^\infty \omega(\boldsymbol{q},n)\,\mathrm{d}n\right] . \end{aligned} \tag{1.3}$$

Both terms in Eq. (1.3) are divergent but their difference is finite and can be calculated by various mathematical methods. We shall here just quote the result

$$E(h) = -\frac{\hbar c\pi^2 S}{720h^3} , \tag{1.4}$$

where S is the area of the plates. This leads to an attractive force between the plates given by

$$\mathcal{F}(T=0) = -\frac{\partial E(h)}{\partial h} = -\frac{\hbar c\pi^2 S}{240h^4} . \tag{1.5}$$

At a finite temperature ($T > 0$) the force should be calculated using the free energy F instead of the energy E as a proper thermodynamic potential. For high temperatures or large thicknesses ($k_B T h \gg \hbar c$), where the thermal fluctuations of the field

overwhelm the quantum fluctuations, the Casimir force reads

$$\mathcal{F} = -\frac{\partial F(h)}{\partial h} = -\frac{k_B T S}{4\pi h^3}\zeta_R(3) \ , \tag{1.6}$$

where k_B is Boltzmann constant and ζ_R is the Riemann zeta function with the value $\zeta_R(3) = 1.202\ldots$. It is worth mentioning that the electromagnetic Casimir force is a special case of the van der Waals force between two dielectric slabs interacting across another dielectric medium, first calculated by Lifshitz in 1955 [4].

As it can be inferred from the above derivation, the Casimir interaction is not specific only to the EM field. It is present in every confined system where the fluctuation spectrum of any physical field is modified due to some boundary conditions. In other words, it is omnipresent but not easily observed due to its usually small magnitude. We shall here give a brief overview of the various fields of physics where the Casimir force has been studied [2].

First of all, the original Casimir calculation, Eq. (1.5), has been refined and extended in various ways. As already mentioned, the contribution due to thermal fluctuations of electromagnetic field should be considered at finite temperatures, leading to the expression (1.6) in the limit of high temperatures [5–12]. Furthermore the corrections concerning finite conductivity and roughness of the plates have been evaluated [13–22]. The generalization to magnetically permeable plates has been performed, which can even change the sign of the force [23–27]. The Casimir interaction has been calculated for rectangular cavities and for spherical, cylindrical, toroidal and wedge geometries [28–34]. There seems to be no a-priori way to predict what the stress on specific geometrical object will be. For example, the Casimir force on the conducting spherical shell tends to expand it, contrary to the attraction obtained between two plates. Moreover, the interaction between the walls of a rectangular cavity can be either attractive or repulsive depending on the relationship between the lengths of the sides. The dynamical Casimir effect, describing the force and radiation from moving plates, has also received much attention [35–39]. In quantum field theory the Casimir effect has found application in the bag model of hadrons in quantum chromodynamics (QCD) [40–42] and in Kaluza-Klein field theories [40, 42–46]. Casimir-type effects naturally arise in cavity quantum electrodynamics (QED) [25] and even in electrical engineering of microchips [47–49]. In gravitational theory, cosmology and astrophysics the Casimir effect arises in spacetimes with nontrivial topology and is related to problems of particle creation by black holes, gravitational collapse and inflation process [42, 50–55]. As a mechanical analog, the acoustic Casimir force has to be mentioned. Larraza et al. managed to measure the force between two closely spaced plates due to the modification of the spectrum of acoustic noise [56–58]. The Casimir idea found application even in maritime physics, where an attractive force between two ships in a rough sea has been attributed to the modification of the wave spectrum in the region between the

ships [59]. A fluctuation-induced interaction is also present between inclusions in biological membranes. Here the thermal fluctuations of a membrane are hindered by the presence of the inclusions which leads to the interaction [60–62]. Many studies have been devoted to the thermal Casimir interaction in correlated fluids [63] – such as critical liquids and binary mixtures of liquids [64–69], super-fluids [70–73], liquid crystals and electrolytes [74–76]. The various studies of the Casimir effect in liquid crystals, the main topic of this thesis, are presented in detail later.

Here we should mention a universal property of the Casimir force in planar geometry which does not depend on details of the studied system: fluctuations with long-range correlations induce long-range interaction while short-correlated fluctuations result in a short-range force decaying with some characteristic length. Typical examples of long-range correlations include critical systems close to the phase transition and systems with a massless Goldstone fluctuation modes due to the broken continuous symmetry of ordering. On the other hand, the sign of the Casimir force depends on the geometry and topology of the system as well as on the specific boundary conditions.

The experimental studies of the Casimir force are vastly outnumbered by the theoretical work. The main reason lies in difficulty of experiments as the Casimir force is usually weak and often screened by other effects. The first documented successful attempts of measuring the electromagnetic Casimir force belong to Sparnaay in 1958 [77]. However, due to the poor accuracy of the measurements only qualitative agreement with theoretical predictions was confirmed. A firm experimental measurement of the Casimir force was reported in 1997 by Lamoreaux [78, 79], almost half a century after the theoretical prediction. Lamoreaux used an electromechanical system based on a torsion pendulum and measured the force between a gold-coated plate and sphere. The agreement with the theory was claimed to be within 5%. Subsequent experiments which relied on the atomic force microscopy (AFM) techniques [80–84] also produced results that were in excellent quantitative agreement with the theory. In recent years a number of new experiments ensued. The force between two crossed cylinders [85], plan-parallel plates [86] and in standard sphere-plane AFM setup was measured [87–91]. In dynamical experiments the influence of the Casimir force on the behavior of micromechanical oscillators was observed [92–95]. The precision of experiments has been greatly improved over the last years and now allows for delicate tests of the theoretical predictions. Furthermore, the Casimir force measurements provide one of the most sensitive tests of the hypothetical new forces predicted by modern theories of fundamental interactions including corrections to Newtonian gravitational law at small distances [95–101].

Although the Casimir force is weak at macroscopic distances, it is important for modern technologies which involve ever smaller length scales where the Casimir force becomes dominant. It is presently unclear whether the Casimir force will present an obstacle or a useful feature in micro- and nano-engineering. For example, the

first microelectromechanical device which shows actuation by the Casimir force was designed by researchers at Bell Labs in 2001 [92]. On the other hand, the Casimir force restricts the yield and performance of nanoscale devices as the movable parts often stick together due to the strong attraction [102–104].

Apart from measurements of the electromagnetic Casimir force, the experiments on other systems have also been performed. The influence of the Casimir force has been observed in the wetting behavior of liquid helium on a metallic surface [70, 71]. The thickness of the helium film formed on the metal depends on the strength of the interaction between the surfaces of the film. When the system is cooled down to the fluid/super-fluid phase transition the fluctuations become critical and the magnitude of the Casimir force strongly increases which is reflected in thinning of the wetting film. Similar experiments were performed with binary liquid mixtures [67, 105–107] where a sharp increase of the wetting film thickness was observed near the critical (demixing) point due to the enhanced Casimir interaction. Casimir interaction is also expected to have an important role in physics of colloids where a long-range attraction would eventually lead to the flocculation of dispersed particles [69]. Such a flocculation of colloidal particles has actually been observed in binary liquid mixtures but the precise interpretation of experimental results is still unclear [108–110].

1.1 Casimir force in liquid crystals

Having briefly described the Casimir interaction in various fields of physics, ranging from biophysics to cosmology, we proceed with a thorough overview of the studies of the Casimir force in liquid-crystal systems. Liquid-crystalline phases are intermediate states of matter between a liquid and a crystal phase [111]. They are formed by anisotropic molecules, usually elongated or disc-shaped. There exist a variety of distinct liquid-crystalline phases which are characterized by orientational and in some cases also by partial orientational order of constituent molecules. It has been established long ago in light-scattering experiments [112] that thermal fluctuations of ordering have an important role in liquid-crystal systems. These fluctuations are the source of the Casimir interaction when the system is confined by external boundaries. The richness of different phases, phase transitions, order parameters and couplings between them makes the liquid-crystalline systems especially attractive for studying the phenomenology of the Casimir interaction.

1.1.1 Nematic liquid crystals

Nematic phase is the simplest liquid-crystalline phase (Fig. 1.2). Molecules in a nematic phase are liquid-like in a sense that there is no long-range positional order and the translational motion of the molecules is random. However, there exists a long-range orientational order. Molecules tend to orient with their long axes parallel

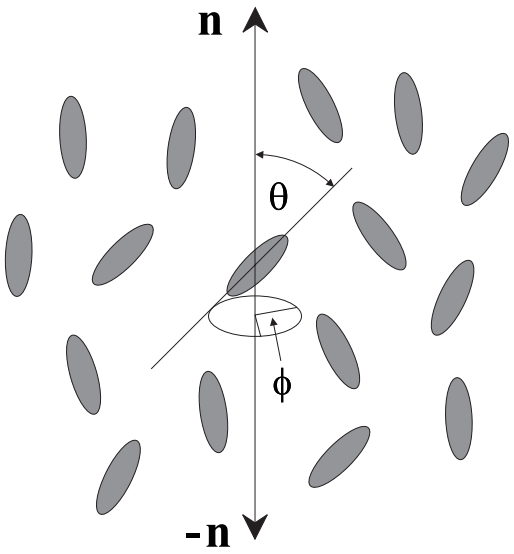

Figure 1.2 Nematic liquid crystal phase. The average orientation of molecules is described by a headless unit vector **n** called the director. The directions **n** and $-\mathbf{n}$ are physically equivalent. The angle θ gives the tilt of a molecule with respect to the director. The polar angle ϕ is used to describe biaxial ordering.

to each other. This orientational order is described by director **n**, which is a unit vector giving the average local direction of orientation of molecules. The degree of orientational order is measured by the order parameter $S = \langle 3/2 \cos^2\theta - 1/2 \rangle$, where θ is the angle between the director **n** and long axes of the molecule, while the brackets denote the thermodynamic average. Nematic ordering is usually uniaxial, except in some special systems. The biaxial ordering is described by the biaxial director $\mathbf{n}_b$, perpendicular to **n**, and the degree of biaxiality $P = \langle \sin^2(\theta)\cos(2\phi) \rangle$, where ϕ is the polar angle of molecular orientation. In equilibrium, with no external forces acting on the system, the director tends to be uniform over the whole sample. The energy cost of a director-field deformation is given by the Frank elastic free-energy [113]

$$F = \frac{1}{2}\int \left[K_1(\nabla\cdot\mathbf{n})^2 + K_2(\mathbf{n}\cdot\nabla\times\mathbf{n})^2 + K_3(\mathbf{n}\times\nabla\times\mathbf{n})^2\right] \mathrm{d}V \ . \qquad (1.7)$$

Here K_1, K_2 and K_3 are splay, twist and bend elastic constants. A more complete description of nematic systems is given by the tensor order parameter Q which incorporates all aspects of nematic ordering – director (**n**), degree of ordering (S), and biaxiality ($\mathbf{n}_b, P$). The Q tensor is a traceless symmetric tensor based on some macroscopic quantity which is zero in the isotropic phase and non-zero in the nematic phase. The magnetic susceptibility tensor χ is usually used for this purpose and the order parameter tensor is defined as $\mathsf{Q} = C(\chi - \frac{1}{3}\mathsf{I}\,\mathrm{Tr}\chi)$, where C is a normalization constant and I a unit tensor. The free energy density of a nematic system close to

the nematic-isotropic phase transition is then described by a Landau-type expansion

$$f = \frac{1}{2}A(T - T^\star)\,\mathrm{Tr}\mathbb{Q}^2 - \frac{1}{3}B\,\mathrm{Tr}\mathbb{Q}^3 + \frac{1}{4}C(\mathrm{Tr}\mathbb{Q}^2)^2 + \frac{1}{2}L\nabla\mathbb{Q}\vdots\nabla\mathbb{Q}\ , \tag{1.8}$$

where A, B, C and L are material constants and $T^\star$ is supercooling limit of isotropic phase.

The first study of the Casimir force in a nematic system was performed by Ajdari et al. in 1991 [114, 115]. They calculated the force in a nematic homeotropic cell (Fig. 1.3), consisting of two infinite parallel plates separated by the distance h which enforce homeotropic orientation of the director $[\mathbf{n}(z = 0) = \mathbf{n}(z = h) = (0, 0, 1)]$. These imposed boundary conditions hinder the thermal fluctuations of the nematic

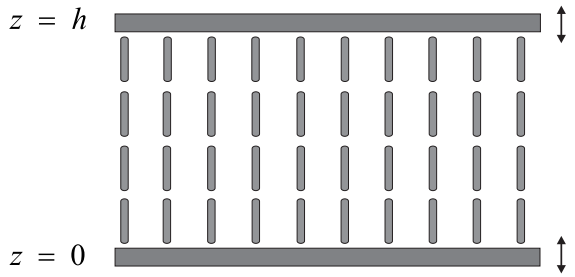

Figure 1.3 Homeotropic nematic cell with the director structure $\mathbf{n} = \mathbf{n}_z$. The arrows indicate the enforced orientation of the director at the plates.

director in the cell, thus modifying the spectrum of fluctuations which leads to the Casimir interaction. The Casimir force in this configuration is equal to

$$\mathcal{F}_{Cas} = -\frac{k_B T S}{8\pi h^3}\zeta_R(3)\left(\frac{K_3}{K_1} + \frac{K_3}{K_2}\right)\ . \tag{1.9}$$

We note here that this force is equal to the thermal EM Casimir force between two metallic plates [Eq. (1.6)], apart from factor including the ratio of elastic constants. This demonstrates the universality of the Casimir interaction which does not depend on specific details of the studied system but on the type of fluctuation modes and on imposed boundary conditions. We also note that director fluctuations in nematic liquid crystals are an example of massless Goldstone fluctuation modes, which try to recover broken continuous symmetry of a high temperature – in this case isotropic – phase. The work of Ajdari was extended by Ziherl et al. [116] who evaluated the contributions of fluctuations of biaxiality and degree of nematic order to the Casimir force. These contributions are equal to

$$\mathcal{F}_{Cas} = -\frac{kTS}{4\pi}\frac{1}{h^3}\sum_{k=1}^{\infty}\frac{\exp\left(-2hk/\eta_i\right)}{k^3}\left(\frac{1}{2} + \frac{h}{\eta_i}k + \frac{h^2}{\eta_i^2}k^2\right)\ , \tag{1.10}$$

where η_i are the corresponding correlation lengths of fluctuations. In the limit of large thicknesses ($h/\eta_i \gg 1$) this force decays as $\exp(-2h/\eta_i)/h$. This is a

demonstration of another universal feature of the Casimir force – massive short-range correlated fluctuations result in a short-range Casimir force, decaying exponentially with some characteristic length equal to the correlation length of fluctuation modes in question. It was established that these short-range contributions are important only close to the nematic-isotropic phase transition where the correlation lengths of the massive modes are strongly increased. Otherwise the long-range contribution of the director fluctuations [Eq. (1.9)] dominates the Casimir force in nematics. These basic results [Eqs. (1.9,1.10)] were also generalized for finite anchoring strengths, where the ordering at the plates is not fixed but can deviate from a preferred value [116, 117]. It was established that finite surface coupling reduces the magnitude of the Casimir force and can even modify its thickness dependence and sign. It is interesting to note that in the case of no surface coupling between the plates and liquid crystal the Casimir force is exactly the same as in the case of infinitely strong anchoring. These two limiting cases correspond to the so-called Neumann and Dirichlet boundary conditions, respectively. The structure of the eigen-modes in the two cases is different, but the energy spectra are identical which leads to identical Casimir forces. Even more interesting is the case of mixed (Dirichlet-Neumann) boundary conditions where the force changes the sign and becomes repulsive [114, 117].

Further studies addressed different aspects of the Casimir force in nematic liquid crystals. Li and Kardar evaluated corrections to the Casimir force due to the roughness of the plates [118, 119]. Ziherl et al. studied the force in a pre-nematic wetting system with inhomogeneous equilibrium order [120]. They found that the Casimir force in such a system is repulsive and short-range. Much attention has been paid to the so-called frustrated systems such as the hybrid and Fréedericksz cell [121]. The hybrid cell is similar to the homeotropic cell (Fig. 1.3) except that now one

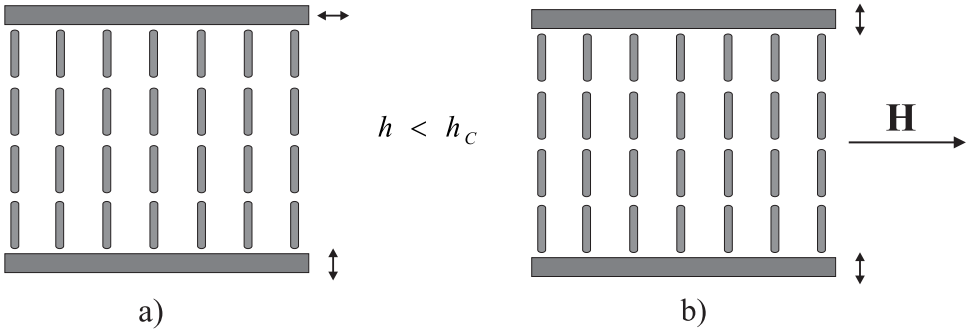

Figure 1.4 Frustrated systems: a) hybrid cell; b) Fréedericksz cell – the magnetic field tends to rotate the director parallel to the plates. The arrows indicate the preferred orientation of director at the plates. In thin enough cells the equilibrium director structure is uniform. When increasing the thickness, the structural transition to a deformed director structure takes place at $h = h_c$.

of the plates imposes a planar orientation of the director (Fig. 1.4a). In thick cells this mismatch between the plate-induced order results in a deformed equilibrium director field. However, in thin cells it is energetically more favorable to maintain homogeneous director configuration thus violating one (the weaker) of the boundary conditions. Such a system is said to be frustrated as it can not adjust to all imposed external conditions. Due to this frustration the order is destabilized and the fluctuations of the director are enhanced which leads to additional contributions to the Casimir force. When the anchoring strengths at the plates of a hybrid cell are very different, the Casimir force exhibits typical crossovers from attraction to repulsion when varying the thickness of the cell. When the critical thickness of the structural transition to the inhomogeneous director profile is approached, the Casimir force diverges logarithmically. The geometry of a hybrid cell is often characteristic for thin nematic films on a solid substrate [122]. In a Fréedericksz cell the frustration is caused by an external magnetic field which tends to orient the director parallel to the plates while the plates induce a homeotropic director orientation (Fig. 1.4b). In thin cells or in weak magnetic fields the director structure is homogeneous and dictated by the boundary conditions. The destabilizing effect of magnetic field enhances the director fluctuations which again results in additional terms to the ordinary director Casimir force. At large enough fields or cell thicknesses the classical Fréedericksz transition to the deformed director structure takes place. The Casimir force again exhibits logarithmic divergence at this transition. Similar studies of frustrated systems were performed for chiral nematics where the frustration arises from inability of a system to synchronize the intrinsic chiral helix with the confining boundaries [123]. Bartolo et al. considered the Casimir force between small spherical impurities in nematic solvent and obtained $1/h^7$ dependence of the force [124]. The Casimir force in confined nematic polymers was discussed in Ref. [125]. It was predicted that at large distances the Casimir force should exhibit a faster algebraical decay ($1/h^5$) than in ordinary nematics ($1/h^3$). In a recent work Karimi et al. studied the Casimir force in a nematic cell with patterned plates, covered by stripes of different anchoring conditions [126]. Finally, the existence of a long-range Casimir torque between plates with anisotropic anchoring energies was predicted [127].

1.1.2 Smectic liquid crystals

Smectic liquid crystals possess, in addition to orientational order, a one-dimensional positional order. Molecules are arranged in parallel layers. The diffusion of molecules within the layers is liquid-like, but the diffusion between the layers is hindered. This leads to modulation of density in direction perpendicular to the layers (denoted as z-direction here)

$$\rho(z) = \rho_0 \left[1 + \mathrm{Re}\left(\Psi \exp\left(i \frac{2\pi z}{d_0} \right) \right) \right] , \tag{1.11}$$

where d_0 is the thickness of smectic layers and $\Psi = \psi \exp(i\phi)$ is the complex order parameter whose modulus ψ describes the amplitude of density wave and the phase ϕ is related to the position of the layers. However, it should be stressed that positional order in smectics is not very pronounced, as the variations of the density are small, and there are no sharp boundaries between the layers. This positional order is said to be quasi-long-range, because according to the Landau-Peierls theorem no true long-range order can exist in one dimension as the thermal fluctuations destabilize it. However, the break-down of positional order in smectics would occur at macroscopic scales which is irrelevant for all current experimental setups. There exist various smectic phases. In this thesis, we focus on the smectic-A phase, where the molecules are oriented perpendicular to the layers, and the smectic-C phase, where the molecules are tilted with respect to the layer normal (Fig. 1.5).

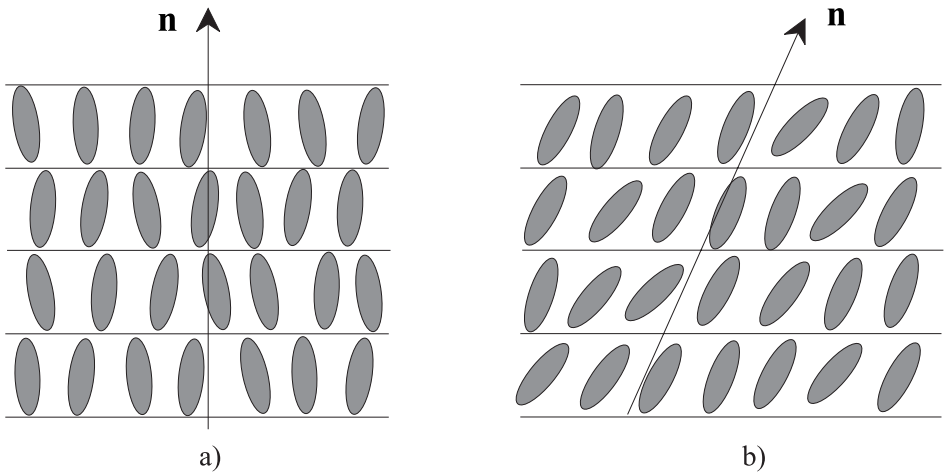

Figure 1.5 Smectic liquid crystals. Molecules are arranged in layers (the figure is schematic): a) smectic-A phase; b) smectic-C phase. In the smectic-A phase the molecules are on average oriented along the layer normal, while in the smectic-C phase the molecules are tilted with respect to the layer normal.

In the simplest model the deformations of smectic structure are described by layer displacement $u(\mathbf{r})$ whereas the degree of smectic order is assumed to be constant and the director is assumed to rigidly follow the layers. The elastic free-energy is then given by

$$F = \frac{1}{2} \int \left[B(\nabla_{\parallel} u)^2 + K(\nabla_{\perp}^2 u)^2 \right] \mathrm{d}V \,, \tag{1.12}$$

where the first term describes the compression or dilation of layers and the second term gives the energy of layer bending (Fig. 1.6). The indices $\parallel$,$\perp$ denote the direction parallel and perpendicular to the layer normal, respectively. A more complete model which incorporates all aspects of smectic ordering will be presented in the following section.

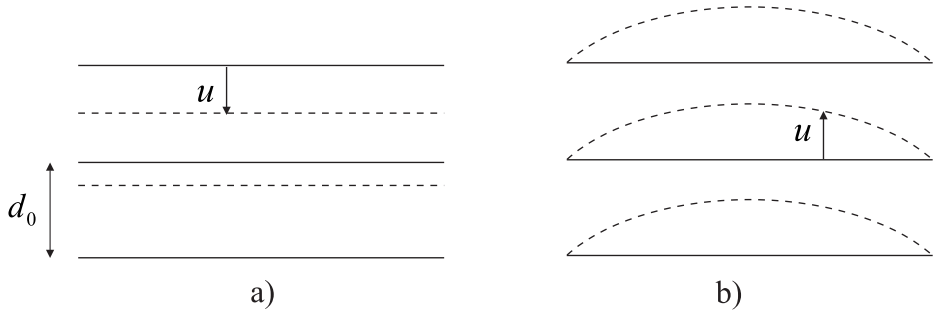

Figure 1.6 a) Compression of smectic layers; b) Bending of smectic layers.

The first study of the Casimir force in smectic systems was published by Mikheev in 1989 [128]. He considered the force in a homeotropic smectic cell induced by fluctuations of smectic layers, taking as a starting point the Eq. (1.12). In this geometry the layers are oriented parallel to the plates and the boundary condition require that the layers at the plates are fixed and do not fluctuate. This hindering of the fluctuations leads to the Casimir force between the plates given by

$$\mathcal{F}_{Cas} = -\frac{k_B T S}{16\pi h^2}\zeta_R(2)\sqrt{\frac{B}{K}}\,. \tag{1.13}$$

We see that the Casimir force in smectics decays with even smaller power (h^{-2}) compared to the nematic decay (h^{-3}). This is a result of a different energy dispersion of fluctuations in smectics. Additional length dimension in smectic Casimir force is provided by the characteristic length $\lambda = \sqrt{K/B}$ which is usually about of a size of a layer thickness. Mikheev actually considered even a more general case of smectic films. The geometry of these systems is the same as that of a homeotropic cell, however, the fluctuations of the surfaces are rather than forbidden only suppressed by the surface tension. In this case, the Casimir force still retains h^{-2} dependence and is given by

$$\mathcal{F}_{Cas} = -\frac{k_B T S}{16\pi h^2}\sqrt{\frac{B}{K}}\,\mathrm{Li}_2\left[\frac{(\gamma_1-\sqrt{KB})(\gamma_2-\sqrt{KB})}{(\gamma_1+\sqrt{KB})(\gamma_2+\sqrt{KB})}\right]\,, \tag{1.14}$$

where Li_2 is a dilogarithm function defined by $\mathrm{Li}_2(x) = \sum_{n=1}^{\infty} x^n n^{-2}$, while γ_1 and γ_2 are surface tensions at the upper and lower surface of the film, respectively. In free-standing smectic films $\gamma_1 = \gamma_2$, but generally the surface tensions can be different. Finite surface tensions reduce the magnitude of the Casimir force compared to the case of hard boundaries. In case of dissimilar boundary conditions (weak/strong anchoring) the force changes sign and is repulsive. The results of Mikheev were later reproduced and extended by Ajdari et al. for bookshelf geometry, where smectic layers are oriented perpendicular to the confining plates, and for columnar liquid crystals [114, 115]. A somewhat different system was addressed in Ref. [129] where

the Casimir force due to the fluctuations of Ψ in a presmectic liquid was studied. Contrary to the long-range smectic Casimir force, the presmectic interaction is short-range, exhibiting typical behavior characteristic for "massive" fluctuation modes [Eq. (1.10)].

Oliveira and Lyra studied the Casimir force in smectic films within discrete model of smectic elasticity [130]. The obtained results were very similar to that of continuous model used in Refs. [114, 115, 128]. They found that in the case of a very special value of surface tension $\gamma = \gamma_c = \sqrt{KB}$ the force decays as h^{-4}, which is much faster as the usual h^{-2} behavior. This work was extended by the inclusion of external magnetic field [131, 132]. The ordering effect of magnetic field results in a faster (h^{-3}) decay of the Casimir force at large thicknesses. In the case of asymmetric boundary conditions the impact of the magnetic field changes the sign of the force from the usual repulsion at small thicknesses to the attraction at large thicknesses of the film. The crossover thickness (from repulsion to attraction) decreases with inverse square of the magnetic field ($h_c \propto 1/H^2$). Furthermore the Casimir force in a free-standing film near the Sm-A – nematic phase transition was studied [133]. Strong increase of the force close to the transition was predicted as a result of a strong nonuniformity of equilibrium smectic and nematic order profiles. This increase would make the Casimir force the dominant long-range interaction in such a system. The discrete formalism was also applied to hexatic smectics, where the Casimir force due to the fluctuations of the bond ordering was examined [134].

1.1.3 Search for experimental evidence

There has been no unambiguous confirmation of the Casimir force in liquid-crystalline systems so far. The reason probably lies in the fact that there are many other forces present in confined liquid crystals, such as mean-field force originating from non-uniform equilibrium ordering and dielectric van der Waals force, which often dominate and thus mask the Casimir force. The potential experiments for detecting the Casimir force can be generally divided into two types. Firstly, the forces in liquid crystal systems can be measured directly using the surface force apparatus (SFA) or atomic force microscope (AFM) [135, 136]. Secondly, the impact of the Casimir force could be observed indirectly in different phenomena concerning liquid crystal films.

The possibilities of detecting the Casimir force in nematic liquid crystals were thoroughly discussed in Ref. [137]. It was found that the sensitivity of the AFM and SFA suffices for detection of the Casimir force only in very thin samples, up to about 40 nm thickness. Furthermore, the behavior of the Casimir force in nematics strongly depends on specific boundary conditions, which should be therefore well-controlled in order to allow for the identification of the Casimir interaction. Moreover, in plane-sphere or cylinder-cylinder geometry employed in AFM and SFA experimental

setups the deformation of the equilibrium director field is difficult to avoid. This leads to the mean-field elastic force which is usually much stronger than the Casimir force. Although the magnitude of the Casimir force could be somewhat enhanced by using a suitable material with large ratio of elastic constants (K_3/K_1 or K_3/K_2), it seems that the direct measurement of the force in nematic systems is a formidable task. As for indirect observations, it was argued that the Casimir force should drive the spinodal-dewetting of thin nematic films on a silicon substrate [122, 138, 139]. However, the explanation of this phenomena is not completely clear yet [140]. The Casimir force also naturally arises in colloidal systems but with particles of micron-size the leading interaction in this systems comes from elastic deformation of director field. If the size of the particles were reduced to a few tens of nanometers then the elastic deformation would vanish and the Casimir force would dominate [117].

Due to the longer range of the Casimir force in smectics, the AFM and SFA setups are precise enough to detect the Casimir force in samples of up to about 1 μm thickness, which is much more than in nematics. Furthermore, the smectic layers are much "stiffer" than the nematic director. Therefore, a smectic system adjusts to the curved surfaces of AFM and SFA setups by formation of an array of edge dislocation loops, whereas the smectic layers do not bend considerably [141]. This facilitates the interpretation of the results as there is no additional mean-field force due to the elastic deformations of layers present. The force measurements in smectics have indeed been performed [136, 141–146] and the force profile was found to be comprised of quasiperiodic parabolas due to the compression (or dilation) of layers. These parabolas are often superposed on an attractive background whose origin is not fully understood yet. However, it seems that the Casimir force is about an order of magnitude too small to be responsible for this [141].

There have been many speculations whether the Casimir force in smectics could be observed indirectly. It was proposed that the Casimir force should drive the wetting of isotropic and nematic films by the smectic phase at the free surface of the film close to the corresponding phase transitions [128]. In the case of wetting smectic film formed at the free surface of the isotropic film the Casimir force on the wetting smectic layers is expected to be attractive and the wetting should therefore be incomplete (only a finite number of smectic layers is developed before the whole film undergoes the transition to smectic phase). When the wetting smectic film is formed at the free surface of the nematic film the Casimir force on smectic layers is expected to be repulsive due to the very dissimilar boundaries. The wetting should therefore be complete, with thickness of smectic film continuously increasing and eventually diverging at the phase transition. This kind of behavior was indeed observed experimentally in some systems [147–149], however no analysis confirming the dominant role of the Casimir force has been performed. Similar interactions are expected to be present in free-standing smectic films above the bulk smectic – nematic phase transition temperature, where the layer-thinning transitions take

place [150]. The influence of the Casimir force could also be detected by measuring the contact angle between a free-standing smectic-A film and its meniscus, as this angle provides direct information about the interaction between the free surfaces of the film [151]. The interactions in free-standing films can further be probed in experiments that measure the intensity of light scattered by the capillary waves on the free surfaces of the film [152]. But as stressed above, no unambiguous confirmation of the Casimir force in liquid crystal systems, neither nematic nor smectic, has been obtained yet.

1.1.4 Aim and outline of thesis

The preceding studies of the Casimir force in smectic liquid crystals were concerned with interaction induced by fluctuations of smectic layers [114, 115, 128, 130–133]. It is the aim of this thesis to study the Casimir force considering all aspects of smectic ordering – positional and orientational. This gives, to our knowledge the first, complete picture of the Casimir phenomenon in smectic systems. Our main focus is on the force in smectic-A phase. We further address the behavior of the Casimir force close to the smectic-A to smectic-C phase transition in plain and also in chiral smectics. The presence of the phase transition is expected to result in some special features of the Casimir force, which might facilitate its experimental identification. In the end we consider the problem of the Casimir force in two systems with inhomogeneous equilibrium order. We first address a smectic system with inhomogeneous positional order which results in spatial dependence of smectic elastic constants. Second, we study the effect of a presmectic order on the director fluctuations in a nematic phase. In confined systems, some boundary-induced smectic order is always present. Therefore it is a relevant question how this order influences the long-range Casimir interaction in nematics. The systems with inhomogeneous equilibrium structure represent a special challenge in the theory of the Casimir interaction and the thesis gives a contribution to the yet limited knowledge in this field. Our studies are limited to the plan-parallel geometry. This is a geometry realized in smectic films. Furthermore, the results obtained in planar systems can be generalized (with some restrictions) to the most commonly encountered curved geometries by using Derjaugin approximation [153]. Some of the results presented in the thesis have been published in two papers in *Physical Review E* [154, 155].

The outline of the thesis is as follows. In Chapter 2 we present the theoretical models used in this thesis and describe the procedure for calculating the Casimir force. In Chapter 3 we consider the Casimir force in confined smectic-A systems. In Chapter 4 we address the force in the vicinity of smectic-A to smectic-C phase transition. In Chapter 5 we study the force in two systems with inhomogeneous equilibrium order. At the end we summarize the obtained results and outline some of the open questions in the field.

2

Theoretical model

2.1 Free energy of smectic-A phase

Positional order in smectics is described by a complex order parameter $\Psi = \psi \exp(i\phi)$. The modulus ψ gives the magnitude of positional ordering and is related to the magnitude of the density wave as described by Eq. (1.11). The argument ϕ is related to deformations of smectic layers, $\phi = q_0 u = (2\pi/d_0)u$, where u is the layer displacement and d_0 the period of smectic layers. The orientational order of molecules is described by the director $\mathbf{n}$. The free energy of a smectic system is then given by a phenomenological Landau – de Gennes type expansion [111, 156, 157]. This expansion includes three parts. The first part f_L describes the free energy density of positional ordering:

$$f_L = \frac{1}{2}a|\Psi|^2 + \frac{1}{4}b|\Psi|^4 + \frac{1}{2}C_\parallel|\nabla_\parallel\Psi|^2 + \frac{1}{2}d_1|\nabla_\perp^2\Psi|^2 + \frac{1}{2}d_2|\nabla_\parallel^2\Psi|^2 + \frac{1}{4}d_3|\nabla_\perp\nabla_\parallel\Psi|^2 \ . \quad (2.1)$$

The first two terms in f_L describe the smectic-A – nematic phase transition, and $a = \alpha(T - T_{NA})$ with T_{NA} being the temperature of the phase transition and $b > 0$. The rest gives the various contributions to elastic free energy weighted by the elastic constants $C_\parallel$, d_1, d_2 and d_3. The subscripts $\parallel$ and $\perp$ denote directions parallel and perpendicular to the layer normal, respectively. We shall seldom employ the elastic contributions in full generality as the lowest order elastic terms are usually sufficient to describe smectic systems. The second part f_N to the total smectic free energy comes from the energy cost of deformations of orientational order and is given by the usual nematic Frank elastic energy:

$$f_N = \frac{1}{2}K_1(\nabla \cdot \mathbf{n})^2 + \frac{1}{2}K_2[\mathbf{n} \cdot (\nabla \times \mathbf{n})]^2 + \frac{1}{2}K_3[\mathbf{n} \times (\nabla \times \mathbf{n})]^2 \ . \quad (2.2)$$

Here K_1, K_2 and K_3 are splay, twist and bend elastic constants, respectively. The third contribution f_{LN} describes the coupling between the orientational and the positional order. In the case of the smectic-A phase it is given by

$$f_{LN} = \frac{1}{2}C_\perp\left|(\nabla_\perp + iq_0\delta\mathbf{n}_\perp)\Psi\right|^2 \ . \quad (2.3)$$

In the case of the smectic-C phase a fourth order term should be included so that

$$f_{LN} = \frac{1}{2}C_{\perp}^{(1)}\Big|(\nabla_{\perp} + iq_0\delta\mathbf{n}_{\perp})\Psi\Big|^2 + \frac{1}{4}C_{\perp}^{(2)}\Big|(\nabla_{\perp} + iq_0\delta\mathbf{n}_{\perp})\Psi\Big|^4 , \tag{2.4}$$

with $C_{\perp}^{(1)} < 0$ and $C_{\perp}^{(2)} > 0$, but we refer to this case in a more specific system later on. The complete free energy can now be written as

$$F = \int (f_L + f_N + f_{LN})\,\mathrm{d}V \ . \tag{2.5}$$

It is useful to expand the free energy density in terms of ψ and ϕ. We obtain

$$\begin{aligned} f_L = {} & \frac{1}{2}a\psi^2 + \frac{1}{4}b\psi^4 + \frac{1}{2}C_{\parallel}\left[(\nabla_{\parallel}\psi)^2 + \psi^2(\nabla_{\parallel}\phi)^2\right] \\ & + \frac{1}{2}d_1\Big\{\left[\nabla_{\perp}^2\psi - \psi(\nabla_{\perp}\phi)^2\right]^2 + \left[2\nabla_{\perp}\phi\cdot\nabla_{\perp}\psi + \psi(\nabla_{\perp}^2\phi)\right]^2\Big\} \\ & + \frac{1}{2}d_2\Big\{\left[\nabla_{\parallel}^2\psi - \psi(\nabla_{\parallel}\phi)^2\right]^2 + \left[2\nabla_{\parallel}\phi\nabla_{\parallel}\psi + \psi\nabla_{\parallel}^2\phi\right]^2\Big\} \\ & + \frac{1}{2}d_3\Big\{\left[\nabla_{\perp}\nabla_{\parallel}\psi - \psi\nabla_{\parallel}\phi\nabla_{\perp}\phi\right]^2 + \left[\nabla_{\parallel}\psi\nabla_{\perp}\phi + \nabla_{\perp}\psi\nabla_{\parallel}\phi + \psi(\nabla_{\perp}\nabla_{\parallel}\phi)\right]^2\Big\} , \end{aligned} \tag{2.6}$$

$$f_{LN} = \frac{1}{2}C_{\perp}\left[(\nabla_{\perp}\psi)^2 + \psi^2\big(\nabla_{\perp}\phi + q_0\delta\mathbf{n}_{\perp}\big)^2\right] \ . \tag{2.7}$$

If no elastic deformations are present in the system, then the equilibrium value of bulk smectic order is given by $\psi_0 = \sqrt{-a/b}$, the phase ϕ is constant [$\phi \neq \phi(\mathbf{r})$] and the director is perpendicular to the layers ($\delta\mathbf{n} = \mathbf{0}$). Above the phase transition temperature T_{NA} in nematic phase there is no bulk smectic order and $\psi_0 = 0$.

2.2 Chiral smectics close to smectic-A* to smectic-C* phase transition

In this thesis, we also address the behavior of the Casimir force close to the smectic-A to smectic-C phase transition. We actually also consider the more complex chiral smectic phases, smectic-A* (Sm-A*) and smectic-C* (Sm-C*), as this brings no conceptual difficulties to our calculations and the results can be straightforwardly applied to the non-chiral phases.

Chiral molecules, which lack the mirror symmetry and therefore distinguish left- and right-handed types, form chiral liquid crystal phases [158–160]. The chiral Sm-A* phase exhibits the same structure as its non-chiral counterpart, but its physical properties are different. On the other hand, the chirality modifies the structure of Sm-C* phase. The molecules in Sm-C* are still tilted with respect to the layer normal as in a non-chiral Sm-C phase. However the direction of the tilt changes gradually from layer to layer such that the director forms a helical structure (Fig. 2.1).

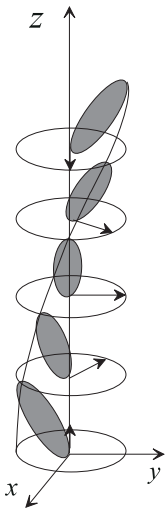

Figure 2.1 Helical structure of chiral Sm-C* phase (the period of the helix on the figure is exaggeratedly short). The direction of the molecular tilt changes gradually from layer to layer. The arrows indicate the orientation of spontaneous polarization.

The period of the helix (~ 1 μm) is incommensurate with the layer thickness and much larger compared to it. Furthermore, the Sm-C* phase can posses spontaneous polarization and is hence ferroelectric. This was discovered experimentally by Meyer et al. in 1975 [161] and later explained by Meyer on pure symmetry grounds [162]. The spontaneous polarization is oriented perpendicular both to the layer normal and to the director.

The ordering in Sm-A* and Sm-C* phases can be described by two two-component order parameters. The primary order parameter, $\boldsymbol{\xi} = (\xi_x, \xi_y)$, represents the projection of the director onto the x-y plane. The secondary order parameter is the spontaneous polarization $\mathbf{P} = (P_x, P_y)$. However, the interaction between the dipole moments of molecules is too weak to drive the Sm-A* – Sm-C* phase transition. In Sm-C* phase, the polarization $\mathbf{P}$ appears only due to the coupling with the tilt $\boldsymbol{\xi}$ and for this reason smectics belong to the class of so-called improper ferroelectrics.

The Sm-A* – Sm-C* phase transition can be conveniently described by a phenomenological Landau-type model. In this model, the free energy density reads

$$\begin{aligned} f = f_A &+ \frac{1}{2}a\left(\xi_x^2+\xi_y^2\right) + \frac{1}{4}b\left(\xi_x^2+\xi_y^2\right)^2 - \Lambda\left(\xi_x\frac{\partial\xi_y}{\partial z} - \xi_y\frac{\partial\xi_x}{\partial z}\right) \\ &+ \frac{1}{2}K_1\left(\frac{\partial\xi_x}{\partial x}+\frac{\partial\xi_y}{dy}\right)^2 + \frac{1}{2}K_2\left(\frac{\partial\xi_x}{\partial y}-\frac{\partial\xi_y}{\partial x}\right)^2 + \frac{1}{2}K_3\left[\left(\frac{\partial\xi_x}{\partial z}\right)^2+\left(\frac{\partial\xi_y}{\partial z}\right)^2\right] \\ &+ \frac{1}{2\varepsilon}\left(P_x^2+P_y^2\right) - \mu\left(P_x\frac{\partial\xi_x}{\partial z}+P_y\frac{\partial\xi_y}{\partial z}\right) + C\left(P_x\,\xi_y - P_y\,\xi_x\right)\ . \end{aligned} \tag{2.8}$$

Here f_A stands for the equilibrium free energy density of Sm-A* phase. The temper-

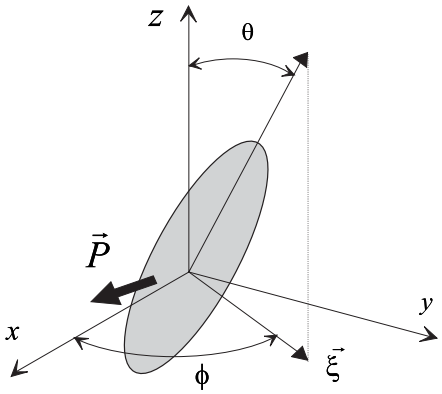

Figure 2.2 Order parameters of the Sm-A* – Sm-C* phase transition: a) tilt of molecules $\boldsymbol{\xi}$; b) spontaneous polarization $\mathbf{P}$. Molecular orientation can be also described by the azimuthal angle θ and the polar angle ϕ. Spontaneous polarization $\mathbf{P}$ is oriented perpendicular to the tilt $\boldsymbol{\xi}$ and the layer normal z.

ature dependence is hidden in coefficient $a = \alpha(T - T_0)$, where T_0 is the temperature of phase transition in an achiral system. The coefficient b must be positive to stabilize the total free-energy. The Lifshitz term $\Lambda\left(\xi_x \frac{\partial \xi_y}{\partial z} - \xi_y \frac{\partial \xi_x}{\partial z}\right)$ is responsible for the helical twist of the director. The three elastic terms give the energy of deformation of director field and are analogous to the Frank elastic energy in nematics. The coefficient $1/2\varepsilon$ in front of $\mathbf{P}^2$ term is independent of temperature, as the polarization does not drive the phase transition. The piezoelectric term $C\left(P_x\,\xi_y - P_y\,\xi_x\right)$ describes the coupling between the tilt and polarization. The flexoelectric term $\mu\left(P_x \frac{\partial \xi_x}{\partial z} + P_y \frac{\partial \xi_y}{\partial z}\right)$ on the other hand describes the appearance of the polarization due to the inhomogeneity of the director structure. It should be mentioned that the Lifshitz and piezoelectric term have a chiral origin while the flexoelectric effect can also be present in achiral smectics.

In Sm-A* phase, the equilibrium value of $|\boldsymbol{\xi}|$ and $|\mathbf{P}|$ is 0. Below the phase transition temperature T_c, in Sm-C* phase, the amplitude of the director tilt varies as $|\boldsymbol{\xi}| = \sqrt{\alpha\left(T_c - T\right)/b}$. The amplitude of the polarization is proportional to the magnitude of tilt $|\mathbf{P}| = \varepsilon\left(\mu q_c + C\right)|\boldsymbol{\xi}|$. The temperature of Sm-A* – Sm-C* phase transition T_c is equal to $T_c = T_0 + \left[\varepsilon C^2 + \left(K_3 - \varepsilon\mu^2\right) q_c^2\right]/\alpha$ and is always higher than the phase transition temperature T_0 in achiral systems. This is due to the coupling between the tilt and polarization and due to the helical structure of Sm-C* phase which has to be unwinded at the transition. The equilibrium pitch of helix is given by $q_c = (\Lambda + \varepsilon\mu C)/(K_3 - \varepsilon\mu^2)$. The classical Landau model presented here does not completely cover the experimentally observed material properties of ferroelectric smectics and has therefore been subject to various improvements and corrections. However all these corrections contribute higher order terms in free energy expansion and are hence not crucial for our analysis of fluctuations which will be limited to

harmonic terms only.

In liquid crystals, the thermal fluctuations of ordering around the equilibrium structure are overdamped. The relaxation times of fast (i.e. high energy) polarization fluctuations ($\tau^{-1} \sim 100$ MHz) are much shorter than typical relaxation times of director fluctuations ($\tau^{-1} \sim 10$ Hz $-$ 1 MHz). This fact justifies the use of adiabatic approximation which is based on assumption that polarization always instantaneously equilibrates with the director movement. This enables us to eliminate the polarization $\mathbf{P}$ from the free energy. Considering the equilibrium conditions $\partial f/\partial P_x = 0$ and $\partial f/\partial P_y = 0$ we obtain for polarization values

$$\begin{aligned} P_x &= \varepsilon\mu\frac{d\xi_x}{dz} - \varepsilon C\xi_y \,, \\ P_y &= \varepsilon\mu\frac{d\xi_y}{dz} + \varepsilon C\xi_x \,. \end{aligned} \tag{2.9}$$

The free energy in the adiabatic approximation then reads

$$\begin{aligned} f = f_A + \frac{1}{2}\widetilde{a}\left(\xi_x^2+\xi_y^2\right) + \frac{1}{4}b\left(\xi_x^2+\xi_y^2\right)^2 - \widetilde{\Lambda}\left(\xi_x\frac{\partial\xi_y}{\partial z} - \xi_y\frac{\partial\xi_x}{\partial z}\right) \\ + \frac{1}{2}K_1\left(\frac{\partial\xi_x}{\partial x}+\frac{\partial\xi_y}{\partial y}\right)^2 + \frac{1}{2}K_2\left(\frac{\partial\xi_x}{\partial y}-\frac{\partial\xi_y}{\partial x}\right)^2 + \frac{1}{2}\widetilde{K}_3\left[\left(\frac{\partial\xi_x}{\partial z}\right)^2+\left(\frac{\partial\xi_y}{\partial z}\right)^2\right], \end{aligned} \tag{2.10}$$

with renormalized coefficients $\widetilde{a}(T) = a(T) - \varepsilon C^2$, $\widetilde{\Lambda} = \Lambda + \varepsilon\mu C$ and $\widetilde{K}_3 = K_3 - \varepsilon\mu^2$.

The free energy expansion can be further simplified by transforming the order parameter into rotating system which follows the helical structure of the Sm-C* phase. The order parameter $\boldsymbol{\xi}$ in the rotating frame is given by $\boldsymbol{\xi} = (\xi_{\shortparallel}, \xi_\perp)$ where $\xi_{\shortparallel}$ is the component parallel to the equilibrium director tilt and $\xi_\perp$ component perpendicular to the equilibrium tilt. The transformation equations read: $\xi_x = \xi_{\shortparallel}\cos q_c z - \xi_\perp \sin q_c z$ and $\xi_y = \xi_{\shortparallel}\sin q_c z + \xi_\perp \cos q_c z$. The equilibrium values of transformed order parameters in Sm-C* phase are $\xi_{\shortparallel} = |\boldsymbol{\xi}| = \sqrt{\alpha\left(T_c - T\right)/b}$ and $\xi_\perp = 0$, while in Sm-A* phase both order parameters are equal to 0. The free energy in rotating frame is now given by

$$\begin{aligned} f = f_A + \left(\frac{1}{2}\widetilde{a}(T) - \frac{1}{2}\widetilde{K}_3\, q_c^2\right)\left(\xi_{\shortparallel}^2+\xi_\perp^2\right) + \frac{1}{4}b\left(\xi_{\shortparallel}^2+\xi_\perp^2\right)^2 + \\ + \frac{1}{2}K\left[\left(\frac{\partial\xi_{\shortparallel}}{\partial x}+\frac{\partial\xi_\perp}{\partial y}\right)^2 + \left(\frac{\partial\xi_{\shortparallel}}{\partial y}-\frac{\partial\xi_\perp}{\partial x}\right)^2\right] + \frac{1}{2}\widetilde{K}_3\left[\left(\frac{\partial\xi_{\shortparallel}}{\partial z}\right)^2+\left(\frac{\partial\xi_\perp}{\partial z}\right)^2\right], \end{aligned} \tag{2.11}$$

with assumption $K_1 = K_2 = K$. The coefficient $(\widetilde{a} - \widetilde{K}_3\, q_c^2)/2$ is of form $\alpha(T - T_c)/2$ and is positive in Sm-A* phase and negative in Sm-C* phase.

2.3 Confined systems

The presence of confining boundaries, and thereby boundary conditions imposed onto fluctuating fields, is the basis of the Casimir interaction. In this thesis we study the Casimir force in two confined systems with plan-parallel geometry: homeotropic cell and free-standing film (Fig. 2.3). The influence of boundaries on both types of smectic ordering – positional and orientational – has to be taken into account.

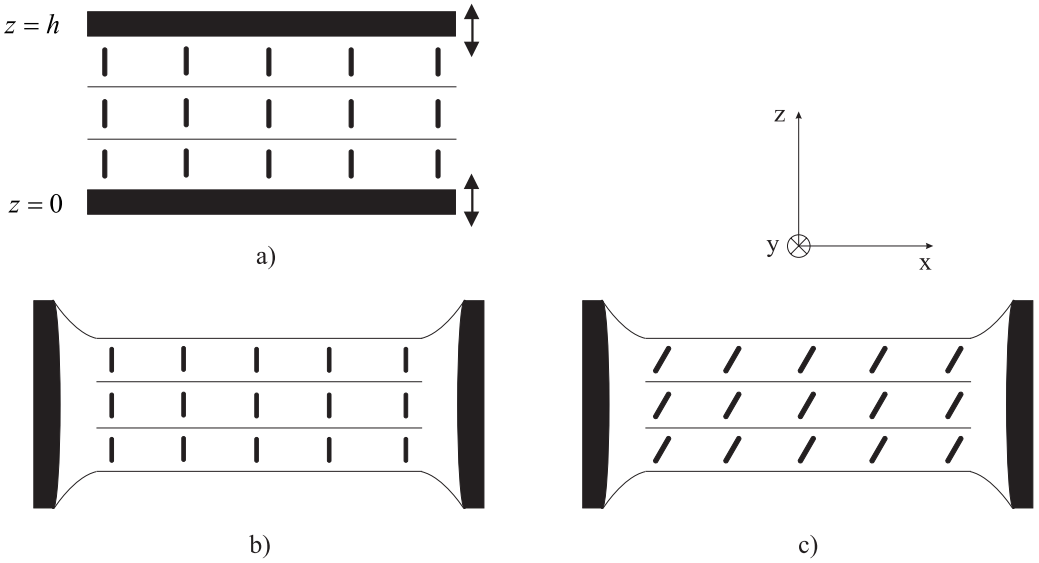

Figure 2.3 Confined systems: a) Homeotropic cell. Smectic material is confined by parallel plates. Smectic layers are aligned parallel to the plates, while the director structure is homeotropic. The arrows indicate the preferential orientation of the director at the plates; b) Free-standing smectic-A film; c) Free-standing smectic-C film. In free-standing films the smectic material is spread over a hole in a metal or a glass plate. The layers align parallel with the free boundaries in contact with air; The setting of coordinate system which is used in the calculations is presented.

The homeotropic cell consists of Sm-A material trapped between two parallel flat plates separated by the distance h. Smectic layers are aligned parallel to the plates. We assume that smectic layers rigidly adjust to the plates. In terms of layer displacement u this gives the boundary condition $u(z{=}0){=}u(z{=}h){=}0$. Furthermore the boundaries affect (usually increase) the degree of positional order ψ. We model this by assuming that the plates induce a fixed magnitude of positional order ψ_S, which gives the boundary conditions $\psi(z=0)=\psi(z=h)=\psi_S$. Finally, the plates favor homeotropic (i.e. perpendicular to the plates) ordering of the director. This director anchoring is described by phenomenological Rapini-Papoular model [163] with the anchoring free energy given by

$$F_S\left[\mathbf{n}\right] = \frac{1}{2} W \int \sin^2\left(\left|\mathbf{n}-\mathbf{n}_S\right|\right) \mathrm{d}S \,, \tag{2.12}$$

where W is the anchoring energy per surface unit and $\mathbf{n}_S$ the preferred director orientation at the boundary. The anchoring energy W depends on chemical and mechanical preparation of the plates and can be in general different for each plate in homeotropic cell. In the case of infinitely strong director anchoring, $W \to \infty$, the director orientation at the boundary is fixed. It is common to express anchoring strengts in terms of extrapolation length $L = K/W$ with K being some appropriate elastic constant of the liquid crystal material.

A free-standing film is formed by spreading the smectic material over a hole in a metal or a glass plate. The layers align parallel with free boundaries. Films consisting of only a few (at least two) up to thousands layers can be produced and stabilized, while monolayers are unstable. Free-standing films are very convenient for studying properties of liquid crystals as a defect-free structure can be obtained relatively easy, which is not the case in liquid-crystal cells. As the film is confined by air and not by hard plates the fluctuations of the boundary layers are not completely suppressed. However, these surface fluctuations increase the area of the free surface and thus the surface tension free energy given by

$$F_S[u] = \frac{1}{2}\gamma \int (\nabla_\perp u)^2 \, \mathrm{d}S \,, \tag{2.13}$$

where γ is the surface tension between the smectic and air. The boundary conditions for ψ and $\mathbf{n}$ can be modeled in same manner as in the homeotropic cell. The preferential orientation of director at a free-surface $\mathbf{n}_S$ depends on the specific smectic phase (Sm-A or Sm-C). In the simplest model we take $\mathbf{n}_S$ to be equal to the equilibrium bulk orientation of the director. This assumes the existence of some "internal anchoring" where the bulk interior dictates the behavior of the boundary layer. In this case the equilibrium director structure of the film is homogeneous because the boundary conditions match the bulk order. However, as the fluctuations of surface layers are suppressed by the surface tension and thus less pronounced than in interior of the film, the boundary layers are often more ordered than the interior ones [164]. Close to the Sm-A – Sm-C phase transition (above T_C) the boundary layers can exhibit Sm-C ordering while the bulk interior is still in Sm-A phase. This kind of system can be modeled by taking appropriate value of $\mathbf{n}_S$ which corresponds to this surface-induced ordering.

2.4 Calculation of Casimir force

The procedure used for calculating the Casimir force is similar for all systems studied in this thesis. We here outline the main steps of the calculation while specific details are presented along with each system.

Let us begin with a definition of the thermodynamic force. In plan-parallel geometry the force is given as a derivative of the free energy F with respect to the

distance between the planar boundaries h

$$\mathcal{F} = -\left(\frac{\partial F}{\partial h}\right)_{V,S,T} . \tag{2.14}$$

Here the total volume and surface area as well as the temperature of the system should be constant. This means that we should always consider a system where confined liquid crystal material is connected to some reservoir of bulk material in order to retain constant volume as the liquid crystal is squeezed in or out of the confined area. The bulk reservoir is realized naturally in the case of free-standing smectic films where a large amount of smectic material gathers at the lateral edges and can flow into or out of the film. For a homeotropic cell the reservoir is provided by immersing the plates into the liquid crystal material. This is indeed the case in the atomic force microscope, with distinction that it is a sphere and not a plate which is immersed into liquid crystal. For the purpose of calculation the presence of a reservoir means that the free energy of a confined system should be measured from the reference free energy of a bulk system.

As it can be inferred from the definition of the force, the main task in the calculation is evaluation of the free energy of a system. Ideally one would start with a Hamiltonian of the system, evaluate the partition function and obtain the total free energy at once. This is however rarely possible and the procedure is then divided into two steps. First the equilibrium structure of a system is determined by minimizing the mean-field free energy described by phenomenological Landau-type models. Then fluctuations around the equilibrium are considered. The total free energy now consists of the mean-field and fluctuations free energy: $F = F_{mf} + F_{fluc}$. If the mean-field free energy F_{mf} depends on the separation between boundaries (this usually happens in systems with inhomogeneous equilibrium order) it gives rise to the mean-field force $\mathcal{F}_{mf}$. The fluctuations on the other hand induce the Casimir force $\mathcal{F}_{Cas}$ which is of main concern to us.

The calculation of the fluctuations free energy in this thesis is performed in the following way. Once the mean-field configuration has been determined the order parameter(s) can be written as a sum of equilibrium and fluctuating part: $\nu = \nu_{mf} + \delta\nu$. Here ν stands for any of the smectic order parameters. The Hamiltonian of fluctuations $H[\delta\nu]$ is obtained by expanding the free energy given by Landau-type models around the equilibrium. We retain only harmonic fluctuation terms in the Hamiltonian and neglect higher order terms. The harmonic approximation is justified as long as the fluctuations are small. However, in the vicinity of phase transitions the fluctuations of ordering can be strongly enhanced and higher order terms could become important. In this case the harmonic model may only give qualitative description of the force and one should be aware of this limitation.

Once the Hamiltonian is known the partition function of fluctuations is obtained

by evaluating a path integral

$$Z_{fluc} = \exp\left(-\beta F_{fluc}\right) = \int_{b.c.} \exp\left(-\beta H[\delta\nu(\mathbf{r})]\right)\, \mathcal{D}\delta\nu(\mathbf{r}) \equiv \sum_{all\ conf.} \exp\left(-\beta H[\delta\nu(\mathbf{r})]\right)\ , \tag{2.15}$$

where $\beta = 1/k_B T$. The path integral is a functional integral which is evaluated by going over all possible configurations of $\delta\nu(\mathbf{r})$ that satisfy the boundary conditions, assigning each configuration a statistical weight $\exp(-\beta H)$. This is analogous to Feynman formulation of quantum mechanics [165], where the propagator of a quantum system is obtained by path integration exploring all possible paths from a state x_1 at time t_1 to a state x_2 at time t_2 (Fig. 2.4), assigning each path a phase factor $\exp(iS/\hbar)$, with S being the action of a system

$$(x_2 t_2 | x_1 t_1) = \sum_{all\ paths} \exp(iS/\hbar)\ . \tag{2.16}$$

The analogy between statistical physics of one-dimensional systems and quantum

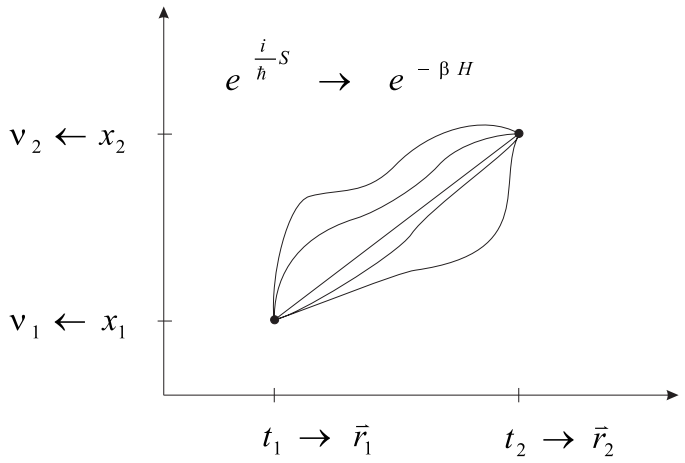

Figure 2.4 Analogy between path integral formulation of quantum mechanics and statistical physics of one-dimensional systems. The time t corresponds to the one-dimensional spatial coordinate $\vec{r}$ and the quantum state x corresponds to the fluctuating field ν. Instead of the quantum phase factor $\exp(iS/\hbar)$ the Boltzmann factor $\exp(-\beta H)$ is used in statistical physics. The system explores all possible paths between the initial and the final state.

mechanics will be readily employed as many results of path integration in quantum systems can be easily transformed and used for evaluation of partition functions [166–168]. The partition function Z_{fluc} can be transformed into a partition function of a one-dimensional system considering the fact that both studied systems, the homeotropic cell and the free-standing film, are extensive in horizontal directions (x-y). We can therefore assume that lateral edges do not influence the liquid crystal

structure. This allows for application of periodic boundary conditions and Fourier transformation of fluctuating fields

$$\delta\nu(\mathbf{r}) = \sum_{\mathbf{q}} \nu_q(z) \exp\left(i\mathbf{q}\cdot\boldsymbol{\rho}\right) \ , \tag{2.17}$$

where $\boldsymbol{\rho} = (x, y)$ and $\mathbf{q} = (q_x, q_y)$ satisfy periodic boundary conditions. The fluctuating field $\nu_q(z)$ now depends only on the coordinate z, which makes the analogy with one-dimensional systems possible. If fluctuation modes with different wave vectors $\mathbf{q}$ are not coupled, the partition function can be factorized as

$$Z_{fluc} = \prod_{\mathbf{q}} Z_{\mathbf{q}} = \prod_{\mathbf{q}} \int \exp\left(-\beta H_q[\nu_q(z)]\right) \mathcal{D}\nu_q(z) \ . \tag{2.18}$$

The generalization to several, possibly coupled fluctuating fields is straightforward

$$Z_{fluc} = \prod_{\mathbf{q}} Z_{\mathbf{q}} = \prod_{\mathbf{q}} \int \exp\left(-\beta H_q[\nu_q^{(1)}(z),\, \nu_q^{(2)}(z),\, \ldots]\right) \mathcal{D}\nu_q^{(1)}(z)\, \mathcal{D}\nu_q^{(2)}(z) \ldots \ . \tag{2.19}$$

The free-energy of fluctuations is given as a sum (or integral) of contributions of individual Fourier modes

$$F_{fluc} = -k_B T \sum_{\mathbf{q}} \ln Z_{\mathbf{q}} = -k_B T \frac{S}{(2\pi)^2} \int \ln Z_{\mathbf{q}} \, \mathrm{d}\mathbf{q} \ . \tag{2.20}$$

Within the continuum model, where the sum or integral over $\mathbf{q}$ is unbounded, the free energy of fluctuations F_{fluc} diverges. This is one of the main problems in calculation of the Casimir force. Many methods have been developed in the theory of Casimir effect to regularize the diverging total free energy and extract the finite interaction part. These methods include dimensional regularization, introduction of a suitable cut-off of wave vectors, Zeta regularization, methods based on Green's function and others [40, 42, 63]. At first it seems that introducing the lower limit of allowed wavelengths of fluctuations, i.e., a cut-off of large $\mathbf{q}$'s, would solve the problem naturally. However, it turned out that the final result can depend on the type of the cut-off procedure which complicates the situation considerably. In this thesis we use a method which is perhaps the most intuitive from physical point of view. As already discussed while defining the thermodynamic force [Eq. (2.14)] the free energy should actually be measured with respect to reference bulk configuration. If the free energy of fluctuations of a reference bulk system can be directly (i.e. analytically) subtracted from the total free energy of fluctuations in confined system the divergence is removed in most cases. One should simultaneously also dispose of constant terms in fluctuations free energy which do not depend on separation between the boundaries of confined system. These terms do not contribute to the force and usually represent the surface tension between the liquid crystal

material and boundaries. Once the finite interaction part has been extracted from the total free energy of fluctuations the Casimir force is obtained straightforwardly by differentiation.

3

Casimir force in smectic-A phase

3.1 Homeotropic smectic-A cell

Our work starts with the study of the Casimir force in the homeotropic smectic-A cell, which was introduced in the previous chapter (Fig. 2.3). The homeotropic smectic cell consists of two plan-parallel plates which align smectic layers and favor homeotropic director orientation. Our calculation starts from the free energy expansion (2.5). Before considering fluctuations, the equilibrium configuration has to be determined. We first assume that the equilibrium degree of smectic order ψ is uniform over the whole cell and equal to bulk value $\psi_0 = \sqrt{-a/b}$ as follows from Eq. (2.6). This assumption holds reasonably well when the system is deep in smectic-A phase far from the nematic – smectic-A phase transition. Close to this transition where the bulk value ψ_0 is small, one should expect inhomogeneous equilibrium profile of ψ due to the surface enhanced order and also due to the coupling with layer compression which can result in melting of smectic order. These effects are neglected in present model but will be discussed later on. We further assume that the homeotropic cell incorporates an integer number of unstressed smectic layers $[u_{mf}(\mathbf{r}) = 0]$. As the plates favor homeotropic orientation of molecules the equilibrium director configuration is given by $\mathbf{n}_{mf} = \mathbf{n}_z = (0, 0, 1)$. Due to normalization condition $|\mathbf{n}| = 1$ there can be only two director fluctuation modes present, which describe transversal components of director n_x and n_y. The fluctuating director is then given by $\mathbf{n} = (n_x, n_y, \sqrt{1 - n_x^2 - n_y^2}) \approx [\delta\mathbf{n}, 1 - \frac{1}{2}(n_x^2 + n_y^2)]$, with $\delta\mathbf{n} = (n_x, n_y)$. The Hamiltonian of fluctuations is obtained by expanding free energy [Eq. (2.5)] around equilibrium configuration (note that $\phi = q_0 u$)

$$H[\delta\psi, u, \delta\mathbf{n}] = H[\delta\psi] + H[u, \delta\mathbf{n}] \,,$$

$$H[\delta\psi] = \int \mathrm{d}V \left[-a\delta\psi^2 + \frac{1}{2} C_\parallel (\nabla_\parallel \delta\psi)^2 + \frac{1}{2} C_\perp (\nabla_\perp \delta\psi)^2 \right] \,,$$

$$H[u,\delta\mathbf{n}] = \frac{1}{2}\int \mathrm{d}V \Bigg\{ B\left(\nabla_{\parallel} u\right)^2 + K_L\left(\nabla_{\perp}^2 u\right)^2 + D\left(\nabla_{\perp} u + \delta\mathbf{n}\right)^2 + \\ + K_1\left(\frac{\partial n_x}{\partial x} + \frac{\partial n_y}{\partial y}\right)^2 + K_2\left(\frac{\partial n_x}{\partial y} - \frac{\partial n_y}{\partial x}\right)^2 + K_3\left[\left(\frac{\partial n_x}{\partial z}\right)^2 + \left(\frac{\partial n_y}{\partial z}\right)^2\right]\Bigg\}, \tag{3.1}$$

where $\delta\psi(\mathbf{r}) = \psi - \psi_0$ are the fluctuations of degree of smectic order, $u(\mathbf{r})$ fluctuations of position of smectic layers and $\delta\mathbf{n}(\mathbf{r}) = (n_x, n_y)$ the director fluctuations (Fig. 3.1). In this expansion we neglected terms of higher than quadratic order in fluctuating

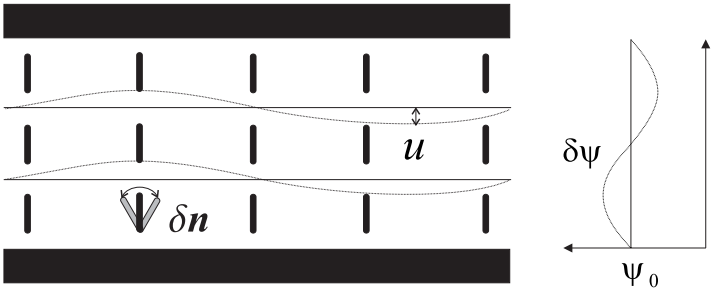

Figure 3.1 Fluctuations in smectic-A homeotropic cell. The fluctuations of degree of smectic order $\delta\psi$, position of smectic layers u and director fluctuations $\delta\mathbf{n}$ are presented schematically.

fields and also discarded some higher order elastic terms, which are not essential to describe the physical properties of smectics. We have introduced the elastic constants

$$B = C_{\parallel} q_0^2 \psi_0^2\,, \quad D = C_{\perp} q_0^2 \psi_0^2 \quad \text{and} \quad K_L = d_1 q_0^2 \psi_0^2 \tag{3.2}$$

to cast the Hamiltonian in a compact form. Within the harmonic approximation, the fluctuations of degree of smectic order are decoupled from layer and director fluctuations which considerably simplifies the calculations. Let us now provide physical meaning of individual terms in Hamiltonian (3.1). The first term in $H[\delta\psi]$ gives the energy of deviation of smectic order magnitude from the preferred value (note that $a < 0$). The remaining terms describe the elastic energy of the inhomogeneity of smectic order. The first and the second term in $H[u,\delta\mathbf{n}]$ are related to the layer compression and to the layer bending, respectively. The third term $D\left(\nabla_{\perp} u + \delta\mathbf{n}\right)^2/2$ describes the coupling between the director and layers. It simply states that if the coupling constant D is positive the director tends to orient perpendicular to the layers ($\delta\mathbf{n} = -\nabla_{\perp} u$). The last three terms in $H[u,\delta\mathbf{n}]$ originate from the Frank director elastic energy.

In addition to bulk Hamiltonian, also the boundary conditions must be modeled. As mentioned in the previous chapter, we assume that the position of the smectic layers is fixed at the plates which gives $u(z=0) = u(z=h) = 0$. Furthermore we assume that the degree of smectic order at the plates is fixed to the equilibrium bulk value $\psi(z=0) = \psi(z=h) = \psi_0$ which gives boundary conditions for fluctuating

field $\delta\psi(z=0) = \delta\psi(z=h) = 0$. This somewhat artificial condition should be considered in the spirit of homogeneous equilibrium order profile which we employ here and should suffice to give at least a qualitative picture of phenomenon. Finally, the homeotropic director anchoring is modeled by Rapini-Papoular model. In the harmonic approximation,

$$H_S\left[\mathbf{n}\right] = \frac{1}{2} W \int \left|\delta\mathbf{n}\right|^2 \mathrm{d}S \,, \tag{3.3}$$

where the integration is performed over confining surfaces.

3.1.1 Fluctuations of degree of smectic order ψ

As the fluctuations of ψ are decoupled from director and layer fluctuations their contribution to the Casimir force can be calculated separately. We first perform the two-dimensional Fourier transformation $\delta\psi(\mathbf{r}) = \sum_{\mathbf{q}} \psi_q(z) \exp\left(i\mathbf{q}\cdot\boldsymbol{\rho}\right)$ and obtain

$$H[\delta\psi] = \sum_{\mathbf{q}} H_{\mathbf{q}}[\delta\psi] = \frac{1}{2} C_{\parallel} S \sum_{\mathbf{q}} \int_0^h \mathrm{d}z \left[(\xi^{-2} + \frac{C_{\perp}}{C_{\parallel}} q^2) \left|\psi_{\mathbf{q}}\right|^2 + \left| \frac{\partial \psi_{\mathbf{q}}}{\partial z} \right|^2 \right] \,, \tag{3.4}$$

where ξ is the correlation length of fluctuations defined by $\xi = \sqrt{-C_{\parallel}/2a}$. As fluctuation modes with different wave-vectors $\mathbf{q}$ are decoupled the partition function for each mode is

$$Z_{\mathbf{q}}[\delta\psi] = \int_{\psi_{\mathbf{q}}(z=0)=0}^{\psi_{\mathbf{q}}(z=h)=0} \exp\left(-\beta H_{\mathbf{q}}[\delta\psi]\right) \mathcal{D}\psi_{\mathbf{q}}(z) \,. \tag{3.5}$$

This partition function is analogous to the quantum propagator of a repelling harmonic oscillator [168] and can thus be readily evaluated (see Appendix A.1)

$$Z_{\mathbf{q}}[\delta\psi] \propto \left[\sinh\left(\sqrt{\xi^{-2} + \frac{C_{\perp}}{C_{\parallel}} q^2}\, h \right) \right]^{-1/2} \,. \tag{3.6}$$

We have disposed of the constant factors that do not depend on separation h and therefore do not contribute to the interaction. The free energy of fluctuations is given by

$$F_{fluc}[\delta\psi] = -k_B T \sum_{\mathbf{q}} \ln Z_{\mathbf{q}}[\delta\psi] = \frac{k_B T S}{4\pi} \int \ln \left[\sinh\left(\sqrt{\xi^{-2} + \frac{C_{\perp}}{C_{\parallel}} q^2}\, h \right) \right] q \, \mathrm{d}q \,. \tag{3.7}$$

From the total fluctuation free energy a finite interaction part has to be extracted. In this case the procedure is fairly straightforward. The free energy can be factorized using the relation $\sinh(x) = \exp(x) \times 1/2 \times [1 - \exp(-2x)]$

$$F_{fluc}[\delta\psi] = \frac{k_B T S}{4\pi} \frac{C_{\parallel}}{C_{\perp}} \int_{\xi^{-1}}^{\infty} \ln \left(\exp\left(ph\right) \times \frac{1}{2} \times \left[1 - \exp\left(-2ph\right)\right] \right) p \, \mathrm{d}p \,. \tag{3.8}$$

where $p^2 = \xi^{-2} + \frac{C_\perp}{C_\parallel} q^2$. The first term in the factorization, $\ln(\exp(ph)) = ph$, is proportional to sample volume Sh and represents the bulk free energy. The second term $\ln(1/2)$ is independent of h and does not contribute to the interaction between plates. The last term, which vanishes in the limit $h \to \infty$, represents the interaction part of free energy

$$F^{int}_{fluc}[\delta\psi] = \frac{k_B T S}{4\pi} \frac{C_\parallel}{C_\perp} \int_{\xi^{-1}}^{\infty} \ln\left(1 - \exp\left(-2ph\right)\right) p \, \mathrm{d}p \; . \tag{3.9}$$

The Casimir force, which is obtained by differentiating F^{int}_{fluc} with respect to h and evaluating the integral, reads

$$\mathcal{F}_{Cas}[\delta\psi] = -\frac{k_B T S}{4\pi} \frac{C_\parallel}{C_\perp} \frac{1}{h^3} \sum_{k=1}^{\infty} \frac{\exp(-2hk/\xi)}{k^3} \left(\frac{1}{2} + \frac{h}{\xi} k + \frac{h^2}{\xi^2} k^2\right) . \tag{3.10}$$

In the limiting case of large thicknesses ($h \gg \xi$) the Casimir force decays as $\exp(-2h/\xi)/h$ and is hence short-range. In the opposite limit of small thicknesses ($h \ll \xi$) the force varies as $1/h^3$. Deep in the smectic-A phase the correlation length ξ is of the order of smectic layer thickness. Close to the smectic-A – nematic phase transition the correlation length increases as $\xi = \sqrt{C_\parallel / 2\alpha (T_{NA} - T)}$.

The result obtained here is equivalent to the force induced by biaxiality and degree-of-order fluctuations in nematics [Eq. (1.10)] and is actually universal for all massive fluctuation modes independent of specific details of the system (assuming the same type of boundary conditions and homogeneity of the system).

3.1.2 Fluctuations of director and smectic layers

Fluctuations of director and smectic layers are coupled and must be considered simultaneously. After Fourier transforming the fluctuating fields the Hamiltonian reads

$$\begin{aligned} H[u, \delta\mathbf{n}] = \frac{1}{2} S \sum_{\mathbf{q}} \int_0^h \mathrm{d}z \Bigg[& B \left| \frac{\partial u_{\mathbf{q}}}{\partial z} \right|^2 + D q^2 \left| u_{\mathbf{q}} \right|^2 + K_L q^4 \left| u_{\mathbf{q}} \right|^2 \\ & + D \left(\left| n_{1\mathbf{q}} \right|^2 + \left| n_{2\mathbf{q}} \right|^2 \right) + iqD \left(u_{\mathbf{q}} n^*_{1\mathbf{q}} - u^*_{\mathbf{q}} n_{1\mathbf{q}} \right) + K_1 q^2 \left| n_{1\mathbf{q}} \right|^2 \\ & + K_2 q^2 \left| n_{2\mathbf{q}} \right|^2 + K_3 \left(\left| \frac{\partial n_{1\mathbf{q}}}{\partial z} \right|^2 + \left| \frac{\partial n_{2\mathbf{q}}}{\partial z} \right|^2 \right) \Bigg] . \end{aligned} \tag{3.11}$$

We applied the transformation of $\delta\mathbf{n}_{\mathbf{q}} = (n_{x\mathbf{q}}, n_{y\mathbf{q}})$ into $(n_{1\mathbf{q}}, n_{2\mathbf{q}})$ where component $n_{1\mathbf{q}}$ represents director fluctuations parallel to $\mathbf{q} = (q_x, q_y)$ and component $n_{2\mathbf{q}}$ fluctuations perpendicular to $\mathbf{q}$. Only $n_{1\mathbf{q}}$ modes are coupled to the layer fluctuations, while $n_{2\mathbf{q}}$ modes represent "pure" director fluctuations. The Fourier transformed surface contribution to the Hamiltonian reads:

$$H_S\left[\mathbf{n}\right] = \frac{1}{2} K_3 S L^{-1} \sum_{\mathbf{q}} \left(\left| n^-_{1\mathbf{q}} \right|^2 + \left| n^+_{1\mathbf{q}} \right|^2 + \left| n^-_{2\mathbf{q}} \right|^2 + \left| n^+_{2\mathbf{q}} \right|^2 \right) \; . \tag{3.12}$$

Here $L = K_3/W$ is the extrapolation length, $n^-_{1,2\mathbf{q}} = n_{1,2\mathbf{q}}(z=0)$ and $n^+_{1,2\mathbf{q}} = n_{1,2\mathbf{q}}(z=h)$.

The fluctuation modes with different wave vectors $\mathbf{q}$ are decoupled and the Hamiltonian can be written as

$$H = \sum_{\mathbf{q}} H_{\mathbf{q}}[n_{1\mathbf{q}}, u_{\mathbf{q}}] + H_{S\mathbf{q}}[n^{\pm}_{1\mathbf{q}}] + H_{\mathbf{q}}[n_{2\mathbf{q}}] + H_{S\mathbf{q}}[n^{\pm}_{2\mathbf{q}}]. \tag{3.13}$$

In order to obtain the free energy of fluctuations, the following partial partition functions have to be evaluated

$$\begin{aligned} Z_{\mathbf{q}}[n_{1\mathbf{q}}, u_{\mathbf{q}}] = \int \mathrm{d}n^-_{1\mathbf{q}} \int \mathrm{d}n^+_{1\mathbf{q}} \, \exp(-\beta H_{S\mathbf{q}}[n^{\pm}_{1\mathbf{q}}]) \\ \times \int_{n_{1\mathbf{q}}(z=0)=n^-_{1\mathbf{q}}}^{n_{1\mathbf{q}}(z=h)=n^+_{1\mathbf{q}}} \int_{u_{\mathbf{q}}(z=0)=0}^{u_{\mathbf{q}}(z=h)=0} \exp(-\beta H_{\mathbf{q}}[u_{\mathbf{q}}, n_{1\mathbf{q}}]) \, \mathcal{D}u_{\mathbf{q}}(z) \mathcal{D}n_{1\mathbf{q}}(z) \, , \end{aligned} \tag{3.14}$$

$$Z_{\mathbf{q}}[n_{2\mathbf{q}}] = \int \mathrm{d}n^-_{2\mathbf{q}} \int \mathrm{d}n^+_{2\mathbf{q}} \, \exp(-\beta H_{S\mathbf{q}}[n^{\pm}_{2\mathbf{q}}]) \int_{n_{2\mathbf{q}}(z=0)=n^-_{2\mathbf{q}}}^{n_{2\mathbf{q}}(z=h)=n^+_{2\mathbf{q}}} \exp(-\beta H_{\mathbf{q}}[n_{2\mathbf{q}}]) \, \mathcal{D}n_{2\mathbf{q}}(z) \, . \tag{3.15}$$

Because of the finite anchoring strength, the director fluctuations at the boundaries are not suppressed completely. This fact is reflected in partition function where integration over all possible values of the director fluctuations at the surfaces is performed, assigning each surface configuration a statistical weight factor corresponding to energy penalty of deviation from easy axis orientation.

The partition function $Z_{\mathbf{q}}[n_{1\mathbf{q}}, u_{\mathbf{q}}]$ is analogous to the quantum propagator of two coupled harmonic oscillators [168, 169] and can be evaluated (see Appendix A.2) to give

$$\begin{aligned} Z_{\mathbf{q}}[n_{1\mathbf{q}}, u_{\mathbf{q}}] \propto [\sinh(\Omega_1 h) \, \sinh(\Omega_2 h)]^{-1/2} \\ \times \left[\Omega_1 S^2 A_1^+ + \Omega_2 C^2 A_2^+ + L^{-1}\right]^{-1/2} \left[\Omega_1 S^2 A_1^- + \Omega_2 C^2 A_2^- + L^{-1}\right]^{-1/2} \, . \end{aligned} \tag{3.16}$$

The partition function $Z_{\mathbf{q}}[n_{2\mathbf{q}}]$ can be evaluated using the analogy with the propagator of a single repelling quantum harmonic oscillator [168]:

$$Z_{\mathbf{q}}[n_{2\mathbf{q}}] \propto \left[\frac{L^{-2} + \Omega_3^2}{2\Omega_3 L^{-1}} \sinh(\Omega_3 h) + \cosh(\Omega_3 h)\right]^{-1/2} \, . \tag{3.17}$$

This result is analogous to the partition function obtained in the previous section [Eq. (3.6)] with a modification due to different boundary conditions. We introduced

the following notation:

$$\Omega_{1,2} = \frac{1}{\sqrt{2}}\frac{1}{\Lambda}\Bigg\{1 + (\rho^2+\lambda^2)q^2 + \frac{K_L}{K_3}\lambda^2\Lambda^2 q^4 \mp \sqrt{\left[1-(\lambda^2-\rho^2)q^2 - \frac{K_L}{K_3}\Lambda^2\lambda^2 q^4\right]^2 + 4\lambda^2 q^2}\Bigg\}^{1/2} , \tag{3.18}$$

$$\Omega_3 = \sqrt{\Lambda^{-2} + \frac{K_2}{K_3}q^2} , \tag{3.19}$$

$$C^2 = \frac{1}{2} + \frac{1}{2}\sqrt{\frac{\left[1+(\rho^2-\lambda^2)q^2 - \frac{K_L}{K_3}\lambda^2\Lambda^2 q^4\right]^2}{\left[1+(\rho^2-\lambda^2)q^2 - \frac{K_L}{K_3}\Lambda^2\lambda^2 q^4\right]^2 + 4q^2\lambda^2}} , \tag{3.20}$$

$$S^2 = 1 - C^2 , \tag{3.21}$$

$$A^{\pm}_{1,2} = \frac{\cosh(\Omega_{1,2}h) \pm 1}{\sinh(\Omega_{1,2}h)} \tag{3.22}$$

and the correlation lengths $\Lambda = (K_3/D)^{1/2}$, $\lambda = (K_3/B)^{1/2}$ and $\rho = (K_1/D)^{1/2}$. The free energy of fluctuations can now be written as

$$F_{fluc}[u,\delta\mathbf{n}] = -k_B T \sum_{\mathbf{q}} \Big(\ln Z_{\mathbf{q}}[n_{1\mathbf{q}}, u_{\mathbf{q}}] + \ln Z_{\mathbf{q}}[n_{2\mathbf{q}}]\Big) = F_{fluc}[n_1, u] + F_{fluc}[n_2] . \tag{3.23}$$

Having calculated the total free-energy of fluctuations, we now identify the interaction part. In $Z_{\mathbf{q}}[n_{1\mathbf{q}}, u_{\mathbf{q}}]$ the bulk contributions are contained in $\sinh(\Omega_i h)$ terms and can be identified by the same factorization as in the previous section. The remaining two factors in $Z_{\mathbf{q}}[n_{1\mathbf{q}}, u_{\mathbf{q}}]$ do not contain bulk terms while thickness independent surface contributions automatically vanishes after differentiation of the free energy and need not be extracted. The factorization of $Z_{\mathbf{q}}[n_{2\mathbf{q}}]$ leads to

$$\frac{L^{-2}+\Omega_3^2}{2\Omega_3 L^{-1}}\sinh(\Omega_3 h) + \cosh(\Omega_3 h) = \exp(\Omega_3 h) \times \left(\frac{\Omega_3^2 + L^{-2}}{4\Omega_3 L^{-1}} + \frac{1}{2}\right) \times \left(1 - \frac{(\Omega_3 - L^{-1})^2}{(\Omega_3 + L^{-1})^2}\exp(-2\Omega_3 h)\right) . \tag{3.24}$$

Now the bulk contribution (the first term), the surface contribution (the second term) and the last interaction term can be easily identified.

The Casimir force consists of four terms

$$\mathcal{F}_{Cas}[u,\delta\mathbf{n}] = \mathcal{F}[n_2; L] + \mathcal{F}_1[n_1, u] + \mathcal{F}_2[n_1, u] + \mathcal{F}_3[n_1, u; L] , \tag{3.25}$$

where

$$\mathcal{F}[n_2; L] = -\frac{k_B T S}{2\pi}\int_0^\infty \frac{\Omega_3 q\,\mathrm{d}q}{\frac{(\Omega_3+L^{-1})^2}{(\Omega_3-L^{-1})^2}\exp(2\Omega_3 h) - 1} , \tag{3.26}$$

$$\mathcal{F}_1[n_1,u] = -\frac{k_BTS}{2\pi}\int_0^\infty \frac{\Omega_1 q\,\mathrm{d}q}{\exp(2\Omega_1 h)-1}\,, \tag{3.27}$$

$$\mathcal{F}_2[n_1,u] = -\frac{k_BTS}{2\pi}\int_0^\infty \frac{\Omega_2 q\,\mathrm{d}q}{\exp(2\Omega_2 h)-1}\,, \tag{3.28}$$

$$\begin{aligned}\mathcal{F}_3[n_1,u;L] &= -\frac{k_BTS}{4\pi}\int_0^\infty q\,\mathrm{d}q\left[\frac{\frac{\Omega_1^2S^2}{1+\cosh(\Omega_1 h)}+\frac{\Omega_2^2C^2}{1+\cosh(\Omega_2 h)}}{\Omega_1S^2A_1^- + \Omega_2C^2A_2^- + L^{-1}}\right]\\ &\quad -\frac{k_BTS}{4\pi}\int_0^\infty q\,\mathrm{d}q\left[\frac{\frac{\Omega_1^2S^2}{1-\cosh(\Omega_1 h)}+\frac{\Omega_2^2C^2}{1-\cosh(\Omega_2 h)}}{\Omega_1S^2A_1^+ + \Omega_2C^2A_2^+ + L^{-1}}\right]\,.\end{aligned} \tag{3.29}$$

The first term $\mathcal{F}[n_2;L]$ represents the contribution of "pure" director fluctuation modes. It is a generalization of Eqs. (1.10 and 3.10) for finite strength of surface interaction. It is also the universal result for all massive fluctuation modes for given boundary conditions and has been already analyzed in Refs. [116, 170] in the context of nematics. Here we summarize these results. The effect of finite anchoring strength can be most easily represented by reduction factor

$$R = \frac{\mathcal{F}[n_2;L]}{\mathcal{F}[n_2;L=0]} \tag{3.30}$$

where $\mathcal{F}[n_2;L=0]$ is the familiar result for infinite anchoring strength

$$\mathcal{F}_{Cas}[n_2;L=0] = -\frac{k_BTS}{4\pi}\frac{K_3}{K_2}\frac{1}{h^3}\sum_{k=1}^{\infty}\frac{\exp(-2hk/\Lambda)}{k^3}\left(\frac{1}{2}+\frac{h}{\Lambda}k+\frac{h^2}{\Lambda^2}k^2\right). \tag{3.31}$$

The term $\mathcal{F}[n_2;L]$ can not be evaluated analytically and therefore numerical integration is necessary. Let us first note that for an infinitely weak anchoring ($L\to\infty$) the force is identical as in the strong anchoring limit ($L=0$) and the reduction factor is equal to 1. The dependence of R on the scaled cell thickness h/Λ for several values of the anchoring strengths is shown in Fig. 3.2. Finite anchoring strength reduces the amplitude of the force. If $L/\Lambda<1$, which corresponds to effectively strong anchoring, the reduction factor first decreases from 1 to a minimum and then saturates at a constant value at large thicknesses h/Λ. This saturation means that the functional dependence of the force at large h/Λ is the same as in the case of strong anchoring, i.e. $\exp(-2h/\Lambda)/h$. If $L/\Lambda>1$, which corresponds to effectively weak anchoring, the reduction factor decreases monotonically to the saturation value. The saturation value of reduction factor can be evaluated analytically and is equal to $R=1-4L/\Lambda$ for strong anchoring ($L/\Lambda\ll1$) and $R=1-4\Lambda/L$ for weak anchoring case ($L/\Lambda\gg1$). In the special case of $L/\Lambda=1$, where the anchoring regime is neither strong nor weak, the force decays much faster, as $\exp(-2h/\Lambda)/h^3$, at large h/Λ [116].

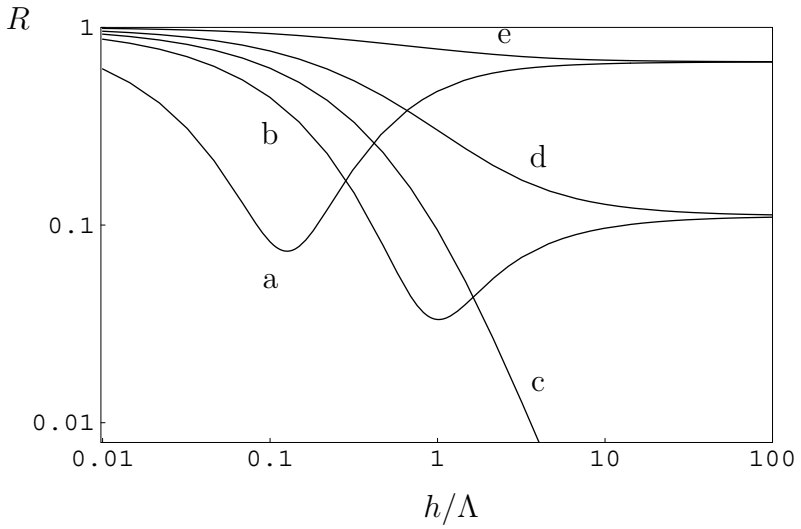

Figure 3.2 Reduction factor R versus the cell thickness h/Λ for different anchoring parameters: a) $L/\Lambda = 0.1$; b) $L/\Lambda = 0.5$; c) $L/\Lambda = 1$; d) $L/\Lambda = 2$; e)$L/\Lambda = 10$; adopted from Refs. [116, 170].

In analogy with eigen-modes of two coupled harmonic oscillators the terms $\mathcal{F}_1[n_1, u]$ and $\mathcal{F}_2[n_1, u]$ represent the contributions of in-phase fluctuations (Fig. 3.3a), where the director follows deformations of layers, and out-of-phase fluctuation modes of the director and layers (Fig. 3.3b). The in-phase fluctuations are massless

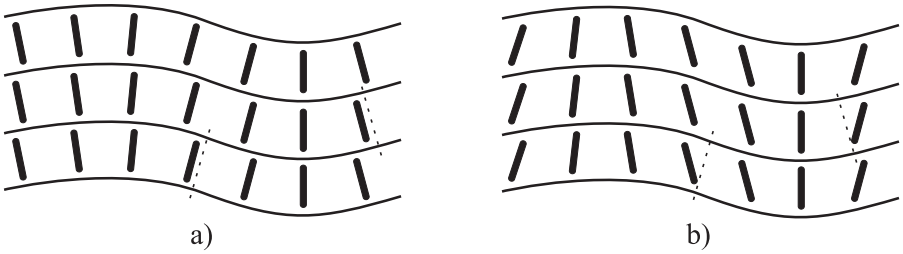

Figure 3.3 Schematic representation of fluctuation modes: a)in-phase fluctuations of director and layers; b)out-of-phase fluctuations of director and layers. The dotted lines indicate the local normal to the layers.

$[\Omega_1(q = 0) = 0]$ therefore the resulting force $\mathcal{F}_1[n_1, u]$ is long-range. In the limit of large thicknesses $\mathcal{F}_1[n_1, u]$ gives the familiar $1/h^2$ smectic Casimir force [Eq. (1.13)]. The out-of-phase fluctuations are massive. Therefore their contribution $\mathcal{F}_2[n_1, u]$ is short range and is qualitatively similar to the pure director fluctuations contribution [Eq. (3.31)]. The last term $\mathcal{F}_3[n_1, u; L]$ is a correction to the $\mathcal{F}_1[n_1, u]$ and $\mathcal{F}_2[n_1, u]$ terms due to the finite director anchoring strengths W at the plates. This correction is short-range and is equal to 0 in the limit of very strong anchoring ($W \to \infty$, $L = 0$).

To summarize, the Casimir force induced by coupled fluctuations of smectic layers and director consists of two director-like short range contributions and of a long range layer-like contribution. The correction due to the finite director anchoring is also short-range which is expected, as this anchoring does not modify the boundary conditions for smectic layers.

To analyze the behavior of $\mathcal{F}_{Cas}[u, \delta\mathbf{n}]$ we compare it to the Casimir force obtained by pure layer fluctuations u, assuming that director is fixed perpendicularly with respect to layers ($D \to \infty$, $\nabla_\perp u = -\delta\mathbf{n}$). In this limiting case the Hamiltonian reads: $H_{lay} = 1/2 \int \mathrm{d}V[B(\partial u/\partial z)^2 + K_L'(\nabla_\perp^2 u)^2]$, where $K_L' = K_L + K_1$. With the boundary conditions $u(z=0) = u(z=h) = 0$ the familiar Casimir force is obtained: $\mathcal{F}_{Cas}^{lay} = -k_B T S \zeta(2)/16\pi h^2 \sqrt{K_L'/B}$ [115, 128]. This force can be conveniently used as a reference because of its simple h^{-2} functional dependence. The comparison between the reference Casimir force $\mathcal{F}_{Cas}^{lay}$ and our result $\mathcal{F}_{Cas}[u, \delta\mathbf{n}]$, where the director degrees of freedom are included, is shown in Fig. 3.4. We used the following material

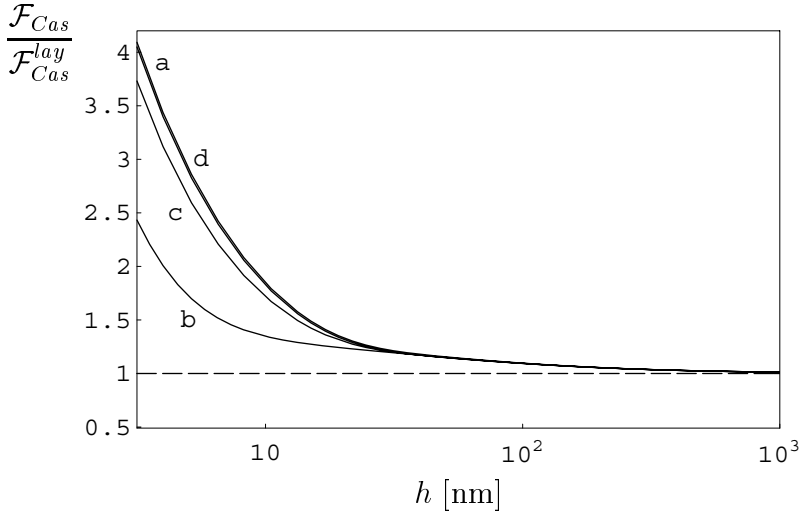

Figure 3.4 Casimir force $\mathcal{F}_{Cas}[u, \delta\mathbf{n}]$ in homeotropic smectic-A cell compared to reference force $\mathcal{F}_{Cas}^{lay}$ for different director anchoring strengths: a) $W \to \infty$, b) $W = 10^{-3}$ J/m^2, c) $W = 10^{-4}$ J/m^2, d) $W = 10^{-5}$ J/m^2.

constants: $B = 2 \times 10^6$ N/m^2, $D = 10^5$ N/m^2, $K_1 = K_2 = K_3 = K_L = 10^{-11}$ N. The full Casimir force $\mathcal{F}_{Cas}[u, \delta\mathbf{n}]$ is significantly larger than the approximate force $\mathcal{F}_{Cas}^{lay}$ only up to the thickness of a few correlation lengths Λ ($\Lambda = 10$ nm) where the short range contributions $\mathcal{F}[n_2; L]$ and $\mathcal{F}_2[n_1, u]$ are important. At larger thicknesses only the long-range contribution of the "in-phase" director-layer fluctuations $\mathcal{F}_1[n_1, u]$ needs to be considered. In the limit of $h/\Lambda \gg 1$ this contribution ($\mathcal{F}_1[n_1, u]$) exactly matches $\mathcal{F}_{Cas}^{lay}$ as can be seen from Fig. 3.4 and can also be shown analytically. A finite strength of the director anchoring generally reduces the magnitude of the Casimir force as was demonstrated in Fig. 3.2. The force is strongest when the anchoring is either very weak or very strong. When the anchoring is somewhere

inbetween these limits, in the sense that the extrapolation length L is comparable to typical lengths of the system, then the magnitude is strongly reduced. This is seen in the case of $W = 10^{-3}$ J/m^2 ($L = 10$ nm) in Fig. 3.4, while in other cases the anchoring does not have an important effect.

The effect of different coupling strengths between the director and smectic layers on the Casimir force is shown explicitly in Fig. 3.5. A reduction of the coupling

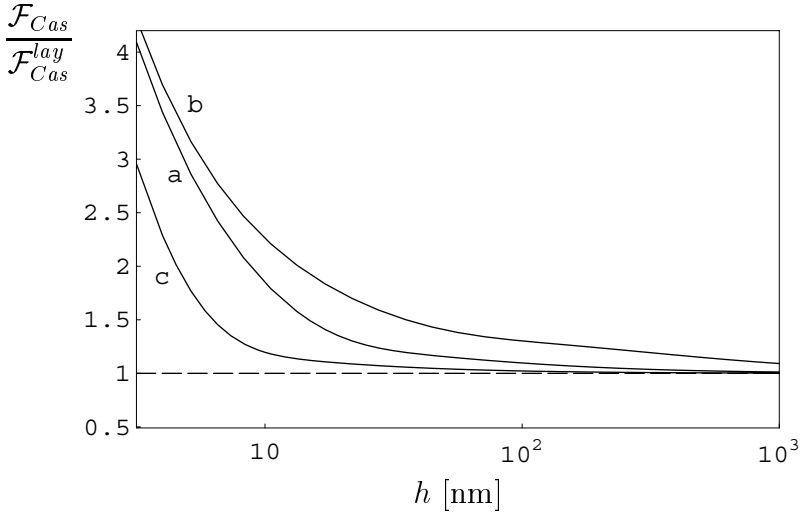

Figure 3.5 Effect of director-layer coupling constant D on the Casimir force: a) $D = 10^5$ N/m^2, b) $D = 10^4$ N/m^2, c) $D = 10^6$ N/m^2. Strong anchoring of the director ($W \to \infty$) is assumed.

constant D results in an increase of the magnitude of the force. This is firstly due to the increased correlation length Λ and hence an increased range of the director-type contributions and secondly also due to the coupling influence on the $\mathcal{F}_1[n_1, u]$ term. This kind of behavior could be observed upon cooling the system from smectic-A to smectic-C phase. In the vicinity of the phase transition the coupling constant changes as $D \propto (T - T_c)$ within the Landau model. Therefore the magnitude of the Casimir force is expected to increase while approaching the phase transition. We address the behavior of the Casimir force close to this phase transition in the next chapter as some other interesting phenomena occur there, which require more detailed treatment.

Another illustrative comparison can be made by comparing the coupled director-layer force $\mathcal{F}_{Cas}[u, \delta\mathbf{n}]$ with its uncoupled counterpart $\mathcal{F}_{Cas}^{unc}$ which is obtained when director and layer fluctuations are treated independently (to avoid confusion it should be noted that the term uncoupled in this context does not imply that the constant D equals 0). The uncoupled force is equal to $\mathcal{F}_{Cas}^{unc} = \mathcal{F}_{Cas}^{lay} + \mathcal{F}_{Cas}^{dir}$, where the director contribution is just twice the contribution of pure director fluctuation modes, $\mathcal{F}_{Cas}^{dir} = 2\mathcal{F}[n_2; L]$. This approximation neglects the fact that deformation of smectic layers also changes the equilibrium director orientation around which the

director fluctuates. Nevertheless, the uncoupled force $\mathcal{F}_{Cas}^{unc}$ represents a first-order approximation of the exact result $\mathcal{F}_{Cas}[u, \delta\mathbf{n}]$. The comparison of the two forces thus reveals the net effect of director-layer coupling and is shown in Fig. 3.6 for different values of coupling constant D. It turns out that the coupling increases the

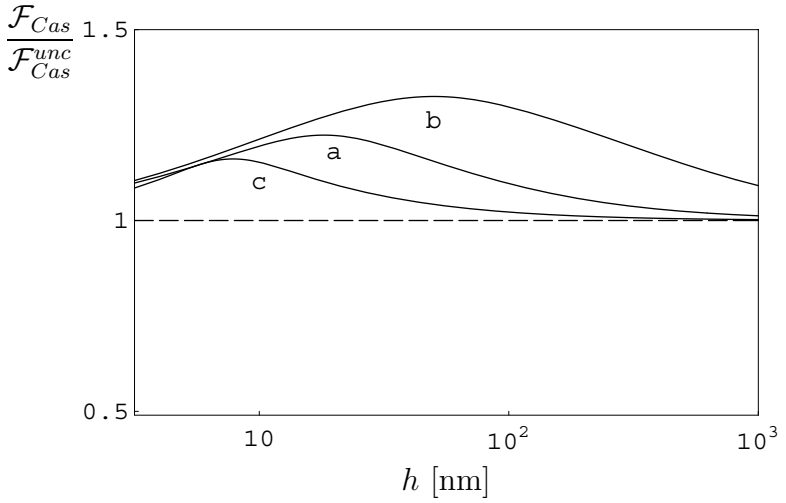

Figure 3.6 Comparison between the "coupled" ($\mathcal{F}_{Cas}[u, \delta\mathbf{n}]$) and "uncoupled" ($\mathcal{F}_{Cas}^{unc}$) Casimir force in homeotropic cell for infinitely strong director anchoring ($W \to \infty$) and various coupling constants D: a) $D = 10^5$ N/m^2, b) $D = 10^4$ N/m^2, c) $D = 10^6$ N/m^2.

magnitude of the force but for no more than a few ten percents. The increase is larger for weak coupling constants D (larger correlation length Λ) and vanishes in the limit of $D \to \infty$ according to our definition of $\mathcal{F}_{Cas}^{unc}$. The profiles in Fig. 3.6 can be explained as follows. In the limit of very large thicknesses ($h \gg \Lambda$) the terms $\mathcal{F}_1[n_1, u]$ and $\mathcal{F}_{Cas}^{lay}$, which are the only long-range contributions, are equal and the ratio between the "coupled" and "uncoupled" force is 1. With decreasing distance the $\mathcal{F}_1[n_1, u]$ term gets larger than $\mathcal{F}_{Cas}^{lay}$ and the ratio increases. At thicknesses comparable to correlation length Λ the short-range contributions from the director and "out-of-phase" fluctuations set in. These director-type contributions are in both – coupled and uncoupled – systems very similar, which results in reducing the difference and consequently the ratio between the two forces at small thicknesses.

3.2 Free-standing smectic-A film

The structure of a free-standing smectic-A film is identical to homeotropic cell. The difference between them lies in fluctuations of surface layers which are allowed in free-standing films but forbidden in a homeotropic cell. This results in modified

surface Hamiltonian which now reads

$$H_S\left[\mathbf{n},u\right]=\frac{1}{2}W\int\left|\delta\mathbf{n}\right|^2\mathrm{d}S\ +\frac{1}{2}\gamma\int\left(\nabla_\perp u\right)^2dS\ . \tag{3.32}$$

The bulk Hamiltonian $H[u,\delta\mathbf{n}]$ remains unchanged. The same goes for $H[\delta\psi]$, therefore the fluctuations of degree of smectic order ψ are not considered here. Fourier transforming Eq. (3.32) we obtain

$$\begin{aligned}H_S\left[\mathbf{n},u\right]=&\frac{1}{2}K_3SL^{-1}\sum_{\mathbf{q}}\left(\left|n_{1\mathbf{q}}^-\right|^2+\left|n_{1\mathbf{q}}^+\right|^2+\left|n_{2\mathbf{q}}^-\right|^2+\left|n_{2\mathbf{q}}^+\right|^2\right)\\&+\frac{1}{2}K_3S\chi^{-1}\sum_{\mathbf{q}}q^2\left(\left|u_{\mathbf{q}}^-\right|^2+\left|u_{\mathbf{q}}^+\right|^2\right)\ .\end{aligned} \tag{3.33}$$

Here $\chi=K_3/\gamma$ is the extrapolation length, $u_{\mathbf{q}}^-=u_{\mathbf{q}}(z=0)$ and $u_{\mathbf{q}}^+=u_{\mathbf{q}}(z=h)$. As only $n_{1\mathbf{q}}$ and $u_{\mathbf{q}}$ modes are coupled it suffices to recalculate $Z_{\mathbf{q}}[n_{1\mathbf{q}},u_{\mathbf{q}}]$ while $Z_{\mathbf{q}}[n_{2\mathbf{q}}]$ remains the same as in a homeotropic cell. The modified partition function now reads

$$\begin{aligned}Z_{\mathbf{q}}[n_{1\mathbf{q}},u_{\mathbf{q}}]=&\int\mathrm{d}n_{1\mathbf{q}}^-\int\mathrm{d}n_{1\mathbf{q}}^+\int\mathrm{d}u_{\mathbf{q}}^-\int\mathrm{d}u_{\mathbf{q}}^+\,\exp(-\beta H_{S\mathbf{q}}[n_{1\mathbf{q}}^\pm,u_{\mathbf{q}}^\pm])\\&\times\int_{n_{1\mathbf{q}}(z=0)=n_{1\mathbf{q}}^-}^{n_{1\mathbf{q}}(z=h)=n_{1\mathbf{q}}^+}\int_{u_{\mathbf{q}}(z=0)=u_{\mathbf{q}}^-}^{u_{\mathbf{q}}(z=h)=u_{\mathbf{q}}^+}\exp(-\beta H_{\mathbf{q}}[u_{\mathbf{q}},n_{1\mathbf{q}}])\,\mathcal{D}u_{\mathbf{q}}(z)\mathcal{D}n_{1\mathbf{q}}(z)\ .\end{aligned} \tag{3.34}$$

The difference between this partition function and the partition function of the homeotropic cell [Eq. (3.14)] is that here integration over all possible surface values of $u_{\mathbf{q}}$ has to be performed while in the former case the surface value of $u_{\mathbf{q}}$ was fixed to 0. This does not pose any conceptual difficulties and the partition function can again be evaluated using the analogy with propagator of two coupled harmonic oscillators

$$\begin{aligned}Z_{\mathbf{q}}[n_{1q},u_q]\propto&\left[\sinh(\Omega_1h)\sinh(\Omega_2h)\right]^{-1/2}\times\Big[\Omega_1\Omega_2\lambda^{-2}A_1^-A_2^-+\chi^{-1}q^2\big(\Omega_1S^2A_1^-\\&+\Omega_2C^2A_2^-\big)+L^{-1}\left(\Omega_1C^2\lambda^{-2}A_1^-+\Omega_2S^2\lambda^{-2}A_2^-\right)+\chi^{-1}L^{-1}q^2\Big]^{-1/2}\\&\times\Big[\Omega_1\Omega_2\lambda^{-2}A_1^+A_2^++L^{-1}\left(\Omega_1C^2\lambda^{-2}A_1^++\Omega_2S^2\lambda^{-2}A_2^+\right)+\chi^{-1}q^2\\&\times\left(\Omega_1S^2A_1^++\Omega_2C^2A_2^+\right)+\chi^{-1}L^{-1}q^2\Big]^{-1/2}\ .\end{aligned} \tag{3.35}$$

Applying the usual decomposition into surface, bulk and interaction terms we extract the interaction part of the fluctuations free energy and thereby the Casimir force. This can be written as

$$\mathcal{F}_{Cas}[u,\delta\mathbf{n}]=\mathcal{F}[n_2;L]+\mathcal{F}_1[n_1,u]+\mathcal{F}_2[n_1,u]+\mathcal{F}_3[n_1,u;L,\chi]\ . \tag{3.36}$$

The first three terms are identical as in homeotropic cell. The last term $\mathcal{F}_3[n_1, u; L, \chi]$ which describes the effect of finite director and layer anchoring strengths becomes more complicated

$$\mathcal{F}_3[n_1,u;L,\chi]=-\frac{k_BTS}{4\pi}\sum_{i=1,2}\int_0^\infty q\,\mathrm{d}q\Big[\Omega_1\Omega_2\lambda^{-2}\Big(\frac{\Omega_1A_2^\mp}{1\pm\cosh(\Omega_1h)}+\frac{\Omega_2A_1^\mp}{1\pm\cosh(\Omega_2h)}\Big)$$
$$+\chi^{-1}q^2\Big(\frac{\Omega_1^2S^2}{1\pm\cosh(\Omega_1h)}+\frac{\Omega_2^2C^2}{1\pm\cosh(\Omega_2h)}\Big)+L^{-1}\lambda^{-2}\Big(\frac{\Omega_1^2C^2}{1\pm\cosh(\Omega_1h)}$$
$$+\frac{\Omega_2^2S^2}{1\pm\cosh(\Omega_2h)}\Big)\Big]\times\Big[\Omega_1\Omega_2\lambda^{-2}A_1^\mp A_2^\mp+\chi^{-1}q^2\Big(\Omega_1S^2A_1^\mp+\Omega_2C^2A_2^\mp$$
$$+L^{-1}\Big)+L^{-1}\lambda^{-2}\Big(\Omega_1C^2A_1^\mp+\Omega_2S^2A_2^\mp\Big)\Big]^{-1}. \tag{3.37}$$

$\mathcal{F}_3$ is a sum of two contributions ($i = 1, 2$) which differ only by sign alternation ($\pm$) in some terms. As the boundary conditions now also affect the layer fluctuations, the correction due to the finite surface anchoring $\mathcal{F}_3[n_1, u; L, \chi]$ is long-range.

The effect of the finite surface tension γ on the Casimir force in free-standing smectic films is shown in Fig. 3.7. We compare the force in a free-standing film to the corresponding force in a homeotropic cell for a specific director anchoring strength $W = 10^{-5}$ J/m^2 (the director anchoring is not essential in this case, and choosing some other value of W leads to very similar results). As it is seen from Fig. 3.7, the

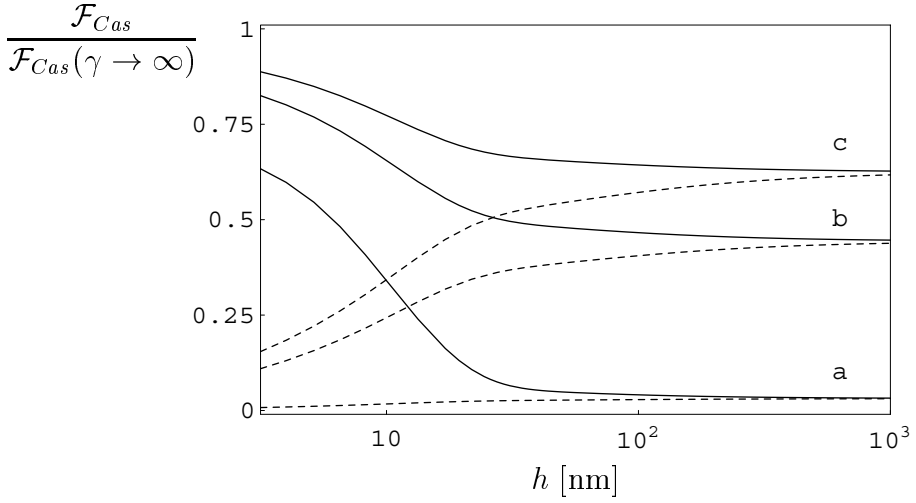

Figure 3.7 Casimir force $\mathcal{F}_{Cas}[u, \delta\mathbf{n}]$ in free-standing film compared to the force in homeotropic cell [$\mathcal{F}_{Cas}(\gamma \to \infty)$] for the director anchoring strength $W = 10^{-5}$ J/m^2, coupling constant $D = 10^5$ N/m^2, and different surface tensions: a) $\gamma = 10^{-2}$ J/m^2, b) $\gamma = 5 \times 10^{-2}$ J/m^2, c) $\gamma = 10^{-1}$ J/m^2. The dashed lines represent $\mathcal{F}_{Cas}^{lay}(\gamma)$.

finite surface tension γ reduces the magnitude of the Casimir force. This effect was

already predicted by Mikheev [128] in a model considering only positional fluctuations of smectic layers u. He obtained the following result for the force (dashed lines in Fig. 3.7): $\mathcal{F}_{Cas}^{lay}(\gamma) = -k_BTS/16\pi h^2\sqrt{K_L'/B}\ \mathrm{Li}_2\left[(\gamma - \sqrt{K_L'B})/(\gamma + \sqrt{K_L'B})\right]^2$, where Li_2 is the dilogarithm function. Our result is in agreement with $\mathcal{F}_{Cas}^{lay}(\gamma)$ in the limit of large thicknesses h where the director-type contributions are not important. At smaller thicknesses h the short-range contributions of director degrees of freedom become important. These contributions are similar in a free-standing film and in a homeotropic cell, therefore the difference between the compared forces is reduced.

It is again instructive to compare the "coupled" Casimir force [Eq. (3.36)] to the "uncoupled" force where the director and layer fluctuations are treated independently: $\mathcal{F}_{Cas}^{unc} = \mathcal{F}_{Cas}^{lay}(\gamma) + 2\mathcal{F}[n_2; L]$. As shown in Fig. 3.8 the net effect of coupling is to increase the magnitude of the force, similar as in the homeotropic cell. The in-

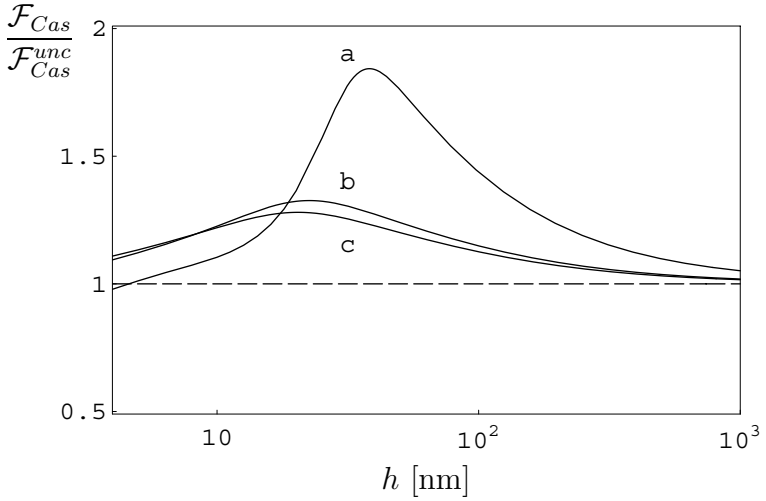

Figure 3.8 Comparison between the "coupled" ($\mathcal{F}_{Cas}[u, \delta\mathbf{n}]$) and "uncoupled" ($\mathcal{F}_{Cas}^{unc}$) Casimir force in a free-standing film for the director anchoring strength $W = 10^{-5}$ J/m^2, coupling constant $D = 10^5$ N/m^2, and different surface tensions: a) $\gamma = 10^{-2}$ J/m^2, b) $\gamma = 5 \times 10^{-2}$ J/m^2, c) $\gamma = 10^{-1}$ J/m^2.

crease is substantial in the case of a small surface tension γ (Fig. 3.8a), while it does not exceed a few ten percents otherwise. This can be explained considering that in a coupled system the fluctuations of surface layers are hindered primarily by surface tension and also indirectly by director anchoring. So even if the surface tension is small the strong director anchoring effectively contributes to the binding of surface layers. This is not the case in a "decoupled" system, where layer fluctuations are independent of director, and therefore the reduction of the magnitude of the force due to weak surface tension γ is stronger. In the case of a strong surface tension the additional effect of director anchoring on surface layers is not significant.

3.3 Casimir force in slightly dilated or compressed cell

In Sec. 3.1 we considered the Casimir force in homeotropic cell whose thickness h corresponded to an integer value of smectic layers with equilibrium period d_0. In this section we study what happens if one of the plates is displaced so that the smectic film is slightly dilated or compressed (Fig. 3.9). If the upper plate is displaced by

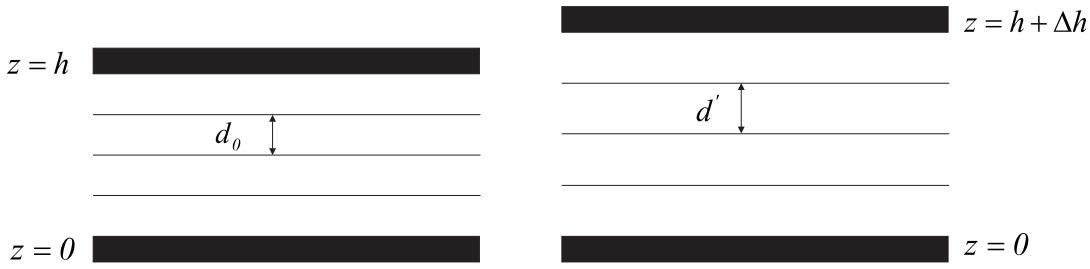

Figure 3.9 Homeotropic cell whose thickness corresponds to an integer number of smectic layers with equilibrium thickness d_0 on the right and slightly stretched homeotropic cell on the left. In the latter case the smectic layers are still equidistant but with increased period d'.

Δh than the equilibrium profile of layer displacement is given by $u_{mf}(z) = z\Delta h/h$. The smectic layers are still equidistant but with increased period d'. For the sake of simplicity, we continue the calculation by considering only fluctuations of smectic layers. This can be justified by the fact that according to Eq. (3.1) the director fluctuations are coupled to transverse gradient of layer displacement $\nabla_\perp u$ which is not affected by the mean-field structure. Therefore we assume that director-layer coupling effects would be similar as in the undeformed homeotropic cell. The possibility of a stress-induced director tilt is here neglected. We furthermore assume that dilation or compression of the cell does not affect the degree of smectic order ψ which is justified when the system is deep in smectic phase where smectic order is well developed.

Starting with elastic free energy of layer deformations

$$F_{lay} = \frac{1}{2}\int \left[B\left(\frac{\partial u}{\partial z}\right)^2 + K_L\left(\nabla_\perp^2 u\right)^2 \right] \mathrm{d}V \tag{3.38}$$

and writing the layer displacement profile as $u(\mathbf{r}) = u_{mf}(z) + \delta u(\mathbf{r})$ we obtain the mean-field free energy

$$F_{lay}^{mf} = \frac{1}{2} BS \frac{\Delta h^2}{h} \tag{3.39}$$

and the Hamiltonian of fluctuations

$$H[\delta u] = \frac{1}{2}\int \left[2B\frac{\Delta h}{h}\frac{\partial(\delta u)}{\partial z} + B\left[\frac{\partial(\delta u)}{\partial z}\right]^2 + K_L\left(\nabla_\perp^2 \delta u\right)^2 \right] \mathrm{d}V\ . \tag{3.40}$$

The mean-field elastic deformation results in a mean-field force given by

$$\mathcal{F}_{mf} = -\frac{\partial F_{lay}^{mf}}{\partial(\Delta h)} = -BS\frac{\Delta h}{h} \,. \tag{3.41}$$

The mean field force is proportional to relative strain $\Delta h/h$ of the smectic film. In the case of dilation ($\Delta h > 0$) the mean field force is attractive while in the case of compression ($\Delta h < 0$) it is repulsive.

The calculation of the Casimir force proceeds in a standard manner. Performing the Fourier transformation $\delta u(\mathbf{r}) = \sum_{\mathbf{q}} \delta u_{\mathbf{q}}(z) \exp(i\mathbf{q}\boldsymbol{\rho})$ we obtain

$$\begin{aligned} H[\delta u] = \sum_{\mathbf{q}} H_{\mathbf{q}} = \frac{1}{2} S \int_0^h \mathrm{d}z \sum_{\mathbf{q}} \Bigg(B \left| \frac{\partial(\delta u_{\mathbf{q}})}{\partial z} \right|^2 + K_L q^4 \left| \delta u_{\mathbf{q}} \right|^2 + \\ + 2B \frac{\Delta h}{h} \frac{\partial(\delta u_{\mathbf{q}})}{\partial z} \, \delta_{\mathbf{q},\mathbf{0}} \Bigg) \,. \end{aligned} \tag{3.42}$$

The boundary conditions at hard plates require $\delta u_{\mathbf{q}}(z=0) = \delta u_{\mathbf{q}}(z=h) = 0$. We now note that the last term in $H[\delta u]$ can be integrated over z and thus transformed into surface term. As we require the fluctations to vanish at the plates, this surface term does not contribute to the Hamiltonian. The partition function is now obtained in usual manner

$$Z[\delta u] = \prod_{\mathbf{q}} Z_{\mathbf{q}} = \prod_{\mathbf{q}} \int_{\delta u_{\mathbf{q}}(z=0)=0}^{\delta u_{\mathbf{q}}(z=h)=0} \exp\left(-\beta H_{\mathbf{q}}\right) \, \mathcal{D}(\delta u_{\mathbf{q}}) \,, \tag{3.43}$$

and can be evaluated using the familiar analogy with the propagator of harmonic oscillator giving

$$Z_{\mathbf{q}} \propto \left[\sinh\left(\sqrt{\frac{K_L}{B}} q^2 h \right) \right]^{-\frac{1}{2}} \,. \tag{3.44}$$

Identifying surface, bulk and interaction parts of partition function we arrive at the interaction free-energy

$$F_{fluc}^{int}[\delta u] = \frac{k_B T S}{4\pi} \int_0^\infty \ln\left(1 - \exp\left(-2\sqrt{K_L/B}\, q^2 h \right) \right) q \, \mathrm{d}q \,. \tag{3.45}$$

This integral can be evaluated analytically leading to the standard layer-induced smectic Casimir force

$$\mathcal{F}_{Cas}^{lay} = -\frac{k_B T S}{16\pi h^2} \zeta_R(2) \sqrt{\frac{B}{K_L}} \,. \tag{3.46}$$

Therefore the conclusion is that the Casimir force in slightly dilated or compressed cell is the same as in nondeformed system.

This was an example of a system with non-trivial equilibrium configuration which did not result in modification of the Casimir force. Here we wish to investigate

this further and draw a more general conclusion about the connection between the equilibrium order parameter profile and the Casimir force. We start formally with a general quadratic free energy expansion

$$F = \int_{z'}^{z''} \left[a(z)\dot{\eta}^2 + 2b(z)\dot{\eta}\eta + c(z)\eta^2 + 2d(z)\dot{\eta} + 2e(z)\eta \right] \mathrm{d}z \ . \tag{3.47}$$

For simplicity we consider a one-dimensional system and the dot denotes the derivative with respect to this dimension z. The mean-field profile of an arbitrary order parameter η is obtained by Euler-Lagrange extremality equation

$$a\ddot{\eta}_{mf} + \dot{a}\dot{\eta}_{mf} + (\dot{b} - c)\eta_{mf} + \dot{d} - e = 0 \ , \tag{3.48}$$

while obeying some boundary conditions $\eta_{mf}(z') = \eta'$ and $\eta_{mf}(z'') = \eta''$. We now introduce fluctuations around the mean-field configuration and write the order parameter as $\eta(z) = \eta_{mf}(z) + \delta\eta(z)$. This leads to Hamiltonian of fluctuations

$$\begin{aligned} H = \int_{z'}^{z''} \Big[& a\delta\dot{\eta}^2 + 2b\delta\dot{\eta}\delta\eta + c\delta\eta^2 + 2d\delta\dot{\eta} + 2e\delta\eta + 2a\dot{\eta}_{mf}\delta\dot{\eta} + \\ & + 2b(\dot{\eta}_{mf}\delta\eta + \eta_{mf}\delta\dot{\eta}) + 2c\eta_{mf}\delta\eta \Big] \mathrm{d}z \ . \end{aligned} \tag{3.49}$$

Performing some per partes integrations, considering the Euler-Lagrange equation for η_{mf} and assuming fixed boundary conditions $[\delta\eta(z') = \delta\eta(z'') = 0]$, the Hamiltonian is considerably simplified

$$H = \int_{z'}^{z''} \Big[a(z)\delta\dot{\eta}^2 + 2b(z)\delta\dot{\eta}\delta\eta + c(z)\delta\eta^2 \Big] \mathrm{d}z \ . \tag{3.50}$$

Here we stress the following important facts. There are no linear terms in the Hamiltonian due to the extremality of mean-field configuration. The coefficients of quadratic terms in Hamiltonian are the same as in the free energy expansion [Eq. (3.47)]. Most importantly, the Hamiltonian of fluctuations does not depend on the mean-field configuration. Because of this a non-trivial mean-field configuration does not influence the Casimir force. We again need to stress that this considerations are valid for quadratic free-energy and fixed boundary conditions which do not allow for fluctuations at boundaries. The studied case of a dilated/compressed smectic cell was just a special example to which the above general conclusion can be applied.

It is important to note that in the case of strained smectic cell the coefficients of quadratic terms $a(z)$ and $c(z)$ in Hamiltonian are independent of coordinate z, whereas the coefficient $b(z)$ is 0. This enabled a straightforward evaluation of the Casimir force. In the last chapter of this thesis, we consider a different type of systems where equilibrium structure dictates a spatial dependence of coefficients of quadratic terms η^2 and $\dot{\eta}^2$. This complicates the calculations considerably and has a strong impact on the Casimir force.

3.4 Importance of Casimir force in smectic-A systems

Here we compare the magnitude of the Casimir force with other interactions present in confined smectic systems. First of all, there is ubiquitous van der Waals interaction between materials with different dielectric and optical properties. For planar geometry the van der Waals force is given by [153]

$$\mathcal{F}_W = -\frac{AS}{6\pi h^3} , \tag{3.51}$$

where A is a Hamaker constant which is a sum of entropic and dispersion terms, $A = A_{\nu=0} + A_{\nu>0}$. For very thin systems the Hamaker constant can be efficiently approximated by

$$A = A_{\nu=0} + A_{\nu>0} = \frac{3}{4} k_B T \left(\frac{\epsilon_1 - \epsilon_2}{\epsilon_1 + \epsilon_2} \right)^2 + \frac{3\hbar\omega_e}{16\sqrt{2}} \frac{(n_1^2 - n_2^2)^2}{(n_1^2 + n_2^2)^{3/2}} , \tag{3.52}$$

where ϵ_1 and n_1 are the static dielectric constant and refractive index of confining boundaries (plates or air), ϵ_2 and n_2 are the static dielectric constant and refractive index of smectic material and $\omega_e = 2\pi \cdot 3 \cdot 10^{15}$ s^{-1} is the plasma frequency taken to be equal for all media. As smectics are anisotropic, the dielectric constant ϵ_2 and refractive index n_2 should be replaced by effective values given by $\bar{\epsilon}_2 = \sqrt{\epsilon_\parallel \epsilon_\perp}$ and $\bar{n}_2 = \sqrt{n_\parallel n_\perp}$, where indices $\parallel$ and $\perp$ denote directions parallel and perpendicular to the layer normal, respectively [171]. At small thicknesses h the dispersion term in Eq. (3.52) dominates. However, at larger thicknesses, above $h \approx 10$ nm, the retardation effects come into play and the dispersion term decays faster, as $1/h^4$. Finally, at very large separations the dispersion term becomes negligible compared to the entropic term, which is unaffected by the retardation effects, and the van der Waals force recovers the $1/h^3$ dependence.

For evaluation of the van der Waals force we use dielectric constants and refractive indices of 8CB smectic liquid crystal at 27° C: $\epsilon_\parallel = 13.6$, $\epsilon_\perp = 5.1$, $n_\parallel = 1.67$, $n_\perp = 1.52$ [172]. The magnitude of the Casimir force is evaluated using the material constants given in the previous sections. We first consider free-standing films where smectic material is bounded by air and hence $\epsilon_1 = 1$, $n_1 = 1$. In a very thin film of $h = 10$ nm the Casimir force is equal to about 625 pN/μm^2 while the van der Waals force is almost ten times larger. At thickness $h = 20$ nm the Casimir force amounts to about 100 pN/μm^2 while the van der Waals force is still about six times larger. We should mention that because we used the Eq. (3.52), which neglects retardation effect, the magnitude of the van der Waals force is here a bit overestimated. In thick films we can neglect the dispersion contribution in the van der Waals force and retain only the entropic part. The ratio between the Casimir and van der Waals force is then given by $\mathcal{F}_{Cas}/\mathcal{F}_W \approx h/\lambda$ where smectic correlation length $\lambda = \sqrt{K_L'/B}$ is

of order of layer thickness ($d_0 \approx 3$ nm). This shows that in thick films the Casimir force dominates over the van der Waals force.

For the homeotropic cell we assume that the smectic material is bounded by glass plates and we use the dielectric constant and refractive index of BK 7 glass: $\epsilon_1 = 6.2$, $n_1 = 1.51$. In this case the van der Waals force is much smaller than in free-standing films, due to the similar dielectric properties of smectic and glass. At cell thickness $h = 10$ nm the Casimir force is equal to about 800 pN/μm^2 while the van der Waals force is about ten times smaller. At thickness $h = 20$ nm the Casimir force amounts to about 145 pN/μm^2 and the van der Waals force is about fifteen times smaller. In thick cells the ratio between the Casimir force and van der Waals force is given by $\mathcal{F}_{Cas}/\mathcal{F}_W \approx 40h/\lambda$, so the Casimir force again dominates.

We can conclude that in thin smectic systems either of the two compared forces, van der Waals or Casimir, can be dominant, depending on specific values of dielectric constants and refractive indexes. In thick smectic systems however, the Casimir force is always dominant due to the slower power law decay.

Further we compare the Casimir force with the force caused by dilation or compression of smectic layers which is given by

$$\mathcal{F}_{mf}^{lay} = -BS\frac{\Delta h}{h} \,. \tag{3.53}$$

Here Δh is the compression or dilation of the system from equilibrium thickness. We take the deformation of about one tenth of layer thickness $\Delta h \approx 0.3$ nm and the compression constant $B = 2 \times 10^6$ N/m^2. For the cell of thickness $h = 10$ nm the mean field force is equal to $\mathcal{F}_{mf}^{lay}/S \approx 60000$ pN/μm^2 and for the thickness $h = 20$ nm it amounts to $\mathcal{F}_{mf}^{lay}/S \approx 30000$ pN/μm^2. This is orders of magnitude stronger than the Casimir force and the ratio between the forces becomes even larger in thick systems. Therefore it is essential to avoid elastic deformations of smectic layers or in some other way eliminate the elastic mean-field force from experimental data when attempting to detect the Casimir interaction.

4

Casimir force in vicinity of smectic-A to smectic-C phase transition

The Casimir force in vicinity of Sm-A to Sm-C phase transition is discussed within the Landau model for chiral smectics described in Sec. 2.2. This model takes into account only director degrees of freedom described by the director tilt vector $\boldsymbol{\xi}$. The director fluctuations slow down critically at the Sm-A – Sm-C transition and represent the so-called soft-mode of the phase transition. On the other hand, the positional smectic order does not change considerably at this transition and therefore the exclusive consideration of director degrees of freedom is somewhat justified. But as we have argued in the previous chapter, the effect of coupling between the smectic layers and the director can not be always neglected. Hence the results presented here are not quantitatively exact but give a qualitative picture of the phenomenon. The use of the simplified model enables us to obtain some results which could not be derived within the full description of smectics and also enable to expose some characteristics of the Casimir force more clearly as in the cumbersome case of coupled director-layer system. Although we employ a model originally designed to describe chiral smectics the application to less complex non-chiral systems is trivial. Therefore the obtained results are valid for a general Sm-A – Sm-C system, either chiral or non-chiral. Some specifics related only to chiral systems will be pointed out explicitly.

We start our analysis with the free energy expansion Eq. (2.11). The Hamiltonian of fluctuations is obtained by expanding the free energy around the equilibrium configuration. We write the order parameter $\boldsymbol{\xi} = (\xi_{\shortparallel}, \xi_{\perp})$ as a sum of a mean-field value and a fluctuating part, $\boldsymbol{\xi} = \boldsymbol{\xi}_0 + \delta\boldsymbol{\xi} = (\xi_{\shortparallel 0} + \delta\xi_{\shortparallel}, \xi_{\perp 0} + \delta\xi_{\perp})$, and insert it into the free energy expression [Eq. (2.11)]. We neglect higher order fluctuation terms, keeping only the harmonic part of the Hamiltonian. From here on, the Sm-A and Sm-C phases have to be treated separately. In the Sm-A phase the mean-field value of the order parameter $\boldsymbol{\xi}$ is equal to 0 as the molecules are oriented perpendicular to the layers. In the Sm-C phase where the molecules are tilted with respect to

the layer normal, the mean-field value of $\xi_{\shortparallel}$ is equal to $\xi_{\shortparallel 0} = \sqrt{\alpha\left(T_c - T\right)/b}$, while $\xi_{\perp 0} = 0$. The Hamiltonian densities of fluctuations then read

$$\begin{aligned} h = & \frac{1}{2}K_3 \left\{ \begin{array}{c} \eta^{-2}\left(\delta\xi_{\shortparallel}^2 + \delta\xi_{\perp}^2\right) \\ \rho^{-2}\delta\xi_{\shortparallel}^2 \end{array} \right\} + \frac{1}{2}K_3 \left[\left(\frac{\partial\left(\delta\xi_{\shortparallel}\right)}{\partial z} \right)^2 + \left(\frac{\partial\left(\delta\xi_{\perp}\right)}{\partial z} \right)^2 \right] \\ & + \frac{1}{2}K \left[\left(\frac{\partial\left(\delta\xi_{\shortparallel}\right)}{\partial x} + \frac{\partial\left(\delta\xi_{\perp}\right)}{\partial y} \right)^2 + \left(\frac{\partial\left(\delta\xi_{\shortparallel}\right)}{\partial y} - \frac{\partial\left(\delta\xi_{\perp}\right)}{\partial x} \right)^2 \right] , \end{aligned} \tag{4.1}$$

where in the first term the upper line corresponds to the Sm-A phase and the lower to the Sm-C phase. We have introduced the correlation lengths of fluctuations: $\eta = \left(\widetilde{a}/K_3 - q_c^2\right)^{-1/2}$ and $\rho = \left[2\left(-\widetilde{a}/K_3 + q_c^2\right)\right]^{-1/2}$.

In the Sm-A phase two degenerate types of fluctuation modes are present, $\delta\xi_{\shortparallel}$ and $\delta\xi_{\perp}$. Both these modes represent the tilt of molecules away from the layer normal and are massive. Upon approaching the phase transition, their mass, which is proportional to $\eta^{-2} = \alpha(T - T_c)$, goes to 0. This means that a uniform tilt of the director over the whole sample does not cost any energy and the phase transition to the smectic-C phase occurs. The tilt fluctuations therefore represent the soft mode of this continuous phase transition. The relaxation time of tilt fluctuations, which is related to their energy, becomes very large and eventually diverges at the phase transition (critical slow down) as shown in Fig. 4.1. In the Sm-C phase the degeneration of fluctuation modes is broken. The fluctuation mode $\delta\xi_{\shortparallel}$ is massive and represents fluctuations of the tilt angle amplitude of molecules. These so-called amplitude fluctuations are analogous to the tilt fluctuations in Sm-A, but their correlation length ρ is different. The so-called phase fluctuations $\delta\xi_{\perp}$ do not change the amplitude of the tilt but represent the rotation of director around the z axis. As a uniform rotation of director in whole sample does not modify the energy of the system, the phase fluctuations are massless with infinite correlation length. This is an example of a zero-energy Goldstone fluctuation mode which tries to restore the continuous symmetry of a high-temperature phase.

In chiral smectics, the fluctuations of orientational order result in inhomogeneity of spontaneous polarization. This leads to the appearance of space charge and Coulomb interaction in the system [161, 173–177]. We are not able to establish the importance of this effect in our systems at present. However, as this interaction is especially prominent in systems with a large value of spontaneous polarization, it is reasonable to assume that our results apply at least for chiral materials with a small value of spontaneous polarization.

4.1 Homeotropic cell

In a homeotropic cell the confining boundaries favor perpendicular orientation of director at the plates ($\boldsymbol{\xi}_S = \mathbf{0}$). This director anchoring can be described by the

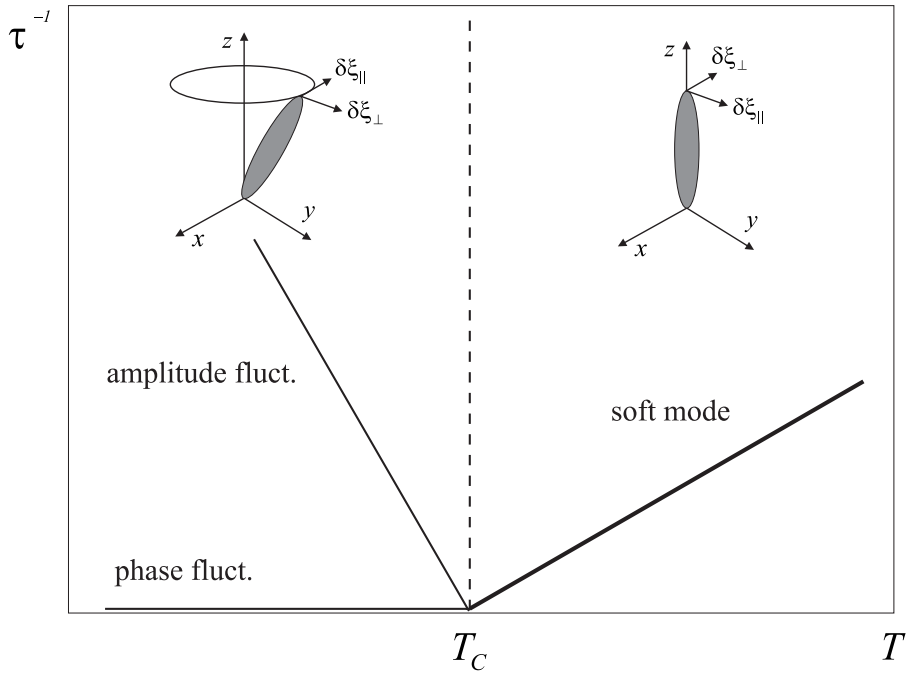

Figure 4.1 Schematic spectrum of fluctuation modes close to Sm-A – Sm-C phase transition [160]. In Sm-A phase ($T > T_C$) there are two degenerate massive fluctuation modes which slow down critically at the transition (soft modes). In Sm-C phase ($T < T_C$) the degeneracy is split into zero-energy Goldstone phase fluctuations and massive amplitude fluctuations. The inverse relaxation time of fluctuation modes τ^{-1} is proportional to their energy.

Rapini-Papoular free-energy model

$$F_S[\boldsymbol{\xi}] = \frac{1}{2}W_1 \int \sin^2(|\boldsymbol{\xi}|)\,\mathrm{d}S_1 + \frac{1}{2}W_2 \int \sin^2(|\boldsymbol{\xi}|)\,\mathrm{d}S_2\ . \tag{4.2}$$

Here we allow for different director anchoring strengths at each of the plates. As a consequence of these boundary conditions, the Sm-A structure in the homeotropic cell can be supercooled below the bulk Sm-A – Sm-C phase transition temperature T_C. In this case the system is in a frustrated state as it can not simultaneously adjust to the imposed boundary conditions and satisfy the tendency of the smectic to tilt. Due to the frustration, the director fluctuations are enhanced. Therefore we have to consider the cases of a "normal" ($T > T_C$) and "supercooled" ($T < T_C$) homeotropic cell separately, even though the equilibrium structure is the same in both cases. When the temperature is lowered to the maximum supercooling value T_{max} the structural transition to a deformed Sm-C structure occurs.

The maximum supercooling temperature T_{max} of course depends on the thickness of the cell. The relation between the critical thickness h_c and the corresponding temperature T_{max}, where the transition occurs, is obtained by minimizing the mean-field free energy of the system. As we expect the transition to be continuous it suffices

to consider only the lowest order terms in free energy expansion [see Eq. (2.11)]

$$F = \frac{1}{2}K_3 \int \left[-(\sqrt{2}\rho)^{-2}\xi_{\shortparallel}^2 + \left(\frac{\mathrm{d}\xi_{\shortparallel}}{\mathrm{d}z}\right)^2 + L_1^{-1}\xi_{\shortparallel}^2\delta(z) + L_2^{-1}\xi_{\shortparallel}^2\delta(z-h) \right] \mathrm{d}V \ . \quad (4.3)$$

Here we introduced the anchoring extrapolation lengths $L_i = K_3/W_i$ and assumed that the mean-field profile depends only on z direction. Applying the Euler–Lagrange formalism we obtain the bulk differential equation

$$\frac{\mathrm{d}^2\xi_{\shortparallel}}{\mathrm{d}z^2} + (\sqrt{2}\rho)^{-2}\xi_{\shortparallel} = 0 \ , \quad (4.4)$$

and the boundary equations

$$\left(\frac{\mathrm{d}\xi_{\shortparallel}}{\mathrm{d}z}\right) - L_1^{-1}\xi_{\shortparallel} \overset{(z=0)}{=} 0 \ , \qquad \left(\frac{\mathrm{d}\xi_{\shortparallel}}{\mathrm{d}z}\right) + L_2^{-1}\xi_{\shortparallel} \overset{(z=h)}{=} 0 \ . \quad (4.5)$$

The solution of the bulk equation is given by $\xi_{\shortparallel}(z) = C_1 \sin(z/\sqrt{2}\rho) + C_2 \cos(z/\sqrt{2}\rho)$. Considering the boundary conditions we obtain a system of two equations for coefficients C_1 and C_2

$$\frac{L_1}{\sqrt{2}\rho}C_1 - C_2 = 0 \ , \quad (4.6)$$

$$\left[\frac{L_2}{\sqrt{2}\rho} + \tan\left(\frac{h}{\sqrt{2}\rho}\right)\right] C_1 + \left[1 - \frac{L_2}{\sqrt{2}\rho}\tan\left(\frac{h}{\sqrt{2}\rho}\right)\right] C_2 = 0 \ . \quad (4.7)$$

This system has a nontrivial solution only if the determinant of coefficients is 0, which finally leads us to the relation

$$h_c = \sqrt{2}\rho \operatorname{arccot}\left(\frac{L_1 L_2 - (\sqrt{2}\rho)^2}{\sqrt{2}\rho(L_1 + L_2)}\right) \ . \quad (4.8)$$

Here the temperature dependence hides in correlation length $\rho = [2\alpha(T_c - T_{max})]^{-1/2}$. For the limiting case of the infinitely strong anchoring ($L_1 = 0$, $L_2 = 0$) the critical thickness is equal to

$$h_c = \sqrt{2}\pi\rho \ . \quad (4.9)$$

The transition from the Sm-A to the Sm-C structure in the homeotropic cell is analogous to the Fréedericksz transition in a nematic homeotropic cell [178]. While the Fréedericksz transition is driven by the quadratic coupling between an external magnetic field and the director, in our case the transition is induced by an "internal", temperature dependent, smectic field. We consider only the case of $h < h_c$ (or $T > T_{max}$), where the equilibrium structure between plates is a homogeneous Sm-A. The problem of the Casimir force in deformed Sm-C structure ($h > h_c$ or $T < T_{max}$) belongs to the class of inhomogeneous systems, some of which are addressed in the next chapter.

4.1.1 Casimir force above T_c

The Casimir force in the Sm-A homeotropic cell above the bulk phase transition temperature T_c can be obtained by following a standard procedure. First the fluctuating fields are Fourier transformed, $\delta\xi_{\shortparallel,\perp}(\mathbf{r}) = \sum_{\mathbf{q}} \widetilde{\xi}_{\shortparallel,\perp}(\mathbf{q},z)\exp(i\mathbf{q}\boldsymbol{\rho})$, and the Hamiltonian is reduced to an ensemble of independent harmonic oscillators, $H = \sum_{\mathbf{q}} \left(H_{\mathbf{q}}[\widetilde{\xi}_{\shortparallel}] + H_{\mathbf{q}}[\widetilde{\xi}_{\perp}] \right)$. In the Sm-A phase, the fluctuation modes $\widetilde{\xi}_{\shortparallel}$ and $\widetilde{\xi}_{\perp}$ are degenerate so the Hamiltonians $H_{\mathbf{q}}[\widetilde{\xi}_{\shortparallel}]$ and $H_{\mathbf{q}}[\widetilde{\xi}_{\perp}]$ are identical and read

$$\begin{aligned} H_{\mathbf{q}}[\widetilde{\xi}_{\shortparallel,\perp}] = \frac{1}{2}K_3 S \int_0^h \left[\left(\eta^{-2} + \frac{K}{K_3}q^2 \right) \widetilde{\xi}^{\,2}_{\shortparallel,\perp} + \left(\frac{\mathrm{d}\widetilde{\xi}_{\shortparallel,\perp}}{\mathrm{d}z} \right)^2 \right] \mathrm{d}z \\ + \frac{1}{2}K_3 S \left(L_1^{-1}\widetilde{\xi}^{-\,2}_{\shortparallel,\perp} + L_2^{-1}\widetilde{\xi}^{+\,2}_{\shortparallel,\perp} \right) , \end{aligned} \tag{4.10}$$

where $\widetilde{\xi}^{-}_{\shortparallel,\perp} = \widetilde{\xi}_{\shortparallel,\perp}(z=0)$, and $\widetilde{\xi}^{+}_{\shortparallel,\perp} = \widetilde{\xi}_{\shortparallel,\perp}(z=h)$. The partition function for harmonic oscillators can be readily evaluated and we obtain

$$Z_{\mathbf{q}}[\widetilde{\xi}_{\shortparallel,\perp}] \propto \left[\frac{L_1^{-1}L_2^{-1} + p^2}{p(L_1^{-1} + L_2^{-1})} \, \sinh(ph) \, + \, \cosh(ph) \right]^{-\frac{1}{2}} , \tag{4.11}$$

where we introduced notation $p^2 = \eta^{-2} + \frac{K}{K_3}q^2$. Having identified and eliminated the bulk and surface contribution in partition function by the usual factorization we acquire the interaction part of free energy

$$F^{int}_{fluc} = \frac{k_B T S}{2\pi}\frac{K_3}{K}\int_{1/\eta}^{\infty} \ln\left(1 - \frac{(p - L_1^{-1})(p - L_2^{-1})}{(p + L_1^{-1})(p + L_2^{-1})}\exp(-2ph) \right) p \, \mathrm{d}p \, , \tag{4.12}$$

and by differentiation the Casimir force

$$\mathcal{F}_{Cas} = -\frac{k_B T S}{\pi}\frac{K_3}{K}\int_{1/\eta}^{\infty} \frac{p^2 \, \mathrm{d}p}{\frac{(p+L_1^{-1})(p+L_2^{-1})}{(p-L_1^{-1})(p-L_2^{-1})}\exp(2ph) - 1} \, . \tag{4.13}$$

This result is analogous to the short-range Casimir force induced by pure director fluctuation modes in the coupled director-layer system [Eqs. (3.26, 3.31)] which was discussed in the previous chapter. A new feature here is the generalization to asymmetric anchoring conditions with anchoring strength W_1 at one plate and W_2 at the other. Therefore we here focus on specifics of anchoring effect on the Casimir force.

Some profiles of the Casimir force for different sets of anchoring strengths are shown in Fig. 4.2. Presented is the reduced amplitude of the Casimir force as compared to the force in the case of symmetric infinitely strong anchoring conditions [see Eq. (3.31)]:

$$R = \frac{\mathcal{F}_{Cas}(L_1, L_2, h, \eta)}{\mathcal{F}_{Cas}(L_1 = 0, L_2 = 0, h, \eta)} \, . \tag{4.14}$$

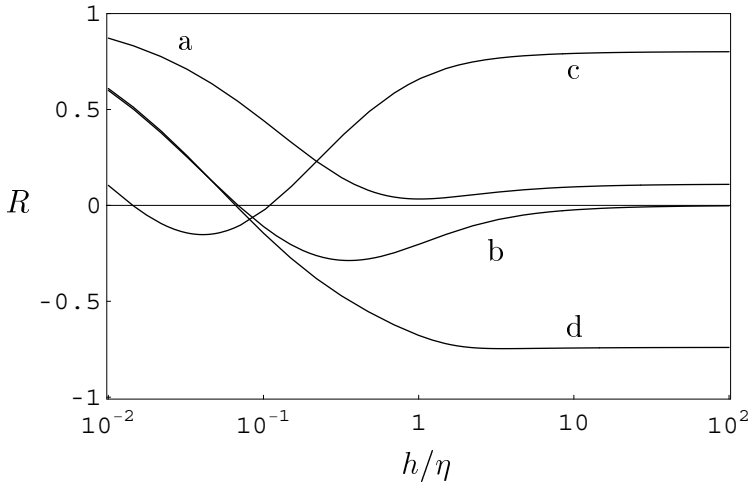

Figure 4.2 Casimir force in the homeotropic cell for $T > T_c$. The dependence of the reduced amplitude R on the parameter h/η is presented for different sets of anchoring strengths: a) $L_1/\eta = 0.5$, $L_2/\eta = 0.5$; b) $L_1/\eta = 1$, $L_2/\eta = 0.05$; c) $L_1/\eta = 0.1$, $L_2/\eta = 0.01$; d) $L_1/\eta = 10$, $L_2/\eta = 0.05$.

The profiles in Fig. 4.2 can be explained by the interplay of four characteristic lengths: the distance between plates h, the correlation length of fluctuations η, and the two extrapolation lengths L_1 and L_2. It is known from the previous studies of the Casimir effect [121] that in the case of symmetric boundary conditions (strong-strong or weak-weak anchoring at the plates) the force is attractive, whereas in the case of antisymmetric boundary conditions (strong-weak anchoring at the plates) the force is repulsive. In our system it is not very obvious which parameters determine the effective anchoring strengths. It seems (Fig. 4.2) that there are actually two different regimes. When $h/\eta < 1$ the effective anchoring strengths are determined by ratios L_1/h and L_2/h. In the case of $L_i/h < 1$ the anchoring is effectively strong, and correspondingly if $L_i/h > 1$ the anchoring is effectively weak. In the second regime, where $h/\eta > 1$, the effective anchoring strengths are determined by parameters L_1/η and L_2/η, using the same criteria as in the first regime. This can be explained if we recall that the anchoring is effectively strong when the interaction between the substrate and liquid crystal is stronger than the internal interaction in liquid crystal [111]. The strength of the surface interaction is measured by the extrapolation lengths L_i. The internal interaction includes two contributions, as can be seen from Eq. (4.1): the massive contribution whose strength is characterized by η^{-1}, and the elastic contribution which scales as h^{-1}. At small h/η the elastic contribution dominates, and the effective strength of the anchoring is obtained by comparing parameters L_i and h. At large h/η the massive contribution is dominant, and consequently the effective strength of the anchoring depends on parameters L_i and η.

All the lengths in Fig. 4.2 are scaled by the correlation length η. The values of parameters L_i/h change by varying the parameter h/η. Therefore the Casimir force in the first regime ($h/\eta < 1$) exhibits cross-overs from attractive to repulsive and vice versa [Figs. 4.2(b)-(d)]. The parameters L_i/η are fixed, therefore the character of the force in the second regime ($h/\eta > 1$) does not change. It should be kept in mind that η is temperature dependent, and that the character of the force is consequently also temperature dependent. At large separations ($h/\eta \gg 1$) the reduced amplitude R saturates at a constant value. This shows that in this regime the force has the same functional form as the leading term in the case of infinitely strong anchoring, which decays as $\exp(-2h/\eta)/h$. The saturation value is the largest when the anchoring at the plates is either very strong or very weak. It can be shown that in the case of very strong anchoring at both plates ($L_1/\eta, L_2/\eta \ll 1$) the reduced amplitude saturates at $R = 1 - 2(L_1/\eta + L_2/\eta)$ [Fig. 4.2(c)], whereas in the case of very weak anchoring at both plates ($L_1/\eta, L_2/\eta \gg 1$) the saturation value is $R = 1 - 2(\eta/L_1 + \eta/L_2)$. In the antisymmetric case where the anchoring at one plate is very weak ($L_1/\eta \gg 1$) and at the other very strong ($L_2/\eta \ll 1$) the reduced amplitude saturates at $R = -1 + 2(\eta/L_1 + L_2/\eta)$ [Fig. 4.2(d)]. The behavior of the force at large separations is substantially modified in the case of $L_i/\eta = 1$, where the anchoring at one or both plates is neither strong nor weak. It can be shown that in the first case the force decays as $\exp(-2h/\eta)/h^2$ and consequently the reduced amplitude goes to zero at $h/\eta \gg 1$ [Fig. 4.2(b)]. In the case of $L_1/\eta = L_2/\eta = 1$ the force decays even faster – as $\exp(-2h/\eta)/h^3$.

4.1.2 Casimir force in frustrated system ($T_{max} < T < T_c$)

The equilibrium structure in frustrated homeotropic cell is still homogeneous Sm-A. Therefore the starting point of our calculation is again Hamiltonian (4.10). However, if $T < T_c$ the value of η^{-2} is negative. The parameter $p^2 = \eta^{-2} + \frac{K}{K_3} q^2$ can now be either positive or negative depending on the value of q. The calculation of partition function is therefore split into two parts. If $p^2 > 0$ then $Z_{\mathbf{q}}$ is the same as in the non-frustrated case

$$Z_{\mathbf{q}}[\widetilde{\xi}_{\shortparallel,\perp}] \propto \left[\frac{L_1^{-1} L_2^{-1} + p^2}{p(L_1^{-1} + L_2^{-1})} \, \sinh(ph) + \cosh(ph) \right]^{-\frac{1}{2}} , \tag{4.15}$$

whereas in the case of $p^2 < 0$ it is equal to

$$Z_{\mathbf{q}}[\widetilde{\xi}_{\shortparallel,\perp}] \propto \left[\frac{L_1^{-1} L_2^{-1} + p^2}{p(L_1^{-1} + L_2^{-1})} \, \sin(|p|h) + \cos(|p|h) \right]^{-\frac{1}{2}} . \tag{4.16}$$

The bulk and surface terms can be easily removed from $Z_{\mathbf{q}}$ for $p^2 > 0$, while in the case of $p^2 < 0$ the partition function contains only pure interaction contribution.

The interaction free energy of fluctuations is now given by

$$\begin{aligned} F_{fluc}^{int} = & \frac{k_B T S}{2\pi}\frac{K_3}{K}\int_0^\infty \ln\left(1-\frac{(p-L_1^{-1})(p-L_2^{-1})}{(p+L_1^{-1})(p+L_2^{-1})}\exp(-2ph)\right) p\,\mathrm{d}p \\ & + \frac{k_B T S}{2\pi}\frac{K_3}{K}\int_0^{(\sqrt{2}\rho)^{-1}} \ln\left(\frac{L_1^{-1}L_2^{-1}-p^2}{p(L_1^{-1}+L_2^{-1})}\,\sin(ph)\,+\,\cos(ph)\right) p\,\mathrm{d}p\,, \end{aligned} \tag{4.17}$$

and after the differentiation the Casimir force, consisting of two terms $\mathcal{F}_{Cas} = \mathcal{F}_1 + \mathcal{F}_2$, reads

$$\begin{aligned} \mathcal{F}_{Cas} = & -\frac{k_B T S}{\pi}\frac{K_3}{K}\Bigg[\int_0^\infty \frac{p^2\,\mathrm{d}p}{\frac{(p+L_1^{-1})(p+L_2^{-1})}{(p-L_1^{-1})(p-L_2^{-1})}\exp(2ph)-1} \\ & + \frac{1}{2}\int_0^{(\sqrt{2}\rho)^{-1}} \frac{(L_1^{-1}L_2^{-1}-p^2)\cot(ph)-p(L_1^{-1}+L_2^{-1})}{(L_1^{-1}L_2^{-1}-p^2)+p(L_1^{-1}+L_2^{-1})\cot(ph)}\,p^2\,\mathrm{d}p\Bigg]\,. \end{aligned} \tag{4.18}$$

Note that $(\sqrt{2}\rho)^{-2} = -(\eta^{-2})$. It is instructive to consider the Casimir force in the limiting case of infinitely strong anchoring ($L_1 = 0$, $L_2 = 0$)

$$\mathcal{F}_{Cas}(L_1 = 0, L_2 = 0) = -\frac{k_B T S}{4\pi}\frac{K_3}{K}\left[\frac{\zeta(3)}{h^3} + 2\int_0^{(\sqrt{2}\rho)^{-1}} \cot(ph)p^2\,\mathrm{d}p\right]\,. \tag{4.19}$$

The first term in $\mathcal{F}_{Cas}$ has the typical form of the Casimir interaction induced by massless fluctuation modes with infinite correlation lengths. This term is actually the same as the interaction induced by director fluctuations in the homeotropic nematic cell. Its dependence on anchoring conditions was analyzed in detail in Refs. [117, 137]. Here we reproduce these results in Fig. 4.3 where the ratio R between the term $\mathcal{F}_1$ in case of finite director anchoring and infinitely strong anchoring (h^{-3} force) is given

$$R = \frac{\mathcal{F}_1(L_1, L_2 \neq 0; \tilde{h})}{\mathcal{F}_1(L_1 = L_2 = 0; \tilde{h})}\,. \tag{4.20}$$

Here $\tilde{h} = h/\sqrt{L_1 L_2}$ is the scaled thickness, and the ratio is plotted for $L_2/L_1 =$ 1,10,10^2,10^3,10^4,10^5,10^6. Finite anchoring strengths in general reduce the magnitude of the Casimir force. If the extrapolation lengths L_1 and L_2 are similar (symmetric anchoring) the force is attractive at all thicknesses. In case of dissimilar boundary conditions (asymmetric anchoring) the force exhibits crossovers from attraction to repulsion and vice versa. This can be explained by noting that effective anchoring strength is determined by parameters L_i/h which give the ratio of surface and elastic energies of liquid crystal. In case of $L_i/h < 1$ the anchoring is effectively strong and in case of $L_i/h > 1$ the anchoring is effectively weak. The limits $\tilde{h} \to \infty$ and $\tilde{h} \to 0$ correspond to very strong and very weak effective anchoring, respectively. Therefore the reduction factor in these limits is equal to $R = 1$. In the intermediate range one

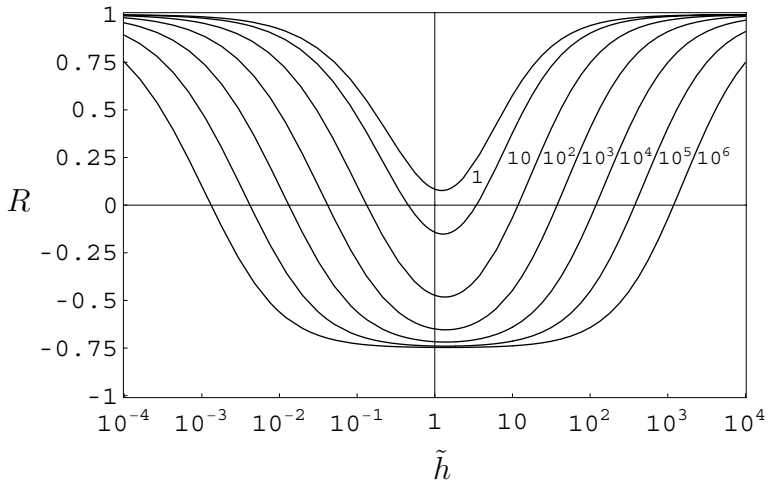

Figure 4.3 Reduction factor $R = \mathcal{F}_1(L_1, L_2 \neq 0; \tilde{h})/\mathcal{F}_1(L_1 = L_2 = 0; \tilde{h})$ for various anchoring parameters $L_2/L_1 = 1,10,10^2,10^3,10^4,10^5,10^6$ [117, 137].

of the extrapolation lengths can be shorter and the other larger than h. This gives mixed boundary conditions (strong–weak) which results in repulsive Casimir force.

The characteristics of the second term in $\mathcal{F}_{Cas}$ are shown in Fig. 4.4 by comparing it to the same reference force as $\mathcal{F}_1$. The reduction factor is now defined as

$$Q = \frac{\mathcal{F}_2(L_1, L_2, \rho, h)}{\mathcal{F}_1(L_1 = L_2 = 0; h)} \, . \tag{4.21}$$

The term $\mathcal{F}_2$ is for small values of h/ρ attractive and of about the same order

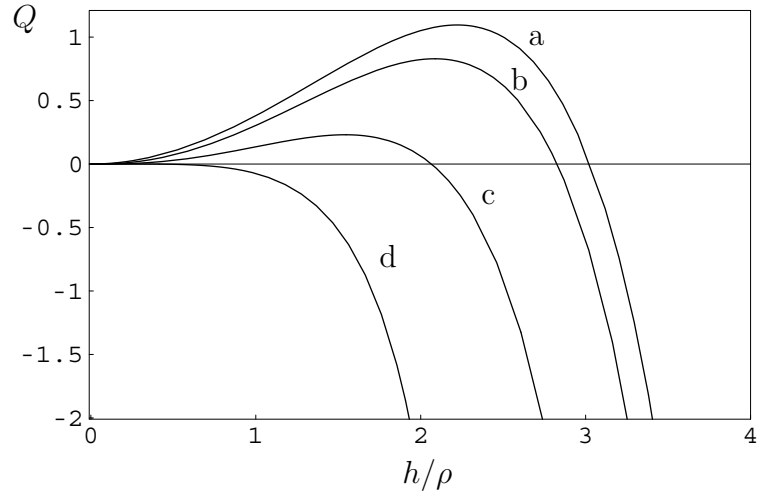

Figure 4.4 Reduction factor $Q = \mathcal{F}_2(L_1, L_2, \rho, h)/\mathcal{F}_1(L_1 = L_2 = 0; h)$ for various anchoring parameters: a) $L_1/\rho = 0, L_2/\rho = 0$; b) $L_1/\rho = 0.1, L_2/\rho = 0.1$; c) $L_1/\rho = 0.05, L_2/\rho = 1$; d) $L_1/\rho = 0.05, L_1/\rho = 10$.

of magnitude as $\mathcal{F}_1$. Then with increasing h/ρ it becomes repulsive and finally

diverges at the structural transition to the deformed Sm-C structure. The critical thickness, and consequently also the maximum magnitude of attraction, increases with stronger anchoring as described by Eq. (4.8).

It is also illustrative to present temperature dependence of the Casimir force in a homeotropic smectic cell at some fixed thickness h. Above the bulk phase transition temperature T_c the force is given by Eq. (4.13) and below T_c in a frustrated system the force is described by Eqs. (4.18 and 4.19). The temperature profile is presented in Fig. 4.5 for various anchoring parameters. The behavior of the force in the

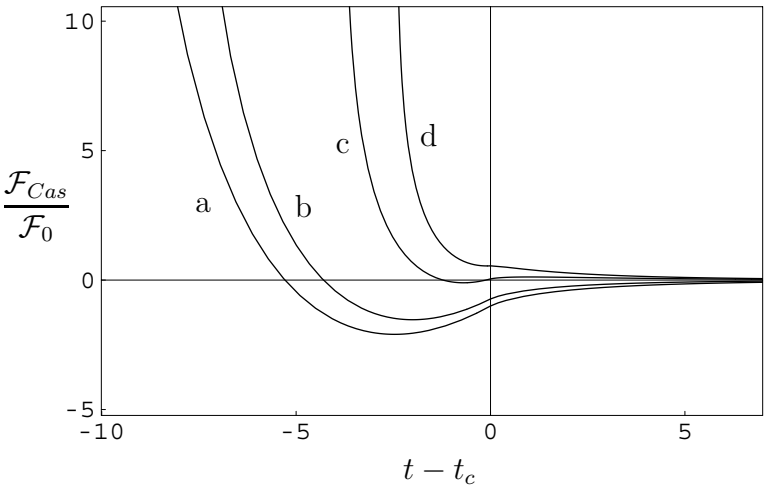

Figure 4.5 Temperature profile of the Casimir force in a homeotropic cell. We introduced a unitless temperature $t = \alpha h^2 T/K_3$. The amplitude of the force is given in the natural unit $\mathcal{F}_0 = |\mathcal{F}_1(L_{1,2} = 0)| = k_B T S K_3 \zeta_R(3)/4\pi K h^3$ (we neglect a weak temperature dependence of $\mathcal{F}_0$). The force is plotted for different sets of anchoring strengths: a) $L_1/h = 0$, $L_2/h = 0$; b) $L_1/h = 0.1$, $L_2/h = 0.01$; c) $L_1/h = 1$, $L_2/h = 0.05$; d) $L_1/h = 10$, $L_2/h = 0.05$.

regime $t > t_c$ was commented along with Fig. 4.2. On supercooling the system ($t < t_c$) the force approaches a local minimum, and eventually it diverges at the structural transition to the Sm-C structure. The stronger the anchoring at the plates, the deeper the supercooling limit, and the more pronounced the minimum. The repulsive divergence of the fluctuation-induced force is characteristic for second order transitions and is logarithmic. Close to the transition the leading term diverges as $\mathcal{F}_{Cas}^{div} \propto \ln\left(\sin(h/\sqrt{2}\rho)\right)$ (in the case of strong anchoring). The behavior of this system is analogous to the nematic Freedericksz cell [121], as we have already mentioned.

To summarize, the frustration enhanced fluctuations affect the Casimir force in two ways. Firstly, the force becomes long-range and behaves like as the modes were massless. Secondly, there is an additional term present due to frustration which results in repulsive logarithmic divergence of the force at the transition. This is

however not all. As we have discussed in the Sec. 2 the free energy of a bulk reference system has to be subtracted from the total free energy of a confined system in order to obtain the interaction contribution. But in the case of a frustrated system, where $T < T_c$, the bulk reference is no longer in Sm-A but in Sm-C phase. In the Sm-C phase we have massive amplitude fluctuations with correlation length ρ and massless phase fluctuations with infinite correlation length [Eq. (4.1)]. The reference bulk free energy of fluctuations is then given by

$$F_{fluc}^{bulk}[\text{Sm-C}] = \frac{k_B T S}{4\pi}\left[\int_0^\infty \ln\left(\exp\left(\sqrt{Kq^2/K_3+\rho^{-2}}h\right)\right)\, q\,\mathrm{d}q + \int_0^\infty \ln\left(\exp\left(\sqrt{K/K_3}qh\right)\right)\, q\,\mathrm{d}q\right]. \tag{4.22}$$

In frustrated Sm-A cell the bulk term in fluctuations free energy is equal to

$$F_{fluc}^{bulk}[\text{Sm-A}] = \frac{k_B T S}{2\pi}\int_{\sqrt{-\frac{K_3}{K}\eta^{-2}}}^\infty \ln\left(\exp\left(\sqrt{\eta^{-2}+Kq^2/K_3}h\right)\right)\, q\,\mathrm{d}q\,. \tag{4.23}$$

Their difference, contributing to the interaction, is then equal to

$$\Delta F_{fluc}^{bulk} = \frac{k_B T S h}{4\pi}\left[2\int_{\sqrt{\frac{K_3}{2K}\rho^{-2}}}^\infty \sqrt{\frac{K}{K_3}q^2-\frac{1}{2}\rho^{-2}}\, q\,\mathrm{d}q - \int_0^\infty \sqrt{\frac{K}{K_3}}\, q^2\mathrm{d}q - \int_0^\infty \sqrt{\frac{K}{K_3}q^2+\rho^{-2}}\, q\,\mathrm{d}q\right], \tag{4.24}$$

using the relation $-\eta^{-2} = \rho^{-2}/2$. These integrals are unfortunately divergent and so is their difference. This is a consequence of the continuum model, where also fluctuations with infinitely large wave-vectors q are allowed. We first try to avoid the divergence by introducing large wave vector cut-off $q_{max} = Q$. This leads to the force

$$\mathcal{F}_3 = -\frac{\Delta F_{fluc}^{bulk}}{\partial h} = -\frac{k_B T S}{4\pi}\left[\frac{2}{3}\sqrt{\frac{K}{K_3}}\, Q^3\left(1-\frac{K_3}{2KQ^2\rho^2}\right)^{3/2} - \sqrt{\frac{K}{K_3}}\frac{Q^3}{3} - \frac{Q^2\sqrt{1+\frac{KQ^2\rho^2}{K_3}}}{3\rho} + \frac{K_3}{3K\rho^3}\left(1-\sqrt{1+\frac{KQ^2\rho^2}{K_3}}\right)\right]. \tag{4.25}$$

Let us now evaluate the parameters appearing in this expression. Using the material constants $\alpha = 4\times10^4$ N/m^{2}K and $K_3 = 10^{-11}$ N the correlation length $\rho = [2\alpha(T_c - T)/K_3]^{-1/2}$ can vary from approximately 100 nm very close to T_c to about 10 nm when 1 K below the T_c [160]. The value of Q is estimated by $2\pi/l$, where $l \sim 0.1$ nm is the transversal dimension of a liquid crystal molecule. This gives $Q \sim 10^{11}$ m^{-1}.

As $Q \gg \rho^{-1}$ the force $\mathcal{F}_3$ can be simplified to

$$\mathcal{F}_3 = \frac{k_B T S}{4\pi}\left(\sqrt{\frac{K_3}{K}}\frac{Q}{\rho^2} - \frac{K_3}{3K\rho^3}\right) + \mathcal{O}\left(\frac{1}{Q\rho^4}\right) . \tag{4.26}$$

It is thickness independent and consists of a dominant repulsion term, which depends linearly on the cut-off value Q, a small attraction term independent of Q, and lower order terms which go to zero in the limit of $Q \to \infty$. The magnitude of ratio between $\mathcal{F}_3$ and the reference force $\mathcal{F}_1(L_{1,2} = 0)$ is estimated by Qh^3/ρ^2. For thin cells of thickness $h \sim 10$ nm, which are relevant for the frustrated system, this ratio varies from $10 - 10^3$, depending on value of ρ. Therefore one could conclude that term $\mathcal{F}_3$ represents a dominant contribution to the Casimir force in a frustrated homeotropic cell, except very close to the divergence. However we should stress that our regularization procedure, by introducing a cut-off $q_{max} = Q$, is somewhat oversimplified and can not give more than a qualitative picture. Indeed the final result linearly depends on the cut-off value Q which is a signature of a poor regularization procedure. Therefore we try to introduce a slightly more sophisticated regularization. We use exponential cut-off which smoothly discards the contribution of large wave-vectors. Now the following integrals have to be evaluated

$$\begin{aligned}\Delta F^{bulk}_{fluc} = \frac{k_B T S h}{4\pi}\lim_{\lambda\to 0}\Bigg[2\int_{\sqrt{\frac{K_3}{2K}\rho^{-2}}}^{\infty}\sqrt{\frac{K}{K_3}q^2 - \frac{1}{2}\rho^{-2}}\, q\, \exp(-\lambda^2 q^2)\,\mathrm{d}q - \\ - \int_0^{\infty}\sqrt{\frac{K}{K_3}}\, q^2\, \exp(-\lambda^2 q^2)\,\mathrm{d}q - \int_0^{\infty}\sqrt{\frac{K}{K_3}q^2 + \rho^{-2}}\, q\, \exp(-\lambda^2 q^2)\,\mathrm{d}q\Bigg] .\end{aligned} \tag{4.27}$$

This gives

$$\begin{aligned}\Delta F^{bulk}_{fluc} = \frac{k_B T S h}{4\pi}\sqrt{\frac{K}{K_3}}\frac{\sqrt{\pi}}{4\lambda^3}\lim_{\lambda\to 0}\Bigg[2\exp\left(-\frac{\lambda^2 K_3}{2K\rho^2}\right) - 1 - 2\sqrt{\frac{K_3}{K}}\frac{\lambda}{\sqrt{\pi}\rho} \\ - \exp\left(\frac{\lambda^2 K_3}{K\rho^2}\right)\,\mathrm{erfc}\left(\frac{\lambda}{\rho}\sqrt{\frac{K_3}{K}}\right)\Bigg] ,\end{aligned} \tag{4.28}$$

where $\mathrm{erfc}(x)$ is the complementary error function $\mathrm{erfc}(x) = 1 - \mathrm{erf}(x)$. For small arguments $\mathrm{erfc}(x)$ can be expanded in series

$$\mathrm{erfc}(x \ll 1) = 1 - \frac{2x}{\sqrt{\pi}} + \frac{2x^3}{3\sqrt{\pi}} - \frac{x^5}{5\sqrt{\pi}} + \dots . \tag{4.29}$$

Using this expansion we obtain the force

$$\mathcal{F}_3 = \frac{k_B T S}{4\pi}\frac{K_3}{K}\lim_{\lambda\to 0}\left[\sqrt{\frac{K}{K_3}}\frac{\sqrt{\pi}}{2\lambda\rho^2} - \frac{1}{3\rho^3}\right] . \tag{4.30}$$

The $\mathcal{F}_3$ term now consists of a repulsive divergent term and a small attraction term. This result is qualitatively the same as Eq. (4.26) with the inverse cut-off length λ^{-1} taking the role of the maximum wave vector number Q.

At present we still lack the physical interpretation of the $\mathcal{F}_3$ term characteristics. But although we are unable to properly regularize the $\mathcal{F}_3$ contribution to the Casimir force this does not pose any practical difficulties. The force scanning techniques, such as atomic force microscopy and surface force apparatus measurements, actually measure the difference of the force at different thicknesses h and not the absolute magnitude. So the thickness independent contributions to the interaction, such as is $\mathcal{F}_3$, are irrelevant.

Furthermore, as the bulk reference is in Sm-C phase, there is also the mean-field force present in a frustrated Sm-A homeotropic cell. The mean-field force is a consequence of a difference between mean-field free energies of structure between plates (Sm-A) and Sm-C reference as given by Eq. (2.11) and is equal to

$$\mathcal{F}_{mf} = (f_C - f_A)S = -\frac{1}{4}\frac{\alpha^2}{b}(T_c - T)^2 S \,, \tag{4.31}$$

where f_C and f_A are free energy densities of the Sm-C and Sm-A phases. The mean-field force is attractive and thickness independent. The comparison between the mean-field force and the Casimir force [Eq. (4.19)] can be performed using the following set of the material constants: $\alpha = 4 \times 10^4$ N/m^{2}K, $b = 10^6$ N/m^2, $K_3 = K = 10^{-11}$ N, $T_c = 368$ K, [160] and taking the thickness of the cell to be $h = 20$ nm. In the limit of strong anchoring the Sm-A structure could be supercooled to about $T_{max} \approx T_c - 5$ K. Very close to T_c the Casimir force is dominant as the mean-field force is very small there. By supercooling the system the mean-field force becomes larger and prevails over the Casimir force. Even very close to the repulsive divergence the Casimir force does not amount to more than a few ten percent of the mean-field force. However as the mean-field force is thickness independent it can not be measured by differential force scanning techniques, as was mentioned earlier, and would not hinder the detection of the Casimir force.

4.2 Free-standing films

In free-standing films, the smectic material is bounded by free surfaces in contact with air. In our simple model we assume that preferential orientation of director at the free surfaces matches the orientation in the bulk interior of the film. This corresponds to an effective internal anchoring. The mean-field structure of the film is therefore in this model homogeneous. The anchoring is the same at both free surfaces which gives symmetric boundary conditions. We consider two cases: a free-standing Sm-A film ($T > T_c$) and a free-standing Sm-C film ($T < T_c$).

In Sm-A free-standing film the equilibrium bulk value of order parameter $\boldsymbol{\xi}$ is equal to 0 which is also the preferred value at the surface. The surface free energy is then modeled by

$$F_S[\boldsymbol{\xi}] = \frac{1}{2} K_3 L^{-1} \left[\int \sin^2(|\boldsymbol{\xi}|)\, \mathrm{d}S_1 + \frac{1}{2} \int \sin^2(|\boldsymbol{\xi}|)\, \mathrm{d}S_2 \right] . \tag{4.32}$$

The anchoring is at both surfaces characterized by extrapolation length L. The Casimir force is calculated in the same way as in the homeotropic Sm-A cell above T_c and is given by

$$\mathcal{F}_{Cas} = -\frac{k_B T S}{\pi} \frac{K_3}{K} \int_{1/\eta}^{\infty} \frac{p^2\, \mathrm{d}p}{\frac{(p+L^{-1})^2}{(p-L^{-1})^2} \exp(2ph) - 1} . \tag{4.33}$$

This a typical short-range contribution of massive fluctuation modes with correlation length η. Its dependence on anchoring parameters was analyzed in Fig. 3.2.

In Sm-C film the equilibrium bulk value of tilt is equal to $\xi_{\shortparallel 0} = \sqrt{\alpha(T_c - T)/b}$ and equilibrium value of phase parameter $\xi_\perp = 0$. In our model of matching bulk and surface order the director anchoring free energy is given by

$$F_S[\boldsymbol{\xi}] = \frac{1}{2} K_3 \sum_{i=1,2} \left[L_{\shortparallel}^{-1} \int \sin^2(\xi_{\shortparallel} - \xi_{\shortparallel 0})\, \mathrm{d}S_i + L_\perp^{-1} \int \sin^2(\xi_\perp)\, \mathrm{d}S_i \right] . \tag{4.34}$$

Here we allow for different anchoring parameters for each type of fluctuations. Using the Hamiltonian of fluctuations in Sm-C phase [Eq. (4.1)] and performing the Fourier transformation of fluctuating fields we obtain within harmonic approximation $H = \sum_{\mathbf{q}} \left(H_{\mathbf{q}}\, [\widetilde{\xi}_{\shortparallel}] + H_{\mathbf{q}}\, [\widetilde{\xi}_\perp] \right)$, where

$$\begin{aligned} H_{\mathbf{q}}[\widetilde{\xi}_i] = \frac{1}{2} K_3 S \Bigg(\int_0^h \Bigg[\left\{ \begin{array}{c} \rho^{-2} + \frac{K}{K_3} q^2 \\ \frac{K}{K_3} q^2 \end{array} \right\} \widetilde{\xi}_i^{\,2} + \left(\frac{d\widetilde{\xi}_i}{dz} \right)^2 \Bigg] \mathrm{d}z + \\ + \left\{ \begin{array}{c} L_{\shortparallel}^{-1} \\ L_\perp^{-1} \end{array} \right\} \left(\widetilde{\xi}_i^{-\,2} + \widetilde{\xi}_i^{+\,2} \right) \Bigg) . \end{aligned} \tag{4.35}$$

The upper line corresponds to Fourier components $\widetilde{\xi}_{\shortparallel}(\mathbf{q}, z)$ and the lower to $\widetilde{\xi}_\perp(\mathbf{q}, z)$. The Casimir force is calculated following the procedure described in the case of the homeotropic cell. It consists of two terms:

$$\mathcal{F}_{Cas} = -\frac{k_B T S}{2\pi} \frac{K_3}{K} \left[\int_{1/\rho}^{\infty} \frac{r^2\, \mathrm{d}r}{\frac{(r+L_{\shortparallel}^{-1})^2}{(r-L_{\shortparallel}^{-1})^2} \exp(2rh) - 1} + \int_0^{\infty} \frac{r^2\, \mathrm{d}r}{\frac{(r+L_\perp^{-1})^2}{(r-L_\perp^{-1})^2} \exp(2rh) - 1} \right] . \tag{4.36}$$

The first term is a contribution of massive amplitude fluctuations with correlation length ρ. The second term is a long-range contribution of massless phase fluctuations. The characteristics of these terms have already been analyzed in the preceding discussion [Figs. (3.2,4.3)].

Here we investigate the temperature dependence of the Casimir force in a free-standing smectic film which is presented in Fig. 4.6. We present the force only for the limiting case of infinitely strong anchoring; that is $L = 0$ in the Sm-A film and $L_{\shortparallel} = 0$, $L_{\perp} = 0$ in the Sm-C film. Due to the symmetric boundary conditions, the

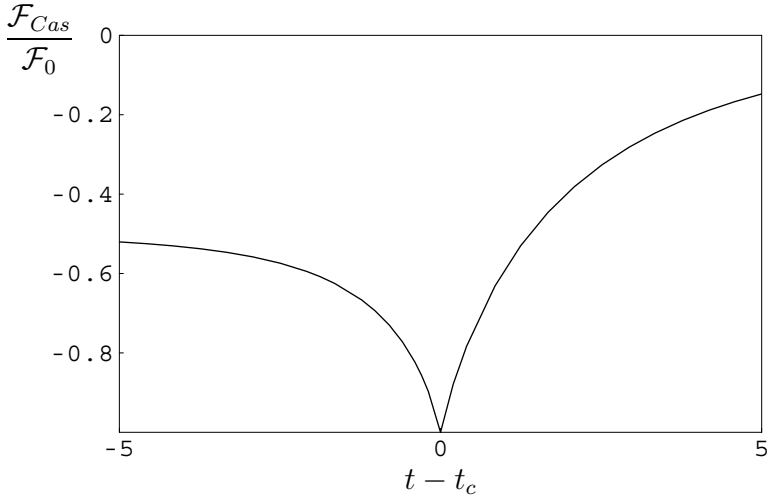

Figure 4.6 Temperature dependence of the Casimir force in a free-standing smectic film. Again the unitless temperature $t = \alpha h^2 T/K_3$ is introduced. The amplitude of the force is given in the natural unit $\mathcal{F}_0 = k_B T S K_3 \zeta_R(3)/4\pi K h^3$ (a weak temperature dependence of $\mathcal{F}_0$ is neglected). Presented is the limiting case of infinitely strong anchoring; $L = 0$ in the Sm-A film and $L_{\shortparallel} = 0$, $L_{\perp} = 0$ in the Sm-C film.

Casimir force in the free-standing smectic film is always attractive. It reaches the maximum at the structural transition from the Sm-A to the Sm-C film ($T = T_c$). Lowering or rising the temperature reduces the amplitude of the force. In the Sm-A film there are two degenerate massive fluctuation modes whose contributions to the Casimir force decay rapidly while rising the temperature. In the Sm-C film the contribution of the massless mode is almost temperature independent, while the contribution of the massive mode again decays rapidly away from $T = T_c$. The profile of the force is therefore asymmetric. There is no divergence of the force at the structural transition from the Sm-A to the Sm-C film as in the homeotropic cell. In our simple model of the smectic film no frustration is induced by the boundary conditions, and consequently the divergence does not occur. The increase of the amplitude is a consequence of the fact that when approaching $T \to T_c$ all fluctuation modes become massless. The implementation of finite anchoring strengths does not significantly alter the temperature profile of the force but merely reduces its amplitude.

4.2.1 Casimir force in free-standing Sm-A films with enhanced surface order

As the fluctuations of surface layers in free-standing films are suppressed by the surface tension, the boundary layers often posses more order than interior ones. Close to the Sm-A – Sm-C phase transition the molecules in boundary layers can already be tilted while the bulk interior is still in the Sm-A phase [164]. We model this surface ordering by demanding that the magnitude of tilt order parameter $\boldsymbol{\xi}$ at the surfaces is equal to a non-zero ξ_S (Fig. 4.7). If we assume that ξ_S, and hence

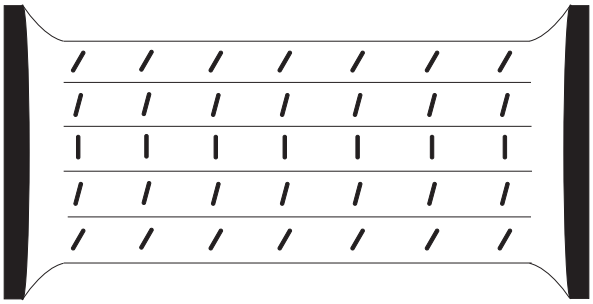

Figure 4.7 Free-standing Sm-A film with enhanced surface order. The molecules in surface layers are tilted while the interior of the film is still in the Sm-A phase.

also interior $|\boldsymbol{\xi}|$, is very small, we can perform the analysis retaining only lowest order terms in the free-energy expansion (2.11)

$$\begin{aligned} f = f_A + \frac{1}{2}K_3\eta^{-2}\left(\xi_{\shortparallel}^2 + \xi_\perp^2\right) + \frac{1}{2}K_3\left[\left(\frac{\partial\xi_{\shortparallel}}{\partial z}\right)^2 + \left(\frac{\partial\xi_\perp}{\partial z}\right)^2\right] \\ + \frac{1}{2}K\left[\left(\frac{\partial\xi_{\shortparallel}}{\partial x} + \frac{\partial\xi_\perp}{\partial y}\right)^2 + \left(\frac{\partial\xi_{\shortparallel}}{\partial y} - \frac{\partial\xi_\perp}{\partial x}\right)^2\right] . \end{aligned} \tag{4.37}$$

Minimization of the free energy leads to the Euler-Lagrange equation

$$\frac{\mathrm{d}^2\xi_{\shortparallel}}{\mathrm{d}z^2} - \eta^{-2}\xi_{\shortparallel} = 0 . \tag{4.38}$$

With boundary conditions $\xi_{\shortparallel}(z = -h/2) = \xi_{\shortparallel}(z = h/2) = \xi_S$ this gives the mean-field profile

$$\xi_{\shortparallel}^{mf}(z) = \xi_S\frac{\cosh(z/\eta)}{\cosh(h/2\eta)} . \tag{4.39}$$

Note that for simplicity we here placed the boundaries at $z = \pm h/2$. The component $\xi_\perp$ is not affected by the surface induced order and $\xi_\perp^{mf} = 0$. The mean-field free-energy of this deformed structure is given by

$$F_{mf} = \frac{K_3 S\xi_S^2}{\eta}\tanh\left(\frac{h}{2\eta}\right) , \tag{4.40}$$

which leads to the mean-field force

$$\mathcal{F}_{mf} = -\frac{\partial F_{mf}}{\partial h} = -\frac{K_3 S \xi_S^2}{2\eta^2 \cosh^2(h/2\eta)} \,. \tag{4.41}$$

This is a well-known short-range attraction characteristic for symmetric systems with enhanced surface order [179].

The Casimir force is calculated in the usual manner. We write the order parameters as $\xi_{\shortparallel} = \xi_{\shortparallel}^{mf} + \delta\xi_{\shortparallel}$ and $\xi_{\perp} = \delta\xi_{\perp}$ and obtain the Hamiltonian density of fluctuations

$$\begin{aligned} h = \frac{1}{2}K_3\eta^{-2}\left(2\xi_{\shortparallel}^{mf}\delta\xi_{\shortparallel} + \delta\xi_{\shortparallel}^2 + \delta\xi_{\perp}^2\right) + \frac{1}{2}K_3\Bigg[\left(\frac{\partial(\delta\xi_{\shortparallel})}{\partial z}\right)^2 + 2\frac{\partial\xi_{\shortparallel}^{mf}}{\partial z}\frac{\partial(\delta\xi_{\shortparallel})}{\partial z} \\ + \left(\frac{\partial(\delta\xi_{\perp})}{\partial z}\right)^2\Bigg] + \frac{1}{2}K\left[\left(\frac{\partial(\delta\xi_{\shortparallel})}{\partial x} + \frac{\partial(\delta\xi_{\perp})}{\partial y}\right)^2 + \left(\frac{\partial(\delta\xi_{\shortparallel})}{\partial y} - \frac{\partial(\delta\xi_{\perp})}{\partial x}\right)^2\right] . \end{aligned} \tag{4.42}$$

Fourier transforming the fluctuating fields and integrating over volume we obtain $H = \sum_{\mathbf{q}} H_{\mathbf{q}}[\delta\xi_{\shortparallel}] + H_{\mathbf{q}}[\delta\xi_{\perp}]$, where

$$\begin{aligned} H_{\mathbf{q}}[\delta\xi_{\shortparallel}] = \frac{1}{2}K_3 S\int_0^h \Bigg[\left(\eta^{-2} + \frac{K}{K_3}q^2\right)\widetilde{\xi}_{\shortparallel}^{\,2} + \left(\frac{\partial\widetilde{\xi}_{\shortparallel}}{\partial z}\right)^2 \\ + 2\left(\eta^{-2}\xi_{\shortparallel}^{mf}\widetilde{\xi}_{\shortparallel} + \frac{\partial\xi_{\shortparallel}^{mf}}{\partial z}\frac{\partial\widetilde{\xi}_{\shortparallel}}{\partial z}\right)\delta_{\mathbf{q},\mathbf{0}}\Bigg]\,\mathrm{d}z \,, \end{aligned} \tag{4.43}$$

$$H_{\mathbf{q}}[\delta\xi_{\perp}] = \frac{1}{2}K_3 S\int_0^h \left[\left(\eta^{-2} + \frac{K}{K_3}q^2\right)\widetilde{\xi}_{\perp}^{\,2} + \left(\frac{\partial\widetilde{\xi}_{\perp}}{\partial z}\right)^2\right]\mathrm{d}z \,. \tag{4.44}$$

The $\delta\xi_{\perp}$ fluctuations are not affected by the deformed mean-field structure and their contribution to the Casimir force is the same as in homogeneous Sm-A film. The Hamiltonian of $\delta\xi_{\shortparallel}$ fluctuations contains additional terms for wave vector $\mathbf{q} = \mathbf{0}$. However, performing a per partes integration over z and considering the Euler-Lagrange equation for the mean-field profile $\xi_{\shortparallel}^{mf}$ [Eq. (4.38)] these additional terms are transformed into a surface term. If we assume fixed boundary conditions, $\delta\xi_{\shortparallel}(z = -h/2) = \delta\xi_{\shortparallel}(z = h/2) = 0$, then this surface term is equal to zero and does not contribute to the Hamiltonian and does consequently also not affect the partition function. Hence the contribution of the $\delta\xi_{\shortparallel}$ fluctuations to the Casimir force is also the same as in a non-deformed film. This is in agreement with the general conclusions of Sec. 3.3.

The free-standing Sm-A film with enhanced surface order represents another example of a system where non-trivial equilibrium structure does not modify the Casimir force, provided the surface induced order is small enough that quadratic approximation of free-energy can be used. A similar study of the Casimir force

was performed for the case of a presmectic system, where confining boundaries enforce enhanced positional order, and the same conclusions were reached [129]. This is therefore a universal result for systems with fixed surface induced order and quadratic free energy.

5

Inhomogeneous systems

Systems with non-trivial equilibrium order pose a special problem in the theory of the Casimir force and were to our knowledge studied only rarely [120, 129, 180]. The main problem in these system lies in the regularization of divergent free energy of fluctuations which can not always be performed analytically. In this thesis we have already studied two systems with non-trivial equilibrium order – a stretched homeotropic cell and a free standing Sm-A film with enhanced surface order. In both cases a non-trivial equilibrium profile resulted in additional linear terms in the Hamiltonian of fluctuations which could be transformed into surface terms and, as argued in Section 3.3, did not affect the Casimir force provided the boundary conditions were fixed. It is not always so simple, though. In this chapter we study two systems with surface induced order where the inhomogeneity of the ordering results in spatial variation of smectic material constants. In this case the Casimir force is considerably modified. The third type of inhomogeneous systems was mentioned in Section 4.1, where in a frustrated Sm-A cell at low enough temperature the transition to the deformed Sm-C structure occurs. In this case the enhanced order, i.e. tilt, is induced by bulk interior whereas the boundaries suppress it. The Casimir force in this kind of system was addressed in Ref. [180] and we do not consider it here, though it has not been indisputably solved yet.

5.1 Casimir force close to smectic-nematic phase transition

In calculation of the Casimir force in a Sm-A homeotropic cell, we assumed that the magnitude of degree of smectic order ψ is constant over the whole sample and equal to the bulk value $\psi_0 = \sqrt{-a/b}$, where a and b are the coefficients in free energy expansion (2.6). Close to the smectic to nematic phase transition where ψ_0 is small, this assumption may not be valid as the surface positional order induced by the confining plates may be much larger than the intrinsic bulk value ψ_0. In

this case we obtain an inhomogeneous equilibrium profile of ψ. If we consider layer fluctuations described by a simple Hamiltonian

$$H = \frac{1}{2}\int \left[B\left(\frac{\partial u}{\partial z}\right)^2 + K_L\left(\nabla_\perp^2 u\right)^2 \right] \mathrm{d}V \ , \tag{5.1}$$

and recall that elastic constants are proportional to the ψ^2

$$B = C_\parallel q_0^2 \psi^2 \ , \qquad\qquad K_L = d_1 q_0^2 \psi^2 \ , \tag{5.2}$$

we obtain a system with a spatial dependence of elastic constants, $B = B(z)$ and $K_L = K_L(z)$.

The first task is therefore to calculate the equilibrium profile $\psi = \psi(z)$. We consider a homeotropic smectic-A cell with plates located at $z = \pm h/2$ and inducing surface smectic order ψ_S (Fig. 5.1). If the layers in the cell are neither stretched nor

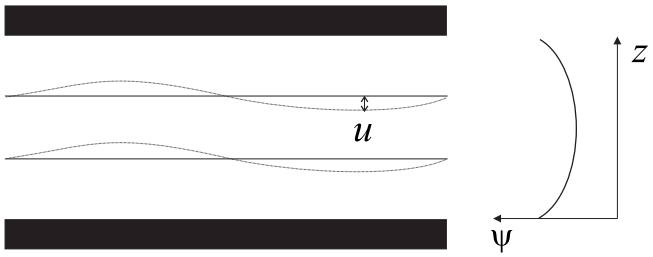

Figure 5.1 Homeotropic smectic-A cell with surface enhanced positional order ψ. The profile of positional order is presented schematically. We consider the Casimir force induced by the fluctuations of smectic layers u.

dilated, the equilibrium profile can be calculated by minimizing the free energy

$$F = \int \left[\frac{1}{2}a\psi^2 + \frac{1}{4}b\psi^4 + \frac{1}{2}C_\parallel \left(\frac{\partial \psi}{\partial z}\right)^2 \right] \mathrm{d}V \ , \tag{5.3}$$

where a is negative in the smectic phase and we neglect higher order elastic terms. In general, the solution can not be obtained analytically. Therefore we first separate the bulk value $\psi_0 = \sqrt{-a/b}$ from the total order parameter and write $\psi = \psi_0 + \tilde{\psi}$. Assuming that $\tilde{\psi}$ is small we can expand the free energy to quadratic order

$$\tilde{F} = F - F_0 = \int \left[-a\tilde{\psi}^2 + \frac{1}{2}C_\parallel \left(\frac{\partial \tilde{\psi}}{\partial z}\right)^2 \right] \mathrm{d}V \ . \tag{5.4}$$

Now the analytical solution is given by

$$\psi(z) = \psi_0 + \tilde{\psi}(z) = \psi_0 + \tilde{\psi}_S \frac{\cosh(z/\xi)}{\cosh(h/2\xi)} \ , \tag{5.5}$$

where $\tilde{\psi}_S = \psi_S - \psi_0$ and $\xi^{-2} = -2a/C_\parallel$.

The spatial dependence of elastic constants B and K is now described by

$$B = C_\parallel q_0^2 \left[\psi_0 + \tilde{\psi}_S \frac{\cosh(z/\xi)}{\cosh(h/2\xi)}\right]^2 \ , \ K_L = d_1 q_0^2 \left[\psi_0 + \tilde{\psi}_S \frac{\cosh(z/\xi)}{\cosh(h/2\xi)}\right]^2 \ . \tag{5.6}$$

Unfortunately it turns out that we are not able to calculate the Casimir force using this full profile, as the partition function of fluctuations can not be evaluated analytically. We therefore neglect the constant ψ_0 contribution, continuing our calculations with the inhomogeneous part of the ψ only:

$$\begin{aligned} B &\to C_\parallel q_0^2 \left[\tilde{\psi}_S \frac{\cosh(z/\xi)}{\cosh(h/2\xi)}\right]^2 = B_S \frac{\cosh^2(z/\xi)}{\cosh^2(h/2\xi)} \ , \\ K_L &\to d_1 q_0^2 \left[\tilde{\psi}_S \frac{\cosh(z/\xi)}{\cosh(h/2\xi)}\right]^2 = K_S \frac{\cosh^2(z/\xi)}{\cosh^2(h/2\xi)} \ . \end{aligned} \tag{5.7}$$

This approximation can not be justified on physical grounds and one should be aware of the inconsistency of our approach. However, we are here mainly interested in the effect of inhomogeneous profile of elastic constants on the Casimir force. Therefore we expect that despite this approximation we will still obtain a qualitative picture of the phenomenon. Our approximation could also be interpreted in the sense that we ad hoc invented a plausible profile of elastic constants and studied its effect on the Casimir force. Furthermore we should mention that in our simple model [Eq. (5.1)], where we consider only layer fluctuations assuming that director is fixed perpendicular to the layers, the constant K_L should also include the contribution of splay director elastic constant K_1 which is proportional to degree of nematic order, $K_1 \propto \psi_N^2$. This would pose no difficulties if the profile of $\psi_N(z)$ could be approximated by the same spatial dependence as $\psi(z)$. Otherwise the Casimir force could not be calculated and we therefore avoid this complication.

We start the calculation of the Casimir force by Fourier transforming the Hamiltonian Eq. (5.1). This transformation is not affected by the $K_L(z)$ and $B(z)$ profiles so we obtain

$$H_{\mathbf{q}}[u] = \frac{1}{2} S K_S \int_{-h/2}^{h/2} \left[\lambda^{-2} \frac{\cosh^2(z/\xi)}{\cosh^2(h/2\xi)} \left|\frac{\partial u_{\mathbf{q}}}{\partial z}\right|^2 + \frac{\cosh^2(z/\xi)}{\cosh^2(h/2\xi)} q^4 \left|u_{\mathbf{q}}\right|^2\right] \mathrm{d}z \ , \tag{5.8}$$

where we introduced the characteristic length $\lambda = \sqrt{K_S/B_S}$. Now the partition function of fluctuations has to be evaluated, where we assume fixed boundary conditions at the plates

$$Z_{\mathbf{q}}[u] = \int_{u_{\mathbf{q}}(z=-\frac{h}{2})=0}^{u_{\mathbf{q}}(z=\frac{h}{2})=0} \exp\left(-\beta H_{\mathbf{q}}[u]\right) \mathcal{D}u_{\mathbf{q}}(z) \ . \tag{5.9}$$

This partition function does not belong to a class of standard path integrals, such as for example path integral of a harmonic oscillator with constant mass and elasticity, but it can be evaluated. For a general quadratic Hamiltonian

$$H = \int_{z'}^{z''} \left[a(z)\dot{x}^2 + 2b(z)\dot{x}x + c(z)x^2 + 2d(z)\dot{x} + 2e(z)x \right] \mathrm{d}z \tag{5.10}$$

the partition function $Z = \int_{x(z')=x'}^{x(z'')=x''} \exp(-\beta H[x(z)])\, \mathcal{D}x(z)$ is given by [168]

$$Z \propto \sqrt{\left(-\frac{\partial^2 H_{cl}(x'', x')}{\partial x' \partial x''} \right)} \ \exp\left(-\beta H_{cl}[x'', x']\right) \ . \tag{5.11}$$

Here H_{cl} is the analog of classical action in quantum mechanics and is obtained by minimizing Hamiltonian H with respect to $x(z)$.

The Euler-Lagrange equation for minimization of the Hamiltonian $H_{\mathbf{q}}[u]$ leads to the differential equation for classical path $u_{\mathbf{q}}^{cl}$

$$\frac{\partial^2 u_{\mathbf{q}}^{cl}}{\partial z^2} + \frac{2}{\xi} \tanh\left(\frac{z}{\xi}\right) \frac{\partial u_{\mathbf{q}}^{cl}}{\partial z} - \lambda^2 q^4 u_{\mathbf{q}}^{cl} = 0 \,, \tag{5.12}$$

with general boundary conditions $u_{\mathbf{q}}^{cl}(z = \pm h/2) = u_{\mathbf{q}}^{\pm}$. The solution of this equation reads

$$\begin{aligned} u_{\mathbf{q}}^{cl} = \Bigg(& \frac{1}{2} u_{\mathbf{q}}^{-} \left\{ \exp\left[\left(\frac{3h}{2} - z \right) \sqrt{\lambda^2 q^4 + \xi^{-2}} \right] - \exp\left[\left(\frac{h}{2} + z \right) \sqrt{\lambda^2 q^4 + \xi^{-2}} \right] \right\} \\ & + \frac{1}{2} u_{\mathbf{q}}^{+} \left\{ \exp\left[\left(\frac{3h}{2} + z \right) \sqrt{\lambda^2 q^4 + \xi^{-2}} \right] - \exp\left[\left(\frac{h}{2} - z \right) \sqrt{\lambda^2 q^4 + \xi^{-2}} \right] \right\} \Bigg) \\ & \times \left[\coth\left(h \sqrt{\lambda^2 q^4 + \xi^{-2}} \right) - 1 \right] \frac{\cosh(h/2\xi)}{\cosh(z/\xi)} \ . \end{aligned} \tag{5.13}$$

It is obvious that for fixed boundary conditions, $u_{\mathbf{q}}^{\pm} = 0$, the classical path $u_{\mathbf{q}}^{cl}$ and hence also H_{cl} are equal to 0. Thus it only remains to evaluate the derivative $\partial^2 H_{cl} / \partial u_{\mathbf{q}}^{+} \partial u_{\mathbf{q}}^{-}$. This calculation is straightforward and leads to the partition function

$$Z_{\mathbf{q}}[u] \propto \left[\sinh\left(\sqrt{\lambda^2 q^4 + \xi^{-2}}\, h \right) \right]^{-\frac{1}{2}} \ . \tag{5.14}$$

After performing the usual extraction of the bulk and surface parts we obtain the interaction part of the fluctuations free energy

$$F_{int} = \frac{k_B T S}{4\pi} \int_0^{\infty} \ln\left(1 - \exp\left(-2\frac{h}{\xi} \sqrt{1 + \xi^2 \lambda^2 q^4} \right) \right) \ q \, \mathrm{d}q \ , \tag{5.15}$$

and the corresponding Casimir force

$$\mathcal{F}_{Cas} = -\frac{k_B T S}{2\pi\xi} \int_0^{\infty} \frac{\sqrt{1 + \xi^2 \lambda^2 q^4}}{\exp\left(2\frac{h}{\xi} \sqrt{1 + \xi^2 \lambda^2 q^4} \right) - 1} \, q \, \mathrm{d}q \ . \tag{5.16}$$

This integral can not be evaluated analytically. We can however obtain the behavior of the force in the limiting cases of small and large thicknesses. In the limit of small thickness, $h/\xi \to 0$, the force is equal to

$$\mathcal{F}_{Cas}\left(h/\xi \to 0\right) = -\frac{k_B T S \zeta_R(2)}{16\pi\lambda h^2} \,. \tag{5.17}$$

This is just the usual layer-fluctuations induced Casimir force [Eq. (1.13)]. Such a behavior can be easily explained by the fact that at very small thicknesses the profile of ψ, and hence also of K and B, is practically constant and there is no effect of inhomogeneity. In the opposite limit of very large thicknesses, $h/\xi \to \infty$, the force is given by

$$\mathcal{F}_{Cas}\left(h/\xi \to \infty\right) = -\frac{k_B T S}{8\sqrt{\pi}\xi^2\lambda}\frac{\exp\left(-2h/\xi\right)}{\sqrt{h/\xi}} \,. \tag{5.18}$$

This is a very interesting result which shows that fluctuations of smectic layers described by a purely elastic Hamiltonian [Eq. (5.1)], due to the space dependent elastic constants induce a short-range Casimir force which decays exponentially as $\exp(-2h/\xi)/\sqrt{h/\xi}$. Such a short-range exponentially decaying force is characteristic for massive fluctuation modes, so the inhomogeneity here obviously acts as some effective mass of fluctuations. The numerically calculated profile of the Casimir force in a broader range of thicknesses is shown in Fig. 5.2.

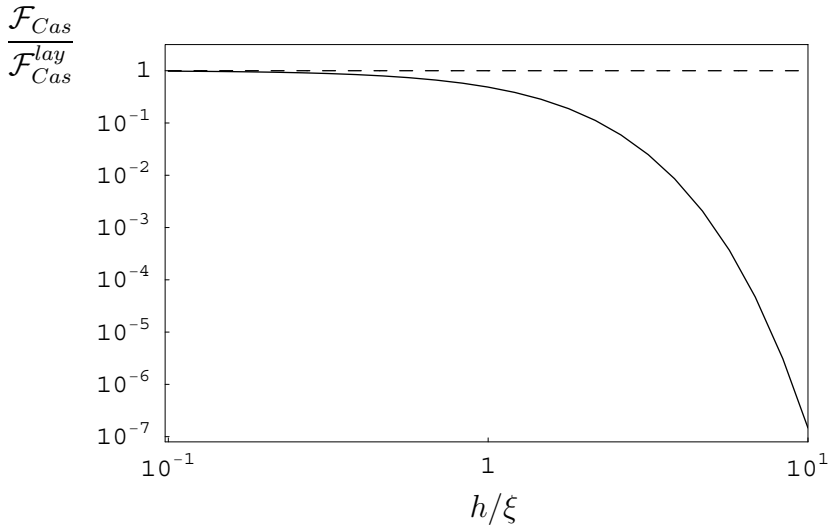

Figure 5.2 The profile of the Casimir force induced by the layer fluctuations in the homeotropic smectic-A cell with a surface enhanced positional order compared to the usual layer-fluctuations induced Casimir force $\mathcal{F}_{Cas}^{lay} = -k_B T S \zeta_R(2)/16\pi\lambda h^2$. At small thicknesses $\mathcal{F}_{Cas}$ is equal to $\mathcal{F}_{Cas}^{lay}$. At large thicknesses it decays much faster, as $\exp(-2h/\xi)/\sqrt{h/\xi}$.

In the end we should again note that the system studied here was somewhat special, as the spatial profiles of K_L and B were taken to be equal and also consider-

ably simplified. This enabled us to obtain an analytical solution which would not be possible in a more general case. Nevertheless, we expect that our simple model still contains some physical reality. In reference to our result we must mention a study of de Oliveira et al. [133] where the Casimir force in a free standing smectic-A film close to the Sm-A – nematic phase transition was studied within discrete model. It was claimed that due to the inhomogeneous profile of elastic constants the magnitude of the force is strongly enhanced. This is obviously in contradiction with our conclusions. As we are not able to reproduce their numerical results we can not make the final judgement whether this contradiction stems from the inconsistency of our model or some other source.

5.1.1 Force induced by fluctuations of degree of smectic order ψ

We can also evaluate the contribution of fluctuations of positional order ψ to the Casimir force. We make use of the fact that in the lowest order the fluctuations of u and ψ are not coupled and start with the harmonic free energy

$$\tilde{F}[\tilde{\psi}] = \int \left[-a\tilde{\psi}^2 + \frac{1}{2} C_{\parallel} \left(\frac{\partial \tilde{\psi}}{\partial z} \right)^2 + \frac{1}{2} C_{\perp} \left(\nabla_{\perp} \tilde{\psi} \right)^2 \right] \mathrm{d}V \ . \tag{5.19}$$

We write $\tilde{\psi} = \tilde{\psi}_{mf} + \delta\tilde{\psi}$, where the mean field part has already been calculated

$$\tilde{\psi}_{mf} = \tilde{\psi}_S \frac{\cosh(z/\xi)}{\cosh(h/2\xi)} \ . \tag{5.20}$$

We now note that this system is equivalent to the case of a free standing smectic-A film with enhanced surface order (Sec. 4.2.1). Therefore we can directly write the mean field force

$$\mathcal{F}_{mf} = -\frac{C_{\parallel} S \tilde{\psi}_S^2}{2\xi^2 \cosh^2(h/2\xi)} \ . \tag{5.21}$$

and the Casimir force

$$\mathcal{F}_{Cas}[\delta\tilde{\psi}] = -\frac{k_B T S}{4\pi} \frac{C_{\parallel}}{C_{\perp}} \frac{1}{h^3} \sum_{k=1}^{\infty} \frac{\exp(-2hk/\xi)}{k^3} \left(\frac{1}{2} + \frac{h}{\xi} k + \frac{h^2}{\xi^2} k^2 \right) . \tag{5.22}$$

The inhomogeneity of equilibrium profile does not affect the Casimir force in this case and we obtain the usual short-range attraction as in a homogeneous system [Eq. (3.10)]. This is just another example of a system described by a quadratic free energy functional and with fixed boundary conditions where the nontrivial equilibrium order profile does not change the Casimir force, as it was discussed in Sec. 3.3.

5.2 Casimir force in presmectic nematic film

Even if the system is in nematic phase there is always some positional order of molecules present in confined geometries. The origin of this presmectic positional order lies in the fact that molecules can not penetrate into the hard boundaries so there is always at least one ordered layer present. How this surface induced order penetrates into the bulk depends on the proximity of the nematic – smectic phase transition. Very close to the transition the positional order extends over large distances, whereas far above the transition it is basically only the boundary layer being ordered. As the orientational fluctuations of director are coupled to the smectic order, this presmectic ordering results in increased energy of director fluctuation modes. The otherwise massless nematic director fluctuations become massive due to the surface induced positional order. It is the aim of this section to calculate the Casimir force due to the director fluctuations in such a nematic system with a presmectic positional order.

We begin by calculating the equilibrium profile of degree of positional order ψ in a homeotropic nematic cell with plates imposing surface smectic order ψ_S (Fig. 5.3). We use the following free energy expression

Figure 5.3 Homeotropic nematic cell with surface induced presmectic order ψ. The profile of positional order is shown schematically. We consider the Casimir force induced by the director fluctuations $\delta\mathbf{n}$.

$$F = \int \left[\frac{1}{2} a\psi^2 + \frac{1}{2} C_{\parallel} \left(\frac{\partial \psi}{\partial z} \right)^2 \right] \mathrm{d}V \ . \tag{5.23}$$

As the system is in a nematic phase the coefficient a is positive and the bulk order ψ_0 is equal to 0. We here consider only the basic elastic term and do not include higher powers of ψ in the expansion as the magnitude of positional order is expected to be small and the quadratic approximation should therefore suffice. Placing the plates at $z = \pm h/2$ we obtain, by minimization of F, the mean-field profile

$$\psi_{mf}(z) = \psi_S \frac{\cosh(z/\xi)}{\cosh(h/2\xi)} \ . \tag{5.24}$$

This is analogous to the profile obtained in the previous section [Eq. (5.20)] with the correlation length now being $\xi^{-2} = a/C_{\parallel}$. The correlation length ξ also represents the characteristic length of penetration of surface smectic order into the bulk. Far from the nematic – smectic phase transition ξ is of order of a molecular length whereas close to the transition its value increases and finally diverges at the transition.

In the one-constant approximation, the nematic free energy density is given by

$$f = \frac{1}{2}D(\delta\mathbf{n})^2 + \frac{1}{2}K\left[(\nabla\cdot\mathbf{n})^2 + (\nabla\times\mathbf{n})^2\right] \ . \tag{5.25}$$

Here $\delta\mathbf{n}$ is the deviation of director from z direction and $D = C_{\perp}q_0^2\psi_{mf}^2$. In usual nematics with no smectic order ($\psi = 0$) D is 0. Here, due to the surface induced smectic order, the director fluctuations become massive with spatially dependent mass

$$D(z) = C_{\perp}q_0^2\psi_S^2\frac{\cosh^2(z/\xi)}{\cosh^2(h/2\xi)} \ . \tag{5.26}$$

The nematic elastic constant K is assumed to be uniform as the nematic order is well developed. In equilibrium, the director is oriented in z direction and the fluctuations are given by $\delta\mathbf{n} = (n_x, n_y)$. This leads to the harmonic Hamiltonian of fluctuations

$$\begin{aligned} H = \frac{1}{2}K\int\Bigg[&\Lambda^{-2}(z)\left(n_x^2+n_y^2\right) + \left(\frac{\partial n_x}{\partial x}+\frac{\partial n_y}{\partial y}\right)^2 + \left(\frac{\partial n_y}{\partial x}-\frac{\partial n_x}{\partial y}\right)^2 + \\ &+\left(\frac{\partial n_x}{\partial z}\right)^2 + \left(\frac{\partial n_y}{\partial z}\right)^2\Bigg]\,\mathrm{d}V \end{aligned} \tag{5.27}$$

where we introduced a spatially dependent correlation length $\Lambda^{-2}(z) = D(z)/K$. After Fourier transformation we obtain $H = \sum_{\mathbf{q}} H_{\mathbf{q}}[n_x] + H_{\mathbf{q}}[n_y]$ with

$$H_{\mathbf{q}}[n_{x\mathbf{q}}] = H_{\mathbf{q}}[n_{y\mathbf{q}}] = H_{\mathbf{q}}[n_{\mathbf{q}}] = \frac{1}{2}KS\int_{-h/2}^{h/2}\left[\left(\Lambda^{-2}(z)+q^2\right)|n_{\mathbf{q}}|^2 + \left|\frac{\partial n_{\mathbf{q}}}{\partial z}\right|^2\right]\mathrm{d}z \ . \tag{5.28}$$

The partition function

$$Z_{\mathbf{q}}[n_{\mathbf{q}}] = \int_{n_{\mathbf{q}}(z=-\frac{h}{2})=0}^{n_{\mathbf{q}}(z=\frac{h}{2})=0}\exp\left(-\beta H_{\mathbf{q}}[n_{\mathbf{q}}]\right)\ \mathcal{D}n_{\mathbf{q}}[z] \tag{5.29}$$

is analogous to the quantum propagator of harmonic oscillator with a time dependent frequency (see Appendix A.1). We assume that the director orientation is fixed at the plates. The partition function is given by

$$Z_{\mathbf{q}}[n_{\mathbf{q}}] \propto \left[g\,(h/2)\right]^{-1/2} \tag{5.30}$$

where $g(z)$ is a solution of differential equation

$$\frac{\partial^2 g(z)}{\partial z^2} - \left(\Lambda^{-2}(z) + q^2\right) g(z) = 0 \tag{5.31}$$

with boundary conditions

$$g\left(z = -\frac{h}{2}\right) = 0 \,, \qquad \frac{\partial g}{\partial z}\left(z = -\frac{h}{2}\right) = 1 \,. \tag{5.32}$$

Here we can not proceed with a general profile of $D(z)$ [Eq. 5.26] but need to make an approximation. We introduce a parabolic profile of $D(z)$

$$D(z) \to C_\perp q_0^2 \psi_S^2 \frac{(z/\xi)^2}{(h/2\xi)^2} \,. \tag{5.33}$$

There exists no physical argument to justify such an approximation, but we again ad hoc introduce a plausible inhomogeneous profile which enables us to continue the calculation, and hope that it still contains some physical reality. With this approximation we can now obtain the partition function as

$$\begin{aligned} Z_{\mathbf{q}}[n_{\mathbf{q}}] \propto \frac{1}{\sqrt{2k}} \Bigg[& -\frac{1}{2} x_0 \left(A + \frac{1}{2}\right) \frac{M[\frac{1}{2}A + \frac{5}{4}, \frac{3}{2}, \frac{1}{8}x_0^2]}{M[\frac{1}{2}A + \frac{1}{4}, \frac{1}{2}, \frac{1}{8}x_0^2]} + \frac{2}{x_0} \\ & + \frac{1}{2} x_0 \left(\frac{1}{3}A + \frac{1}{2}\right) \frac{M[\frac{1}{2}A + \frac{7}{4}, \frac{5}{2}, \frac{1}{8}x_0^2]}{M[\frac{1}{2}A + \frac{3}{4}, \frac{3}{2}, \frac{1}{8}x_0^2]} \Bigg]^{1/2} \,, \end{aligned} \tag{5.34}$$

where $M[a, b, z]$ is the Kummer confluent hypergeometric function [181]. We have introduced the following parameters

$$\alpha = \frac{\xi^2 C_\perp q_0^2 \psi_S^2}{K} \,, \quad A = \frac{h\xi}{4\sqrt{\alpha}} \, q^2 \,, \quad x_0 = \sqrt{\frac{4h\sqrt{\alpha}}{\xi}} \,, \quad k = \sqrt{\frac{h}{4\xi\sqrt{\alpha}}} \,. \tag{5.35}$$

The degree of induced surface order ψ_S is now controlled by parameter α. The free energy of fluctuations is given by

$$F_{fluc} = \frac{k_B T S}{2\pi} \int_0^\infty \ln(Z_{\mathbf{q}}[n_{\mathbf{q}}]) q \, \mathrm{d}q \,, \tag{5.36}$$

where we took into account that there are two degenerate director fluctuation modes present.

The regularization of the fluctuations free energy F_{fluc} can unfortunately not be performed by a simple factorization into bulk, surface and interaction parts, as was the case in previous examples. Therefore we proceed in the following manner. We first calculate the derivative $\partial F_{fluc}/\partial h$. With this we dispose of thickness independent terms. Assuming that interaction part goes to 0 at large thicknesses h, we

numerically calculate $\partial F_{fluc}/\partial h$ at large h's for various wave vectors q. This enables us to evaluate the bulk contribution. In analogy with the previously studied systems we expect the bulk contribution to be constant, $\partial \ln(\exp(rh))/\partial h = r = \text{const}$. However in our case it turns out that the derivative $\partial F_{fluc}/\partial h$ changes very slightly while increasing the distance h. This indicates that the bulk term in partition function can not be described by a simple $\exp(rh)$ dependence, but the correction seems to be very small. Being unable to exactly determine the bulk contribution, our numerical calculations of the force are limited to very small thicknesses h where the interaction part is dominant and the correction due to the uncertainty of regularization is not crucial. The results presented here are hence by no means the final solution of the problem and should serve only as qualitative information of the force behavior. The question of the Casimir force in such systems, with position dependent mass of the fluctuations, remains open for further studies.

The Casimir force calculated using the above described procedure is shown in Figs. 5.4 and 5.5. We first compare the Casimir force in a presmectic nematic with the typical $1/h^3$ nematic force which is present in systems with no smectic order and hence massless director fluctuations (Fig. 5.4):

$$R_1 = \frac{\mathcal{F}_{Cas}(\alpha)}{\mathcal{F}_{Cas}^{nem}} , \tag{5.37}$$

where $\mathcal{F}_{Cas}^{nem} = k_B T S \zeta_R(3)/4\pi h^3$. The thickness is measured in units of correlation length ξ. Various parameters α describe different magnitudes of the surface induced smectic order, where larger α means larger ψ_S. At very small thicknesses the compared forces are equal. This is in agreement with the known results for homogeneous massive systems where in the limit of small thicknesses the force exhibits $1/h^3$ behavior. Such a behavior can be explained by the fact that in very thin cells the elastic contributions (which scale as $1/h$) in the Hamiltonian dominate over the massive term (which scales linearly with h). At larger thicknesses the force in a presmectic system decays faster than $1/h^3$. This is somewhat expected as the fluctuations are massive. The larger the surface induced order, the larger the mass and the faster the decay of the force.

Secondly, we compare the director-induced Casimir force in a presmectic system to the director force in a homogeneous smectic with constant positional order (Fig. 5.5):

$$R_2 = \frac{\mathcal{F}_{Cas}(\alpha)}{\mathcal{F}_{Cas}^{sm}} , \tag{5.38}$$

where

$$\mathcal{F}_{Cas}^{sm} = -\frac{k_B T S}{2\pi} \frac{1}{h^3} \sum_{k=1}^{\infty} \frac{\exp\left(-2hk/\Lambda_S\right)}{k^3} \left(\frac{1}{2} + \frac{h}{\Lambda_S} k + \frac{h^2}{\Lambda_S^2} k^2\right) . \tag{5.39}$$

We defined $\Lambda_S = C_\perp q_0^2 \psi_S^2/K$, meaning that the mass of fluctuations in the homogeneous system is set equal to the boundary value of mass of fluctuations in the

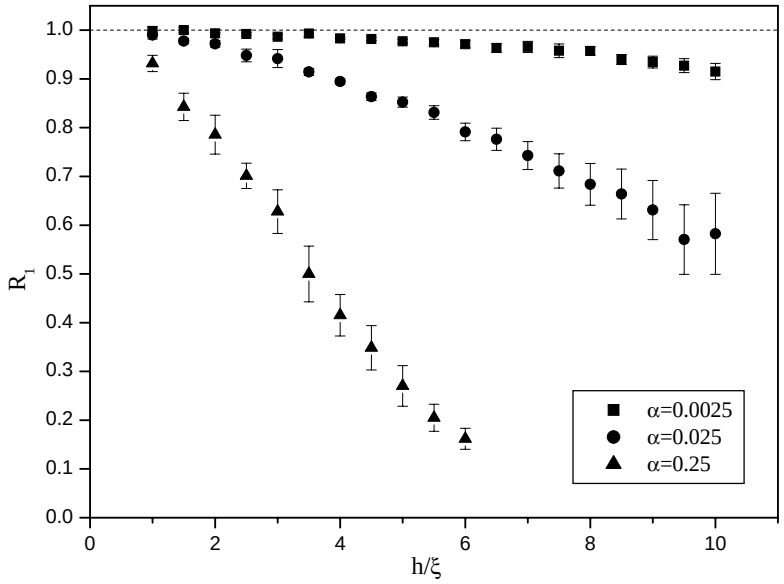

Figure 5.4 Casimir force in a presmectic nematic system compared to the typical $1/h^3$ Casimir force in a nematic system with no smectic order. The different values of α describe the different degrees of the surface induced positional order ψ_S. The error bars indicate the uncertainty stemming from the approximate regularization procedure.

presmectic system. One should note that Λ_S depends on α . The Casimir force in a presmectic system decays slower than in a homogeneous smectic. This is again somewhat expected as an average mass of fluctuations in the presmectic system is smaller than in the homogeneous system, due to the decreased smectic order in the middle of the cell. If we apply the rationale known from homogeneous systems, a larger mass means a shorter correlation length of fluctuations and hence a shorter range of the force. The larger the surface induced smectic order, the larger the difference between the homogeneous and the inhomogeneous system.

Even though we failed to completely solve the problem of the Casimir force induced by director fluctuations in a presmectic system, we can still make some qualitative conclusions. The force in a presmectic nematic system obviously decays faster than the $1/h^3$ force in a pure nematic system without smectic order. As some surface induced positional order is present in every confined system, even deep in the nematic phase, our result indicates that the typical $1/h^3$ nematic director-fluctuations induced force is hardly to be observed in experiments. At present we can not give a more definite answer concerning the behavior of the Casimir force in such systems but we must mention that a complete study should also include the effect of a realistic finite director anchoring at the boundaries which is also known to modify the ideal $1/h^3$ thickness dependence of the Casimir force in nematic systems [137].

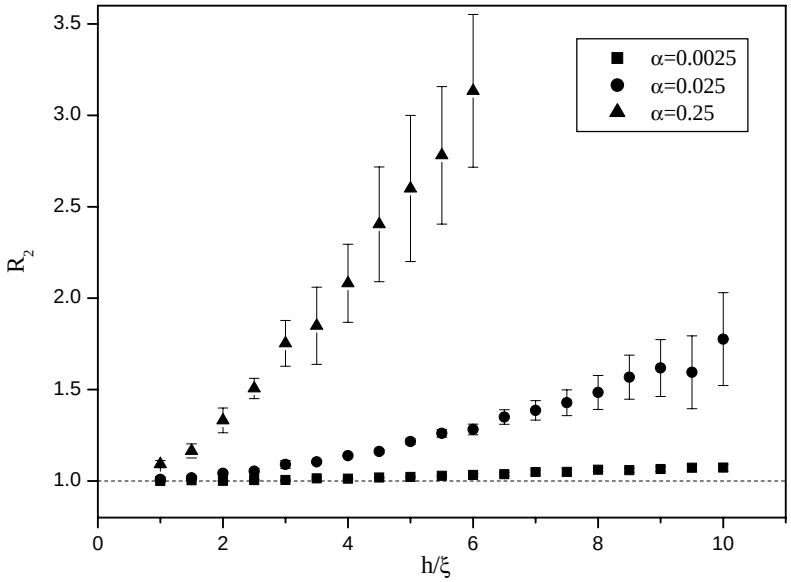

Figure 5.5 Casimir force in a presmectic nematic system compared to the director-fluctuations induced force in a homogeneous smectic system with constant positional order equal to ψ_S. Note that different parameters α correspond to different values of ψ_S so that the reference force $\mathcal{F}_{Cas}^{sm}$ is different for each case. The error bars indicate the uncertainty stemming from the approximate regularization procedure.

6

Conclusion

The majority of studies of the Casimir phenomenon in liquid crystalline systems was concerned with the simplest, i.e. nematic, phase. In this thesis, we tried to reveal the various aspects of the Casimir force in the smectic phase, which possesses a more complex ordering and is thus even more interesting. Many new questions concerning the Casimir effect were raised, but not all the final answers have been given yet.

In Chapter 3 we studied the Casimir force in two smectic-A systems with plan-parallel geometry:a homeotropic cell and a free-standing film. We assumed that the equilibrium structure of the systems was homogeneous. We considered the force induced by thermal fluctuations of positional order (degree of order and position of smectic layers) and by fluctuations of orientational order (director). We also took into account the coupling between the positional and the orientational order. Within the harmonic approximation, the fluctuations of degree of positional smectic order are decoupled from the layer and director fluctuations and were found to contribute a short-range attractive contribution to the total Casimir force. The coupled fluctuations of director and smectic layers result in a long-range Casimir force. It turned out that the effect of director degrees of freedom is important at small thicknesses of the systems whereas at large thicknesses the force can be modeled by considering only layer fluctuations while assuming that the director rigidly follows layer deformations. We evaluated the net effect of the director-layer coupling by comparing the "coupled" force to its "uncoupled" counterpart where director and layer fluctuations were treated independently. We found out that the coupling increases the force by no more than a few ten percent except in some special cases. With results presented in this Chapter we have provided a complete picture, the first to our knowledge, of the Casimir effect in planar smectic-A systems with homogeneous equilibrium structure.

In Chapter 4 we addressed some peculiarities related to the smectic-A to smectic-C phase transition. The theoretical model that we used enabled the study of the plain as well as the chiral smectics. Especially interesting was the case of a frustrated

homeotropic cell, where smectic-A structure is stabilized by the boundaries and supercooled below the bulk phase transition temperature. In this case the fluctuations and the force are enhanced. At the structural transition to a deformed smectic-C structure, the Casimir force exhibits repulsive logarithmic divergence characteristic for continous structural transitions. However, we did not fully solve the problem of the Casimir force in frustrated systems as we were unable to regularize the divergent bulk contribution with our calculation method. Fortunately, this contribution is thickness independent and therefore of no practical importance but the theoretical challenge remains. On the other hand, in free-standing smectic films with no surface-induced frustration the phase transition is characterized by an increased magnitude of the Casimir force but there is no divergence present. We also analyzed the effect of different boundary conditions on the Casimir force induced by massive director fluctuations with finite correlation length in smectic-A phase. We found that in thin cells the effective anchoring strength is determined by the ratio of the anchoring extrapolation lengths and thickness of the system. On the other hand, in thick cells the effective anchoring is determined by the ratio of extrapolation lengths and the correlation length of fluctuations. In the case of symmetric boundary conditions at the plates (effectively strong-strong or weak-weak anchoring) the Casimir force is attractive whereas in the case of asymmetric boundary conditions (effectively strong-weak anchoring) the force is repulsive, in agreement with the previous studies of the Casimir force in other systems.

A special attention was devoted to the Casimir force in systems with non-trivial equilibrium structure, which were only rarely studied in the past. We first considered two systems, dilated or compressed smectic cell and smectic film with enhanced surface order, where the inhomogeneity of equilibrium order did not affect the Casimir force. We came to the conclusion that when the free energy functional of a system is quadratic and the boundary conditions are fixed an inhomogeneous equilibrium ordering does not affect the Hamiltonian of fluctuations and hence does also not affect the Casimir force. In Chapter 5 we considered two systems where the non-trivial equilibrium order resulted in spatial dependence of material constants. In a smectic cell with surface enhanced elastic constants we discovered that the otherwise long-range smectic force becomes short-range. This inhomogeneity thus acts as some effective mass of fluctuating fields. Furthermore we analyzed how the surface-induced presmectic order, which increases the energy of director fluctuations, affects the Casimir force in a nematic system. We found that the magnitude of the force in such a system is reduced as compared to the long-range nematic force. In both systems we had to introduce several approximations in order to calculate the force, therefore the obtained results do not give the final answer on the Casimir force in systems with inhomogeneous equilibrium order. Nevertheless, we believe that an instructive qualitative picture of the phenomenon in such systems has been obtained.

Future perspectives

Undoubtedly, the main challenge in the theory of the Casimir force in liquid crystals is presented by systems with non-trivial equilibrium order and hence spatially dependent Hamiltonian of fluctuations. In this thesis we were able to give a solution for some special examples. The treatment of the more general cases will probably require a more sophisticated calculation and regularization methods. As in real confined systems some inhomogeneity of equilibrium order – either nematic or smectic – is frequently encountered, these open problems are highly relevant.

Some interesting problems concerning the chiral smectics also remain open for further studies. In the thesis we addressed the Casimir force induced by orientational fluctuations, while the polarization fluctuations were eliminated by the adiabatic approximation. However, at least two effects related to the presence of spontaneous polarization should be considered. Firstly, the fluctuations of orientational order result in inhomogeneity of spontaneous polarization, which leads to appearance of space charge and Coulomb interaction in the system. And secondly, the spontaneous polarization can be coupled to an external electric field. It would be interesting to investigate how these two effects affect the behaviour of the Casimir force in chiral smectics.

The main problem in the field remains the lack of experimental evidence of the Casimir interaction. It appears that liquid crystal systems are simply too complex to allow for the detection of the Casimir force, because there is always a variety of other phenomena which mask the Casimir interaction. New possibilities for the observation of the phenomenon could open with the development of colloidal systems with nano-sized dispersed particles, where the fluctuation-induced forces presumably dominate the elastic liquid crystal interaction. We believe that an experimental confirmation of the Casimir force in a liquid-crystalline system would provide a motivation for further studies in this field, as it happened in the case of electromagnetic Casimir effect.

Appendix

Calculation of quantum propagators

Throughout this thesis, we employed the analogy between partition functions of thermal fluctuations in one-dimensional systems and propagators of quantum systems to obtain the free energy of fluctuations. Here we present technical details of propagator evaluation.

The propagator for a quantum system evolving from state x_a at time t_a to a state x_b at time t_b is defined as [167]

$$(x_b t_b | x_a t_a) = \sum_{\substack{\text{all paths} \\ (x_a,t_a)\to(x_b,t_b)}} \exp\left(i\mathcal{A}[x]/\hbar\right) \equiv \int_{(x_a,t_a)\to(x_b,t_b)} \mathcal{D}x \, \exp\left(i\mathcal{A}[x]/\hbar\right) \ . \quad \text{(A.1)}$$

This definition has a simple intuitive interpretation. The amplitude of the propagator is obtained by summing over all paths $x(t)$ along which a system can possibly evolve, assigning each path a phase factor $\exp\left(i\mathcal{A}[x]/\hbar\right)$. Here $A[x]$ is the action of the system defined by

$$\mathcal{A}[x] = \int_{t_a}^{t_b} L(x,\dot{x})\,\mathrm{d}t \ , \quad \text{(A.2)}$$

with $L(x,\dot{x})$ being the Lagrangian of the system.

A.1 Quantum propagator for harmonic oscillator

The action for harmonic oscillator reads

$$\mathcal{A}[x] = \int_{t_a}^{t_b} L(x,\dot{x})\,\mathrm{d}t = \int_{t_a}^{t_b} \frac{1}{2} M\left[\dot{x}^2 - \omega^2(t)x^2\right]\,\mathrm{d}t \ , \quad \text{(A.3)}$$

where we allow for time-dependent frequency $\omega(t)$. For calculation of the propagator it is convenient to employ the splitting of paths into classical and fluctuation part

$$x(t) = x_{cl}(t) + \delta x(t) \ . \quad \text{(A.4)}$$

The classical path $x_{cl}(t)$ is the path which minimizes the action $\mathcal{A}[x]$ and is obtained from Euler-Lagrange equation which gives the equation of motion

$$\ddot{x}_{cl} + \omega^2(t) x_{cl} = 0 \tag{A.5}$$

with boundary conditions $x_{cl}(t_a) = x_a$ and $x_{cl}(t_b) = x_b$. The action is now decomposed into a classical and a fluctuating part

$$\mathcal{A}[x] = \mathcal{A}_{cl}[x_{cl}] + \mathcal{A}_{fl}[\delta x] \tag{A.6}$$

$$\mathcal{A}[x] = \int_{t_a}^{t_b} \frac{1}{2} M \left[\dot{x}_{cl}^2 - \omega^2(t) x_{cl}^2\right] \, \mathrm{d}t + \int_{t_a}^{t_b} \frac{1}{2} M \left[(\delta\dot{x})^2 - \omega^2(t)(\delta x)^2\right] \, \mathrm{d}t \,, \tag{A.7}$$

with boundary conditions for fluctuating part $\delta x(t_a) = \delta x(t_b) = 0$. Due to the extremality of classical action, there is no mixed term between the classical path and fluctuations. Therefore also the propagator is split into a classical and a fluctuation factor

$$(x_b t_b | x_a t_a) = \int \mathcal{D}x \, \exp\left(i\mathcal{A}[x]/\hbar\right) = \exp\left(i\mathcal{A}_{cl}/\hbar\right) F_\omega(t_b, t_a) \,. \tag{A.8}$$

The fluctuation factor

$$F_\omega(t_b, t_a) = \int_{(0,t_a)\to(0,t_b)} \mathcal{D}(\delta x) \, \exp\left(i\mathcal{A}_{fl}[\delta x]/\hbar\right) \,, \tag{A.9}$$

can be evaluated in various ways. We here follow the approach with a discretization of time axis presented in Ref. [166]. First, the time interval $[t_a, t_b]$ is sliced into $N+1$ short intervals of length ϵ. The action $\mathcal{A}_{fl}[\delta x]$ in discretized form reads

$$\mathcal{A}_{fl}^N[\delta x] = \sum_{j=0}^{N} \frac{M}{2\epsilon} \left(\delta x_{j+1} - \delta x_j\right)^2 - \frac{1}{2}\epsilon M \omega_j^2 \left(\delta x_j\right)^2 \,, \tag{A.10}$$

where $\delta x_j = \delta x(t_j)$ and $\omega_j = \omega(t_j)$. The boundary conditions require $\delta x_0 = \delta x(t_a) = 0$ and $\delta x_{N+1} = \delta x(t_b) = 0$. The fluctuation factor is now given as

$$\begin{aligned} F_\omega(t_b, t_a) = \lim_{N\to\infty} \int_{-\infty}^{\infty} \mathrm{d}\delta x_1 \ldots \mathrm{d}\delta x_N \left(\frac{M}{2\pi i\hbar\epsilon}\right)^{(N+1)/2} \\ \times \exp\left\{\frac{i}{\hbar} \sum_{j=0}^{N} \left[\frac{M}{2\epsilon}(\delta x_{j+1} - \delta x_j)^2 - \frac{1}{2}\epsilon M \omega_j^2 (\delta x_j)^2\right]\right\} \,. \end{aligned} \tag{A.11}$$

Some caution is necessary with determination of normalization factor but we shall not deal with this detail here. The calculation of fluctuation factor requires an evaluation of a series of Gaussian integrals. For this purpose it is convenient to introduce the matrix notation. We define a vector η as

$$\eta = \begin{bmatrix} \delta x_1 \\ \vdots \\ \delta x_N \end{bmatrix} \,. \tag{A.12}$$

The argument of exponent in Eq. (A.11) can now be written as $-\eta^T\sigma\eta$ where the matrix σ is given by

$$\sigma = \frac{M}{2\epsilon\hbar i}\begin{bmatrix} 2 & -1 & & & & \\ -1 & 2 & -1 & & & \\ & -1 & 2 & \ddots & & \\ & & & \ddots & & \\ & & & & 2 & -1 \\ & & & & -1 & 2 \end{bmatrix} + \frac{iM\epsilon}{2\hbar}\begin{bmatrix} \omega_1^2 & & & & & \\ & \omega_2^2 & & & & \\ & & \ddots & & & \\ & & & \ddots & & \\ & & & & \omega_{N-1}^2 & \\ & & & & & \omega_N^2 \end{bmatrix} \tag{A.13}$$

The fluctuation factor can now be concisely written as

$$F_\omega(t_b,t_a) = \lim_{N\to\infty}\left(\frac{M}{2\pi i\hbar\epsilon}\right)^{(N+1)/2}\int \mathrm{d}^N\eta\,\exp\left(-\eta^T\sigma\eta\right)\ . \tag{A.14}$$

The matrix σ is of the form $i\tilde{\sigma}$ where $\tilde{\sigma}$ is real and Hermitian. Thus σ can be diagonalized by a unitary matrix

$$\sigma = U^\dagger\sigma_D U\ , \tag{A.15}$$

where σ_D is the diagonal matrix of eigenvalues of σ. Now the above integral can be transformed and directly evaluated

$$\int \mathrm{d}^N\eta\,\exp\left(-\eta^T\sigma\eta\right) = \int \mathrm{d}^N\zeta\,\exp\left(-\zeta^T\sigma_D\zeta\right) = \prod_{\alpha=1}^{N}\sqrt{\frac{\pi}{\sigma_\alpha}} = \frac{\pi^{N/2}}{\sqrt{\det\sigma}}\ , \tag{A.16}$$

where we introduced the coordinate transformation $\zeta = U\eta$ and because U is unitary the Jacobian for going from $\mathrm{d}^N\eta$ to $\mathrm{d}^N\zeta$ is equal to 1. The fluctuation factor is now given by

$$F_\omega(t_b,t_a) = \lim_{N\to\infty}\left[\left(\frac{M}{2\pi i\hbar\epsilon}\right)^{N+1}\frac{\pi^N}{\det\sigma}\right]^{1/2} = \lim_{N\to\infty}\left[\frac{M}{2\pi i\hbar}\times\frac{1}{\epsilon}\frac{1}{\left(\frac{2i\hbar\epsilon}{M}\right)^N\det\sigma}\right]^{1/2}\ , \tag{A.17}$$

and the main task is now the evaluation of determinant $\det\sigma$. We first define the function f such that

$$f(t_b,t_a) = \lim_{N\to\infty}\left[\epsilon\left(\frac{2i\hbar\epsilon}{M}\right)^N\det\sigma\right] \tag{A.18}$$

and a renormalized determinant

$$\left(\frac{2i\hbar\epsilon}{M}\right)^N \det\sigma = \det\left\{\begin{bmatrix} 2 & -1 & & & & \\ -1 & 2 & -1 & & & \\ & -1 & 2 & \ddots & & \\ & & & \ddots & & \\ & & & & 2 & -1 \\ & & & & -1 & 2 \end{bmatrix} - \epsilon^2 \begin{bmatrix} \omega_1^2 & & & & & \\ & \omega_2^2 & & & & \\ & & \ddots & & & \\ & & & \ddots & & \\ & & & & \omega_{N-1}^2 & \\ & & & & & \omega_N^2 \end{bmatrix}\right\} \equiv \det\sigma_N^{'} \equiv p_N \ . \tag{A.19}$$

Next we define truncated $j \times j$ matrices $\sigma_j^{'}$ that consist of the first j rows and columns of $\sigma_N^{'}$ with determinant $\det\sigma_j^{'} = p_j$. By expanding $\sigma_{j+1}^{'}$ in minors, the following recursion formula is obtained

$$p_{j+1} - \left(2 - \epsilon^2\omega_{j+1}^2\right) p_j + p_{j-1} = 0 \ , \tag{A.20}$$

with $p_1 = 2 - \epsilon^2\omega_1^2$ and p_0 is defined to be 1. Rewriting Eq. (A.20) into the form

$$\frac{p_{j+1} - 2p_j + p_{j-1}}{\epsilon^2} + \omega_{j+1}^2 p_j = 0 \tag{A.21}$$

it is apparent that p_N will be obtained by solving a differential equation. Introducing $\phi(t) = \epsilon p_j$ for $t = t_a + j\epsilon$ we obtain, in the limit of $\epsilon \to 0$, the differential equation

$$\frac{\mathrm{d}^2\phi}{\mathrm{d}t^2} + \omega^2(t)\phi = 0 \ . \tag{A.22}$$

The initial conditions for $\phi(t)$ follow from

$$\phi(t_a) = \epsilon p_0 \to 0 \ , \tag{A.23}$$

$$\frac{\mathrm{d}\phi(t_a)}{\mathrm{d}t} = \epsilon\left(\frac{p_1 - p_0}{\epsilon}\right) = 2 - \epsilon^2\omega_1^2 - 1 \to 1 \ , \tag{A.24}$$

in the limit $N \to \infty$ ($\epsilon \to 0$). Finally the function $f(t_b, t_a) = \phi(t_b)$ is obtained by solving the differential equation

$$\frac{\mathrm{d}^2 f(t, t_a)}{\mathrm{d}t^2} + \omega(t)^2 f(t, t_a) = 0 \tag{A.25}$$

with the initial conditions

$$f(t_a, t_a) = 0 \ , \quad \frac{\mathrm{d}f(t, t_a)}{\mathrm{d}t}\,|_{t=t_a} = 1 \ . \tag{A.26}$$

We can now write the propagator of harmonic oscillator in the final form

$$(x_b t_b|x_a t_a) = F_\omega(t_b, t_a) \exp\left(i\mathcal{A}_{cl}/\hbar\right) = \sqrt{\frac{M}{2\pi i\hbar f(t_b, t_a)}} \exp\left(i\mathcal{A}_{cl}/\hbar\right) . \tag{A.27}$$

As an example we can now directly calculate the propagator for harmonic oscillator with constant frequency [$\omega \neq \omega(t)$]. From the Euler-Lagrange equation [Eq. (A.5)] we obtain the classical path

$$x_{cl}(t) = \frac{x_b \sin[\omega(t - t_a)] + x_a \sin[\omega(t_b - t)]}{\sin[\omega(t_b - t_a)]} , \tag{A.28}$$

which starts at the point x_a at time t_a and ends at point x_b at time t_b. The classical action can now be readily evaluated leading to

$$\mathcal{A}_{cl} = \frac{M\omega}{2\sin[\omega(t_b - t_a)]} \left\{(x_a^2 + x_b^2)\cos[\omega(t_b - t_a)] - 2x_a x_b\right\} . \tag{A.29}$$

The function $f(t_b, t_a)$ is obtained straightforwardly from Eqs. (A.25 and A.26)

$$f(t_b, t_a) = \frac{\sin[\omega(t_b - t_a)]}{\omega} . \tag{A.30}$$

The propagator now reads

$$\begin{aligned}(x_b t_b|x_a t_a) = &\sqrt{\frac{M\omega}{2\pi i\hbar \sin[\omega(t_b - t_a)]}} \\ &\times \exp\left\{\frac{iM\omega}{2\hbar\sin[\omega(t_b - t_a)]} \left[(x_b^2 + x_a^2)\cos[\omega(t_b - t_a)] - 2x_b x_a\right]\right\} .\end{aligned} \tag{A.31}$$

A.2 Quantum propagator for two coupled harmonic oscillators

The Lagrangian for two coupled harmonic oscillators can be written as

$$L = \sum_{k=1,2} \frac{1}{2} M_k \left(\dot{x}_k^2 - \omega_k^2 x_k^2\right) - \lambda x_1 x_2 . \tag{A.32}$$

We wish to calculate the propagator

$$(\mathbf{x}_b t_b|\mathbf{x}_a t_a) = \int_{(\mathbf{x}_a, t_a)\to(\mathbf{x}_b, t_b)} \mathcal{D}x_1 \mathcal{D}x_2 \exp\left(\frac{i}{\hbar}\int_{t_a}^{t_b} L(\mathbf{x}, \dot{\mathbf{x}})\,\mathrm{d}t\right) , \tag{A.33}$$

where $\mathbf{x} = (x_1, x_2)$. The calculation presented here follows the approach of Ref. [169].

The first step in evaluation of the propagator is to diagonalize the Lagrangian. This can be done conveniently by applying the following coordinate transformation

$$\begin{bmatrix} x_1 \\ x_2 \end{bmatrix} = \begin{bmatrix} \sqrt{\frac{M}{M_1}}\cos(\phi) & \sqrt{\frac{M}{M_1}}\sin(\phi) \\ -\sqrt{\frac{M}{M_2}}\sin(\phi) & \sqrt{\frac{M}{M_2}}\cos(\phi) \end{bmatrix} \begin{bmatrix} y_1 \\ y_2 \end{bmatrix} . \tag{A.34}$$

Here ϕ is the angle of rotation and M an arbitrary parameter with dimension of mass. This leads to Lagrangian

$$L' = \frac{1}{2}M(\dot{y}_1^2 + \dot{y}_2^2) - \alpha y_1^2 - \beta y_2^2 - \gamma y_1 y_2 \, , \tag{A.35}$$

where

$$\begin{aligned} \alpha &= \frac{1}{2}M\omega_1^2\cos^2(\phi) + \frac{1}{2}M\omega_2^2\sin^2(\phi) - \frac{1}{2}\lambda\frac{M}{\sqrt{M_1M_2}}\sin(2\phi) \, , \\ \beta &= \frac{1}{2}M\omega_1^2\sin^2(\phi) + \frac{1}{2}M\omega_2^2\cos^2(\phi) + \frac{1}{2}\lambda\frac{M}{\sqrt{M_1M_2}}\sin(2\phi) \, , \\ \gamma &= \frac{1}{2}M(\omega_1^2 - \omega_2^2)\sin(2\phi) + \lambda\frac{M}{\sqrt{M_1M_2}}\cos(2\phi) \, . \end{aligned} \tag{A.36}$$

The Jacobian of this coordinate transformation is equal to $J = \sqrt{M_1M_2}/M$ so the path integral measure changes as $\mathcal{D}x_1\mathcal{D}x_2 \to J\mathcal{D}y_1\mathcal{D}y_2$. As we wish to obtain a diagonalized Lagrangian we set the parameter γ to 0 which gives the condition

$$\tan(2\phi) = \frac{2\lambda}{\sqrt{M_1M_2}(\omega_2^2 - \omega_1^2)} \, . \tag{A.37}$$

Solving this equation we obtain two physically equivalent solutions for decoupling angle ϕ, which differ only by interchange of coordinates y_i. One of the solutions is given by

$$\cos(\phi) = \sqrt{\frac{1+R}{2}} \, , \tag{A.38}$$

where

$$R = \frac{\sqrt{M_1M_2(\omega_2^2 - \omega_1^2)^2}}{\sqrt{M_1M_2(\omega_2^2 - \omega_1^2)^2 + 4\lambda^2}} \, . \tag{A.39}$$

With this solution the Lagrangian is transformed into the diagonal form

$$L' = \frac{1}{2}M\left[\dot{y}_1^2 - \Omega_1^2 y_1^2 + \dot{y}_2^2 - \Omega_2^2 y_2^2\right] \, , \tag{A.40}$$

with

$$\begin{aligned} \Omega_1^2 &= \frac{1}{2}\left[\omega_1^2 + \omega_2^2 - \sqrt{(\omega_1^2 - \omega_2^2)^2 + \frac{4\lambda^2}{M_1M_2}}\right] \\ \Omega_2^2 &= \frac{1}{2}\left[\omega_1^2 + \omega_2^2 + \sqrt{(\omega_1^2 - \omega_2^2)^2 + \frac{4\lambda^2}{M_1M_2}}\right] \, . \end{aligned} \tag{A.41}$$

The problem is now reduced to calculation of propagators for two independent harmonic oscillators

$$(\mathbf{x}_b t_b|\mathbf{x}_a t_a) = \frac{\sqrt{M_1 M_2}}{M}\,(y_{1b} t_b|y_{1a} t_a) \times (y_{2b} t_b|y_{2a} t_a) \tag{A.42}$$

and the solution Eq. (A.31) can readily be applied. The final result is obtained by returning to original coordinates

$$\begin{bmatrix} y_1 \\ y_2 \end{bmatrix} = \begin{bmatrix} \sqrt{\frac{M_1}{M}}\cos(\phi) & -\sqrt{\frac{M_2}{M}}\sin(\phi) \\ \sqrt{\frac{M_1}{M}}\sin(\phi) & \sqrt{\frac{M_2}{M}}\cos(\phi) \end{bmatrix} \begin{bmatrix} x_1 \\ x_2 \end{bmatrix} . \tag{A.43}$$

After lengthy but straightforward calculation the propagator for two coupled harmonic oscillators reads

$$\begin{aligned}
(\mathbf{x}_b t_b|\mathbf{x}_a t_a) = {} & \frac{1}{2\pi i\hbar}\left[\frac{M_1 M_2 \Omega_1 \Omega_2}{\sin(\Omega_1\tau)\sin(\Omega_2\tau)}\right]^{1/2} \\
& \times \exp\left\{\frac{i\Omega_1}{2\hbar\sin(\Omega_1\tau)}\Big[\cos(\Omega_1\tau)\Big(M_1 C^2 x_1''^2 + M_2 S^2 x_2''^2 - 2\sqrt{M_1 M_2}SC x_1'' x_2'' \right. \\
& + M_1 C^2 x_1'^2 + M_2 S^2 x_2'^2 - 2\sqrt{M_1 M_2}SC x_1' x_2'\Big) - 2M_1 C^2 x_1' x_1'' \\
& \left. + 2\sqrt{M_1 M_2}SC x_1' x_2'' + 2\sqrt{M_1 M_2}SC x_2' x_1'' - 2M_2 S^2 x_2' x_2''\Big]\right\} \\
& \times \exp\left\{\frac{i\Omega_2}{2\hbar\sin(\Omega_2\tau)}\Big[\cos(\Omega_2\tau)\Big(M_2 C^2 x_2''^2 + M_1 S^2 x_1''^2 + 2\sqrt{M_1 M_2}SC x_2'' x_1'' \right. \\
& + M_2 C^2 x_2'^2 + M_1 S^2 x_1'^2 + 2\sqrt{M_1 M_2}SC x_2' x_1'\Big) - 2M_2 C^2 x_2' x_2'' \\
& \left. - 2\sqrt{M_1 M_2}SC x_2' x_1'' - 2\sqrt{M_1 M_2}SC x_1' x_2'' - 2M_1 S^2 x_1' x_1''\Big]\right\} ,
\end{aligned} \tag{A.44}$$

where $\tau = t_b - t_a$, $S = \sin(\phi)$ and $C = \cos(\phi)$.

Bibliography

[1] H. B. G. Casimir, Proc. Kon. Ned. Akad. Wet. **51**, 793 (1948).

[2] for extensive treatment and literature on the Casimir force, see the review articles by Lamoreaux [Am. J. Phys. **67**, 850 (1999)], Kardar et al. [Rev. Mod. Phys. **71**, 1233 (1999)], Bordag et al. [Phys. Rep. **353**, 1-205, (2001)], Milton [J. Phys. A **37**, R209 (2004)] and Lamoreaux [Rep. Prog. Phys. **68**, 201 (2005)] .

[3] J. Mahanty and B. W. Ninham, *Dispersion Forces* (Academic Press, London, 1976).

[4] E. M. Lifshitz, Zh. Eksp. Teor. Fiz. **29**, 94 (1955), [Sov. Phys. JETP **2**, 73, (1956)].

[5] L. S. Brown and G. J. Maclay, Phys. Rev. **184**, 1272 (1969).

[6] S. Tadaki and S. Takagi, Prog. Theor. Phys. **75**, 262 (1986).

[7] G. Plunien, B. Muller, and W. Greiner, Physica **145A**, 202 (1987).

[8] K. Kirsten, J. Phys. A **24**, 3281 (1991).

[9] N. F. Svaiter, Nuo. Cim. **105A**, 959 (1992).

[10] C. Genet, A. Lambrecht, and S. Reynaud, Phys. Rev. A **62**, 012110 (2000).

[11] M. Bordag, B. Geyer, G. L. Klimchitskaya, and V. M. Mostepanenko, Phys. Rev. Lett. **85**, 503 (2000).

[12] V. M. Mostepanenko *et al.*, J. Phys. A **39**, 6589 (2006).

[13] J. Schwinger, L. L. DeRaad, and K. A. Milton, Ann. Phys. **115**, 1 (1978).

[14] M. Bordag, G. L. Klimchitskaya, and V. M. Mostepanenko, Mod. Phys. Lett. A **9**, 2515 (1994).

[15] M. Bordag, G. L. Klimchitskaya, and V. M. Mostepanenko, Phys. Lett. A **200**, 95 (1995).

[16] M. Bordag, G. L. Klimchitskaya, and V. M. Mostepanenko, Int. J. Mod. Phys. A **10**, 2661 (1995).

[17] M. Bordag and K. Scharnhorst, Phys. Rev. Lett. **81**, 3815 (1998).

[18] V. B. Bezerra, G. L. Klimchitskaya, and V. M. Mostepanenko, Phys. Rev. A **62**, 014102 (2000).

[19] A. Lambrecht and S. Reynaud, Eur. Phys. J. D **8**, 309 (2000).

[20] G. L. Klimchitskaya, U. Mohideen, and V. M. Mostepanenko, Phys. Rev. A **61**, 062107 (2000).

[21] G. L. Klimchitskaya and V. M. Mostepanenko, Phys. Rev. A **63**, 062108 (2001).

[22] C. Genet, A. Lambrecht, P. M. Neto, and S. Reynaud, Europhys. Lett. **62**, 484 (2003).

[23] F. J. Belinfante, Am. J. Phys. **55**, 134 (1987).

[24] D. Kupiszevska, J. of Mod. Optics **40**, 517 (1993).

[25] *Cavity Quantum Electrodynamics*, edited by P. R. Berman (Academic Press, San Diego, 1994).

[26] M. Schaden and L. Spruch, Phys. Rev. A **58**, 935 (1998).

[27] O. Kenneth, I. Klich, A. Mann, and M. Revzen, Phys. Rev. Lett. **89**, 033001 (2002).

[28] T. H. Boyer, Phys. Rev. **174**, 1764 (1968).

[29] K. A. Milton, L. L. De-Raad, and J. Schwinger, Ann. Phys. **115**, 288 (1978).

[30] S. G. Mamayev and N. N. Trunov, Theor. Math. Phys. **38**, 228 (1979).

[31] L. L. DeRaad and K. A. Milton, Ann. Phys. **136**, 229 (1981).

[32] E. Elizalde, Phys. Lett. B **213**, 477 (1988).

[33] I. Brevik and M. Lygren, Ann. Phys. **251**, 157 (1996).

[34] G. J. Maclay, Phys. Rev. A **61**, 052110 (2000).

[35] M. Bordag, G. Petrov, and D. Robashik, Yad. Fiz. **39**, 1315 (1984).

[36] D. A. R. Dalvit and F. D. Mazzitelli, Phys. Rev. A **57**, 2113 (1998).

[37] R. Golestanian and M. Kardar, Phys. Rev. A **58**, 1713 (1998).

[38] G. Plunien, R. Schützhold, and G. Soff, Phys. Rev. Lett. **84**, 1882 (2000).

[39] D. A. R. Dalvit, F. D. Mazzitelli, and X. O. Millan, J. Phys. A **39**, 6261 (2006).

[40] V. M. Mostepanenko and N. N. Trunov, *The Casimir Effect and its Applications* (Clarendon Press, Oxford, 1997).

[41] E. Elizalde, M. Bordag, and K. Kirsten, J. Phys. A **31**, 1743 (1998).

[42] K. A. Milton, *The Casimir Effect* (World Scientific, Singapore, 2001).

[43] S. K. Blau, E. I. Guendelman, A. Taormina, and L. C. R. Wijewardhana, Phys. Lett. B **144**, 30 (1984).

[44] J. S. Dowker, Phys. Rev. D **29**, 2773 (1984).

[45] P. Candelas and S. Weinberga, Nucl. Phys. B **237**, 397 (1984).

[46] D. Birmingham, R. Kantowski, and K. A. Milton, Phys. Rev. D **38**, 1809 (1988).

[47] Y. Srivastava, A. Widom, and M. H. Friedman, Phys. Rev. Lett. **55**, 2246 (1985).

[48] Y. Srivastava and A. Widom, Phys. Rep. **148**, 1 (1987).

[49] I. Brevik, Phys. Rev. D **36**, 1951 (1987).

[50] R. M. Nugayev and V. I. Bashkov, Phys. Lett. A **69A**, 385 (1979).

[51] R. M. Nugayev, Phys. Lett. **91A**, 216 (1982).

[52] I. Brevik and H. Kolbenstvedt, Nuovo Cimento **82B**, 71 (1984).

[53] R. M. Nugayev, Lett. Nuovo Cimento **39**, 331 (1984).

[54] D. Vick, Nuovo Cimento **94B**, 54 (1986).

[55] F. Belgiorno and S. Liberati, Gen. Relat. Gravit. **29**, 1181 (1997).

[56] A. Larraza, C. D. Holmes, R. T. Susbilla, and B. Denardo, J. Acous. Soc. Am. **103**, 2267 (1998).

[57] A. Larraza and B. Denardo, Phys. Lett. A **248**, 151 (1998).

[58] A. Larraza, Am. J. Phys. **67**, 1028 (1999).

[59] S. L. Boersma, Am. J. Phys. **64**, 539 (1996).

[60] M. Goulian, R. Bruinsma, and P. Pincus, Europhys. Lett. **22**, 145 (1993).

[61] R. Golestanian, Europhys. Lett. **36**, 557 (1996).

[62] R. Golestanian, R. M. Goulian, and M. Kardar, Europhys. Lett. **33**, 241 (1996).

[63] M. Krech, *The Casimir Effect in Critical Systems* (World Scientific, Singapore, 1994).

[64] T. W. Burkhardt and E. Eisenriegler, Phys. Rev. Lett. **74**, 3189 (1995).

[65] M. Krech, Phys. Rev. E **56**, 1642 (1997).

[66] A. Hanke, F. Schlesener, E. Eisenriegler, and S. Dietrich, Phys. Rev. Lett. **81**, 1885 (1998).

[67] A. Mukhopadhyay and B. M. Law, Phys. Rev. Lett. **83**, 772 (1999).

[68] N. Uchida, Phys. Rev. Lett. **87**, 216101 (2001).

[69] F. Schlesener, A. Hanke, and S. Dietrich, J. Stat. Phys. **110**, 981 (2003).

[70] R. Garcia and M. H. W. Chan, Phys. Rev. Lett. **83**, 1187 (1999).

[71] R. Garcia and M. H. W. Chan, Phys. Rev. Lett. **88**, 086101 (2002).

[72] X. S. Chen and V. Dohm, Physica B **329**, 202 (2003).

[73] A. Maciolek and S. Dietrich, Europhys. Lett. **74**, 22 (2006).

[74] P. Attard, R. Kjellander, D. J. Mitchell, and B. Jonsson, J. Chem. Phys. **89**, 1664 (1988).

[75] P. Attard, D. J. Mitchell, and B. W. Ninham, J. Chem. Phys. **88**, 4987 (1988).

[76] R. Podgornik and J. Dobnikar, J. Chem. Phys. **115**, 1951 (2001).

[77] M. J. Sparnaay, Physica **24**, 751 (1958).

[78] S. K. Lamoreaux, Phys. Rev. Lett. **78**, 5 (1997).

[79] S. K. Lamoreaux, Phys. Rev. Lett. **81**, 5475 (1998).

[80] U. Mohideen and A. Roy, Phys. Rev. Lett. **81**, 4549 (1998).

[81] A. Roy and U. Mohideen, Phys. Rev. Lett. **82**, 4380 (1999).

[82] A. Roy, C. Y. Lin, and U. Mohideen, Phys. Rev. D **60**, 111101 (1999).

[83] G. L. Klimchitskaya, A. Roy, U. Mohideen, and V. M. Mostepanenko, Phys. Rev. A **60**, 3487 (1999).

[84] B. W. Harris, F. Chen, and U. Mohideen, Phys. Rev. A **62**, 052109 (2000).

[85] T. Ederth, Phys. Rev. A **62**, 062104 (2000).

[86] G. Bressi, G. Carugno, R. Onofrio, and G. Ruoso, Phys. Rev. Lett. **88**, 041804 (2002).

[87] F. Chen, U. Mohideen, G. L. Klimchitskaya, and V. M. Mostepanenko, Phys. Rev. Lett. **88**, 101801 (2002).

[88] F. Chen, U. Mohideen, G. L. Klimchitskaya, and V. M. Mostepanenko, Phys. Rev. A **66**, 032113 (2002).

[89] F. Chen, B. W. Harris, A. Roy, and U. Mohideen, Int. J. Mod. Phys. A **17**, 711 (2002).

[90] F. Chen, U. Mohideen, G. L. Klimchitskaya, and V. M. Mostepanenko, Phys. Rev. A **72**, 020101 (2005).

[91] F. Chen and U. Mohideen, J. Phys. A **39**, 6233 (2006).

[92] H. B. Chan *et al.*, Science **291**, 1941 (2001).

[93] R. S. Decca, D. Lopez, E. Fischbach, and D. E. Krause, Phys. Rev. Lett. **91**, 050402 (2003).

[94] R. S. Decca *et al.*, Phys. Rev. D **68**, 116003 (2003).

[95] G. L. Klimchitskaya *et al.*, Int. J. Mod. Phys. A **20**, 2205 (2005).

[96] V. M. Mostepanenko and I. Y. Sokolov, Phys. Lett. A **125**, 405 (1987).

[97] V. M. Mostepanenko and I. Y. Sokolov, Phys. Lett. A **132**, 313 (1988).

[98] M. Bordag, B. Geyer, G. L. Klimchitskaya, and V. M. Mostepanenko, Phys. Rev. D **58**, 075003 (1998).

[99] M. Bordag, B. Geyer, G. L. Klimchitskaya, and V. M. Mostepanenko, Phys. Rev. D **60**, 055004 (1999).

[100] G. L. Klimchitskaya and U. Mohideen, Int. J. Mod. Phys. A **17**, 4143 (2002).

[101] F. Chen, U. Mohideen, and P. W. Milonni, Int. J. Mod. Phys. A **20**, 2222 (2005).

[102] F. M. Serry, D. Walliser, and G. Maclay, J. Microelectromech. Syst. **4**, 193 (1995).

[103] F. M. Serry, D. Walliser, and G. Maclay, J. Appl. Phys. **84**, 2501 (1998).

[104] E. Buks and M. L. Roukes, Phys. Rev. B **63**, 033402 (2001).

[105] A. Mukhopadhyay and B. M. Law, Phys. Rev. E **62**, 5201 (2000).

[106] A. Mukhopadhyay and B. M. Law, Phys. Rev. E **63**, 041605 (2001).

[107] M. Fukuto, Y. F. Yano, and P. S. Pershan, Phys. Rev. Lett. **94**, 135702 (2005).

[108] D. Beysens and D. Esteve, Phys. Rev. Lett. **54**, 2123 (1985).

[109] T. Narayanan *et al.*, Phys. Rev. E **48**, 1989 (1993).

[110] Y. Jayalakshmi and E. W. Kaler, Phys. Rev. Lett. **78**, 1379 (1997).

[111] P. G. de Gennes and J. Prost, *The Physics of Liquid Crystals* (Clarendon Press, Oxford, 1993).

[112] P. Chatelain, P. Acta Cristallogr. **1**, 315 (1948).

[113] F. C. Frank, Disc. Faraday Soc. **25**, 19 (1958).

[114] A. Ajdari, L. Peliti, and J. Prost, Phys. Rev. Lett. **66**, 1481 (1991).

[115] A. Ajdari *et al.*, J. Phys. II (Paris) **2**, 487 (1992).

[116] P. Ziherl, R. Podgornik, and S. Žumer, Chem. Phys. Lett **295**, 99 (1998).

[117] P. Ziherl, Liq. Cryst. Today **11**, 1 (2002).

[118] H. Li and M. Kardar, Phys. Rev. Lett. **67**, 3275 (1991).

[119] H. Li and M. Kardar, Phys. Rev. A **46**, 6490 (1992).

[120] P. Ziherl, R. Podgornik, and S. Žumer, Phys. Rev. Lett. **82**, 1189 (1999).

[121] P. Ziherl, F. K. P. Haddadan, R. Podgornik, and S. Žumer, Phys. Rev. E **61**, 5361 (2000).

[122] P. Ziherl, R. Podgornik, and S. Žumer, Phys. Rev. Lett. **84**, 1228 (2000).

[123] F. K. pour Haddadan, D. W. Allender, and S. Žumer, Phys. Rev. E **64**, 061701 (2001).

[124] D. Bartolo, D. Long, and J. B. Fournier, Europhys. Lett. **49**, 729 (2000).

[125] J. Dobnikar and R. Podgornik, Europhys. Lett. **53**, 735 (2001).

[126] F. K. pour Haddadan, F. Schlesener, and S. Dietrich, Phys. Rev. E **70**, 041701 (2004).

[127] R. Golestanian, A. Ajdari, and J. B. Fournier, Phys. Rev. E **64**, 022701 (2001).

[128] L. V. Mikheev, Sov. Phys. JETP **69**, 358 (1989).

[129] P. Ziherl, Phys. Rev. E **61**, 4636 (2000).

[130] I. N. de Oliveira and M. L. Lyra, Phys. Rev. E **65**, 051711 (2002).

[131] I. N. de Oliveira and M. L. Lyra, Phys. Rev. E **70**, 050702(R) (2004).

[132] I. N. de Oliveira and M. L. Lyra, Physica A **344**, 595 (2004).

[133] I. N. de Oliveira, M. L. Lyra, and L. V. Mirantsev, Phys. Rev. E **73**, 041703 (2006).

[134] M. L. Lyra, M. Kardar, and N. F. Svaiter, Phys. Rev. E **47**, 3456 (1993).

[135] R. G. Horn, J. N. Israelachvili, and E. Perez, J. Physique **42**, 39 (1981).

[136] *Surfaces and Interfaces of Liquid Crystals*, edited by T. Rasing and I. Muševič (Springer, Berlin, 2004).

[137] P. Ziherl and I. Muševič, Liq. Cryst. **28**, 1057 (2001).

[138] S. Herminghaus *et al.*, Science **282**, 916 (1998).

[139] F. Vandenbrouck, M. P. Valignat, and A. M. Cazabat, Phys. Rev. Lett. **82**, 2693 (1999).

[140] P. Ziherl and S. Žumer, Eur. Phys. J. E **12**, 361 (2003).

[141] P. Richetti, P. Kekicheff, and P. Barois, J. Phys. II France **5**, 1129 (1995).

[142] P. Kekicheff and H. K. Christenson, Phys. Rev. Lett. **63**, 2823 (1989).

[143] P. Richetti, P. Kekicheff, J. L. Parker, and B. W. Ninham, Nature **346**, 252 (1990).

[144] I. Koltover *et al.*, J. Phys. II France **6**, 893 (1996).

[145] M. Ruths, S. Steinberg, and J. N. Israelachvili, Langmuir **12**, 6637 (1996).

[146] B. Cross and J. Crassous, Eur. Phys. J. E **14**, 249 (2004).

[147] J. Als-Nielsen, F. Christensen, and P. S. Pershan, Phys. Rev. Lett. **48**, 1107 (1982).

[148] B. M. Ocko *et al.*, Phys. Rev. Lett. **57**, 923 (1986).

[149] P. S. Pershan, A. Braslau, A. H. Weiss, and J. Als-Nielsen, Phys. Rev. A **35**, 4800 (1987).

[150] E. A. L. Mol *et al.*, Physica B **248**, 191 (1998).

[151] F. Picano, P. Oswald, and E. Kats, Phys. Rev. E **63**, 021705 (2001).

[152] A. Böttger, D. Frenkel, J. G. H. Joosten, and G. Krooshof, Phys. Rev. A **38**, 6316 (1988).

[153] J. Israelachvili, *Intermolecular & Surface Forces* (Academic Press, London, 1985).

[154] B. Markun and S. Žumer, Phys. Rev. E **68**, 021704 (2003).

[155] B. Markun and S. Žumer, Phys. Rev. E **73**, 031702 (2006).

[156] D. N. Moskvin, V. P. Romanov, and A. Y. Val'kov, Phys. Rev. E **49**, 4121 (1994).

[157] P. M. Chaikin and T. C. Lubensky, *Principles of condensed matter physics* (Cambridge University Press, Cambridge, 1995).

[158] V. L. Indenbom, S. A. Pikin, and E. B. Loginov, Kristallografiya **21**, 1093 (1976).

[159] J. W. Goodby *et al.*, *Ferroelectric Liquid Crystals: Principles, Properties and Applications*, *Ferroelectricity and Related Phenomena* (Gordon and Breach Science Publishers, Philadelphia, 1991).

[160] I. Muševič, R. Blinc, and B. Žekš, *The Physics of Ferroelectric and Antiferroelectric Liquid Crystals* (World Scientific, Singapore, 2000).

[161] R. B. Meyer, L. Liebert, L. Strzelecki, and P. Keller, J. Phys. (Paris), Lett. **36**, L69 (1975).

[162] R. B. Meyer, Mol. Cryst. Liq. Cryst. **40**, 33 (1977).

[163] A. Rapini and M. Papoular, J. Phys. Colloq. **30**, C4 (1969).

[164] S. Heinekamp *et al.*, Phys. Rev. Lett. **52**, 1017 (1984).

[165] R. P. Feynman and A. R. Hibbs, *Quantum mechanics and path integrals* (McGraw-Hill, New York, 1965).

[166] L. S. Schulman, *Techniques and Applications of Path Integration* (John Wiley, New York, 1981).

[167] H. Kleinert, *Path Integrals in Quantum Mechanics, Statistics, and Polymer Physics* (World Scientific, Singapore, 1990).

[168] C. Grosche and F. Steiner, *Handbook of Feynman Path Integrals* (Springer, Berlin, 1998).

[169] A. D. S. Dutra, J. Phys. A **25**, 4189 (1992).

[170] P. Ziherl, Ph.D. thesis, University of Ljubljana, Ljubljana, 1998.

[171] A. Šarlah and S. Žumer, Phys. Rev. E **64**, 051606 (2001).

[172] D. A. Dunmur, M. R. Manterfield, W. H. Miller, and J. K. Dunleavy, Mol. Cryst. Liq. Cryst. **45**, 127 (1978).

[173] C. Y. Young, R. Pindak, N. A. Clark, and R. B. Meyer, Phys. Rev. Lett. **40**, 773 (1978).

[174] K. Okano, Jap. J. Appl. Phys. **25**, L846 (1986).

[175] M. Lu, K. A. Crandall, and C. Rosenblatt, Phys. Rev. Lett. **68**, 3575 (1992).

[176] J. Prost and R. Bruinsma, Ferroelectrics **148**, 25 (1993).

[177] R. Bruinsma and J. Prost, J. Phys. II France **4**, 1209 (1994).

[178] G. Barbero and L. R. Evangelista, *An Elementary Course on The Continuum Theory for Nematic Liquid Crystals*, Vol. 3 of *Series on Liquid Crystals* (World Scientific, Singapore, 2001).

[179] S. Marčelja and N. Radić, Chem. Phys. Lett **42**, 129 (1976).

[180] F. K. P. Haddadan, Ph.D. thesis, University of Ljubljana, Ljubljana, 2001.

[181] *Handbook of mathematical functions*, edited by M. Abramowitz and I. A. Stegun (Dower Publ., New York, 1964).

Razširjeni povzetek

Uvod

Zgodovina Casimirjevega pojava sega v leto 1948, ko je nizozemski fizik H. B. G. Casimir napovedal obstoj privlačne interakcije med dvema vzporednima nenaelektrenima kovinskima ploščama [1]. Ta interakcija izvira iz spremenjenega spektra fluktuacij elektromagnetnega polja v ograjenem prostoru v primerjavi s spektrom polja na prostem. Pri absolutni ničli, kjer so prisotne le kvantne ničelne fluktuacije elektromagnetnega polja, je Casimirjeva sila enaka

$$\mathcal{F}_{Cas}(T=0) = -\frac{\hbar c \pi^2 S}{240 h^4} \,, \tag{1}$$

pri čemer je $\hbar$ Planckova konstanta, c hitrost svetlobe, S površina in h razdalja med ploščama. V limiti visokih temperatur, kjer prevladujejo termične fluktuacije polja, Casimirjeva sila znaša

$$\mathcal{F}_{Cas} = -\frac{k_B T S}{4\pi h^3}\zeta_R(3) \,, \tag{2}$$

kjer je k_B Boltzmannova konstanta in ζ_R Riemmanova funkcija zeta.

Casimirjevemu pionirskemu delu je sledila kopica teoretičnih in v zadnjih letih tudi eksperimentalnih študij Casimirjeve sile [2]. Te študije so obravnavale popravke h Casimirjevi sili zaradi končne temperature, končne prevodnosti in deformiranosti kovinskih plošč ter magnetnih efektov [5–27]. Nadalje so študije obravnavale Casimirjevo interakcijo v različnih geometrijah: sferični, cilindrični, toroidni in klinasti [28–34]. Kar nekaj pozornosti je bil deležen tudi dinamični Casimirjev pojav, pri katerem kovinski plošči ne mirujeta, ampak se gibljeta [35–39]. Prva zanesljiva eksperimentalna potrditev obstoja Casimirjeve sile je prišla šele leta 1997, skoraj pol stoletja za teoretično napovedjo. Lamoreaux je z uporabo elektromehanskega sistema uspel izmeriti silo med pozlačeno ploščo in sferično lečo, ki se je zelo dobro ujemala s teoretičnimi napovedmi [78]. Nadaljnji eksperimenti z mikroskopom na atomsko silo so prav tako potrdili obstoj Casimirjeve interakcije [80–84]. V novejših eksperimentih so uspeli izmeriti tudi silo v originalni Casimirjevi konfiguraciji [86], torej med dvema vzporednima ploščama, in silo med dvema prekrižanima valjema [85]. Prav tako so bili izvedeni dinamični eksperimenti, kjer so izmerili vpliv Casimirjeve sile na obnašanje mikromehanskih nihal [92–95].

Casimirjeva sila je univerzalen pojav, ki ni značilen le za elektromagnetno polje, ampak je prisoten v vsakem ograjenem sistemu, kjer robni pogoji spremenijo spekter fluktuacij nekega fizikalnega polja. Tako je Casimirjev pojav prisoten v kvantni kromodinamiki [40–42], kvantni elektrodinamiki [25], kozmologiji in astrofiziki [42, 50–55]. Kot mehanski primer Casimirjeve sile naj navedemo akustični Casimirjev pojav, kjer se interakcija med dvema bližnjima ploščama pojavi zaradi spremenjenega spektra zvočnega šuma [56–58]. Podoben pojav je poznan tudi iz pomorske fizike [59]. Med dvema blizu plovečima ladjama se namreč zaradi spremenjenega spektra vodnega valovanja pojavi močan privlak. Zelo veliko študij je bilo posvečenih Casimirjevemu pojavu v koreliranih tekočinah, kot so kritične tekočine in binarne zmesi tekočin [64–69], superfluidi [70–73], tekoči kristali in elektroliti [74–76]. Vpliv Casimirjeve sile je bil eksperimentalno potrjen pri opazovanju močenja kovinske površine s tekočim helijem [70, 71]. Ravnovesna debelina tvorjenega filma je namreč odvisna od interakcije med površinama filma. V bližini prehoda iz tekoče v supertekočo fazo se amplituda Casimirjeve sile močno poveča, kar se odraža v stanjšanju helijevega filma. Podoben pojav so opazili tudi v binarnih tekočinskih zmeseh [67, 105–107].

Casimirjeva interakcija je na makroskopskih skalah zanemarljiva, na veljavi pa pridobi šele na mikronskih in nanometrskih skalah. Ni še popolnoma jasno, kakšen bo pomen Casimirjeve sile v mikro in nanotehnologiji. Tako so recimo raziskovalci v Bellovih laboratorijih razvili mikroelektromehansko napravo, ki jo poganja prav Casimirjeva sila [92]. Po drugi strani pa Casimirjeva sila omejuje delovanje nanonaprav, saj se premični deli zaradi močnega privlaka pogosto zlepijo skupaj [102–104]. Pričakujemo lahko, da bo z razvojem nanotehnologije poznavanje karakteristik Casimirjevega pojava pridobivalo na pomenu in vplivalo na nadaljni razvoj tega področja fizike.

Casimirjeva sila v tekočih kristalih

Tekočekristalne faze so vmesne faze med kristalnim in tekočim stanjem [111]. Srečamo jih v nekaterih snoveh, zgrajenih iz anizotropnih molekul paličaste ali diskaste oblike. Poznamo vrsto različnih tekočekristalnih faz, ki jih zaznamujeta orientacijska in včasih tudi delna pozicijska urejenost molekul. Pomemben vpliv na fizikalne lastnosti tekočih kristalov imajo termične fluktuacije ureditve, ki so tudi izvor Casimirjeve interakcije v ograjenih tekočekristalnih sistemih. Zaradi obilice različnih faz, faznih prehodov in parametrov urejenosti so tekočekristalni sistemi še posebej zanimivi za študij Casimirjevega pojava.

Nematski tekoči kristali

Najpreprostejša tekočekristalna faza je nematska. V nematski fazi se molekule gibljejo prosto kot v tekočini, vendar pri tem ohranjajo orientacijski red. Skušajo

se urediti čimbolj vzporedno ena drugi. Lokalno povprečno smer urejenosti molekul imenujemo direktor in označujemo z enotskim vektorjem $\mathbf{n}$. Stopnjo orientacijske urejenosti meri paremeter $S = \left\langle \frac{3}{2}\cos^2\theta - \frac{1}{2} \right\rangle$, kjer θ označuje kot med dolgo osjo molekule ter direktorjem in oklepaji zaznamujejo termodinamično povprečje. Nematski tekoči kristali so večinoma enoosno anizotropni. V nekaterih posebnih sistemih pa lahko pride tudi do dvoosnosti nematske ureditve, ki jo opišeta smer dvoosnega direktorja $\mathbf{n}_b$ in stopnja dvoosnega reda P.

V ravnovesju se skušajo molekule v nematskem tekočem kristalu po celotnem vzorcu orientirati v isti smeri. Deformacije direktorskega polja opišemo s Frankovo prosto energijo

$$F = \frac{1}{2}\int \left[K_1(\nabla\cdot\mathbf{n})^2 + K_2(\mathbf{n}\cdot\nabla\times\mathbf{n})^2 + K_3(\mathbf{n}\times\nabla\times\mathbf{n})^2\right] \mathrm{d}V \ , \tag{3}$$

kjer so K_1,K_2 in K_3 pahljačna, zvojna ter upogibna elastična konstanta. Za popolnejši opis nematske faze, ki vključuje tudi stopnjo orientacijskega reda in dvoosnost ureditve, je potrebno vpeljati tenzorski parameter reda Q, ki je brezsleden in simetričen. Definiramo ga na osnovi primerne makroskopske količine, ki je enaka 0 v izotropni fazi in je neničelna v nematski fazi. Ponavadi za ta namen uporabimo tenzor magnetne susceptibilnosti χ in definiramo tenzorski parameter reda kot $\mathsf{Q} = C(\chi - \frac{1}{3}\mathsf{I}\,\mathrm{Tr}\chi)$, pri čemer je C normalizacijska konstanta ter I enotski tenzor. Gostoto proste energije nematskega sistema v bližini faznega prehoda v izotropno fazo lahko sedaj opišemo z Landauovim razvojem

$$f = \frac{1}{2}A(T-T^*)\,\mathrm{Tr}\mathsf{Q}^2 - \frac{1}{3}B\,\mathrm{Tr}\mathsf{Q}^3 + \frac{1}{4}C(\mathrm{Tr}\mathsf{Q}^2)^2 + \frac{1}{2}\mathsf{L}\nabla\mathsf{Q}\vdots\nabla\mathsf{Q} \ , \tag{4}$$

kjer so A, B, C ter L materialne konstante in T^* temperatura maksimalne možne podhladitve izotropne faze.

Prvo študijo Casimirjevega pojava v nematskih tekočih kristalih so objavili Ajdari in sodelavci leta 1991 [114, 115]. Izračunali so Casimirjevo silo v homeotropni nematski celici, ki je sestavljena iz dveh vzporednih plošč, obdanih s tekočekristalnim materialom. Plošči vsiljujeta homeotropno orientacijo direktorja, s čimer vplivata na spekter termičnih fluktuacij in s tem na pojav Casimirjeve sile med ploščama

$$\mathcal{F}_{Cas} = -\frac{k_B T S}{8\pi h^3}\zeta_R(3)\left(\frac{K_3}{K_1} + \frac{K_3}{K_2}\right) \ . \tag{5}$$

Nematska sila je analogna elektromagnetni Casimirjevi sili [enačba (2)], kar je odraz univerzalnosti Casimirjeve interakcije. Le-ta ni odvisna od podrobnosti sistema, temveč le od tipa fluktuacijskih načinov in robnih pogojev. Ajdarijevo delo so nadgradili Ziherl in sodelavci [116], ki so izračunali prispevke h Casimirjevi sili zaradi termičnih fluktuacij stopnje nematskega reda in dvoosnosti ureditve. Ti znašajo

$$\mathcal{F}_{Cas} = -\frac{kTS}{4\pi}\frac{1}{h^3}\sum_{k=1}^{\infty}\frac{\exp\left(-2hk/\eta_i\right)}{k^3}\left(\frac{1}{2} + \frac{h}{\eta_i}k + \frac{h^2}{\eta_i^2}k^2\right) \ , \tag{6}$$

pri čemer so η_i korelacijske dolžine ustreznega fluktuacijskega načina. Za razliko od direktorske Casimirjeve sile [enačba (5)] so ti prispevki kratkega dosega in pri velikih razdaljah upadajo kot $\exp(-2h/\eta_i)/h$. Doseg Casimirjeve sile je v splošnem odvisen od korelacij v sistemu. Tako je v sistemu s fluktuacijskimi korelacijami kratkega dosega Casimirjeva sila prav tako kratkega dosega. Fluktuacijski načini s korelacijami dolgega dosega, kot so direktorske fluktuacije v nematikih, pa dajo Casimirjevo interakcijo dolgega dosega. Zgornja osnovna rezultata [enačbi (5 in 6)] sta bila posplošena tudi za končno jakost površinskega sidranja [116, 117]. Izkaže se, da končna jakost sidranja v splošnem zmanjša velikost Casimirjeve sile in lahko vpliva tudi na njen predznak. V primeru simetričnih robnih pogojev, kjer je sidranje na obeh ploščah ali močno ali šibko, je sila privlačna. V primeru antisimetričnih robnih pogojev, kjer je sidranje na eni površini močno, na drugi pa šibko, postane sila odbojna.

Nadaljnje študije so obravnavale razne vidike Casimirjeve sile v nematskih tekočih kristalih. Li in Kardar sta ocenila popravke k sili zaradi hrapavosti plošč [118, 119]. Ziherl je obravnaval silo v prednematskem sistemu z nehomogeno ravnovesno ureditvijo [120]. Precej pozornosti je bilo posvečene tako imenovanim frustriranim sistemom, kot sta hibridna in Fréederickszova celica [121]. V teh sistemih se ravnovesna nematska struktura ne more prilagoditi vsem zunanjim vplivom – robnim pogojem ali zunanjim poljem. Zaradi te frustracije so fluktuacije ureditve še posebej izrazite, kar se odraža v specifičnem obnašanju Casimirjeve sile. Do podobnega pojava pride tudi v kiralnih nematskih sistemih, kjer frustracija izvira iz dejstva, da se perioda kiralne vijačnice ne ujema z razdaljo med ograjujočima površinama. Omenimo še študije Casimirjeve sile v nematskih polimerih [125], med sferičnimi nečistočami [124] in napoved obstoja Casimirjevega navora med ploščama z anizotropnimi energijami sidranja [127].

Smektični tekoči kristali

Smektične tekoče kristale odlikuje poleg nematske orientacijske urejenosti tudi enorazsežni pozicijski red. V izbrani smeri se gostota molekul periodično spreminja. Ta pozicijska urejenost ni zelo izrazita, saj so variacije gostote majhne. Lahko si predstavljamo, da so molekule v smektiku razporejene v vzporednih plasteh. Vsaka od teh plasti predstavlja dvorazsežno tekočino, znotraj katere se molekule prosto gibljejo. Gibanje med plastmi pa ni povsem prosto, zato pride do modulacije gostote v smeri pravokotno na plasti. Pozicijski smektični red opišemo s kompleksnim parametrom reda $\Psi = \psi \exp(i\phi)$, pri čemer ψ podaja stopnjo pozicijskega reda, medtem ko faza ϕ opisuje lego smektičnih plasti. Pozicijski red dolgega dosega v smektikih je nepravi, saj zaradi Landau-Peierlsove nestabilnosti urejenost dolgega dosega v eni razsežnosti ni mogoča.

Prvo študijo Casimirjevega pojava v smektičnih tekočih kristalih je objavil Mihe-

jev leta 1989 [128]. Obravnaval je silo, ki jo povzročijo fluktuacije smektičnih plasti v ograjenem sistemu. Prosto energijo deformacij plasti lahko zapišemo kot

$$F = \frac{1}{2}\int \left[B(\nabla_{\parallel}u)^2 + K(\nabla_{\perp}^2 u)^2\right] \mathrm{d}V \,, \tag{7}$$

kjer $u(\mathbf{r})$ predstavlja odmik plasti od ravnovesne lege. Prvi člen v prosti energiji opisuje stiskanje, drugi pa upogib smektičnih plasti. V homeotropni smektični celici so plasti v ravnovesju urejene vzporedno z ograjujočima ploščama. Fluktuacije robnih plasti zaradi prisotnosti trdnih sten niso mogoče, kar vodi do Casimirjeve sile med ploščama

$$\mathcal{F}_{Cas} = -\frac{k_B T S}{16\pi h^2}\zeta_R(2)\sqrt{\frac{B}{K}} \,. \tag{8}$$

V primeru smektičnih filmov je ravnovesna struktura enaka kot v homeotropni celici, le da so tu dovoljene tudi fluktuacije površinskih plasti. Amplituda površinskih fluktuacij je odvisna od površinske napetosti med smektikom in ograjujočim medijem. Casimirjeva sila je v tem primeru enaka

$$\mathcal{F}_{Cas} = -\frac{k_B T S}{16\pi h^2}\sqrt{\frac{B}{K}}\,\mathrm{Li}_2\left[\frac{(\gamma_1-\sqrt{KB})(\gamma_2-\sqrt{KB})}{(\gamma_1+\sqrt{KB})(\gamma_2+\sqrt{KB})}\right] \,, \tag{9}$$

kjer je Li_2 dilogaritemska funkcija, definirana kot $\mathrm{Li}_2(x) = \sum_{n=1}^{\infty} x^n n^{-2}$. Površinski napetosti γ_1 in γ_2 na zgornji in spodnji površini filma sta v splošnem lahko različni. Casimirjeva sila je v primeru končne površinske napetosti vedno šibkejša kot v primeru ograditve s trdimi ploščami. Če sta površinski napetosti γ_1 in γ_2 zelo različni, tako da imamo opravka z antisimetričnimi robnimi pogoji, Casimirjeva sila zamenja predznak in postane odbojna.

Posebej moramo omeniti še študije Casimirjevega pojava izvedene v okviru diskretnega opisa smektične faze [130–133]. Rezultati, dobljeni z diskretnim modelom so zelo podobni rezultatom kontinuumskega modela, razen za nekatere zelo specifične vrednosti površinskih napetosti. Nadalje so te študije obravnavale vpliv magnetnega polja na Casimirjevo silo ter obnašanje sile v bližini faznega prehoda iz smektične v nematsko fazo. Napovedale so veliko povečanje amplitude sile v bližini faznega prehoda, kar bi pomenilo, da je Casimirjeva sila dominantna interakcija dolgega dosega v tem področju.

Namen disertacije

Večina dosedanjih študij v smektičnih tekočih kristalih je obravnavala Casimirjevo silo, ki jo povzročajo fluktuacije smektičnih plasti v ograjenih sistemih [114, 115, 128, 130–133]. V tej tezi obravnavamo Casimirjevo silo v smektičnih sistemih upoštevajoč oba vidika ureditve – pozicijskega in orientacijskega. S tem podajamo kompletno sliko Casimirjevega pojava v smektikih. Glavni poudarek disertacije je na študiju

interakcije v smektični A fazi. Nadalje obravnavamo obnašanje Casimirjeve sile v bližini faznega prehoda iz smektične A faze v smektično C fazo. Posebna pozornost je posvečena sistemom z nehomogeno ravnovesno ureditvijo. Kot prvi tak primer obravnavamo smektično A celico, kjer se nehomogenost pozicijskega reda odraža v krajevni odvisnosti elastičnih konstant. Kot drugi primer obravnavamo vpliv površinsko induciranega predsmektičnega reda na direktorsko Casimirjevo silo v nematski fazi. V disertaciji se omejimo na izračun sile v planarni geometriji. To ustreza geometriji prostostoječih filmov, dobljene rezultate pa je možno razširiti na nekatere ukrivljene geometrije s pomočjo Derjaginove aproksimacije. Nekateri rezultati, predstavljeni v tej disertaciji, so bili objavljeni v dveh člankih v reviji *Physical Review E* [154, 155].

Casimirjeva sila v smektični A fazi

Homeotropna smektična A celica

Homeotropna celica sestoji iz dveh vzporednih plošč, ki obdajata smektični material (slika 1). Smektične plasti se uredijo vzporedno s ploščama, medtem ko je

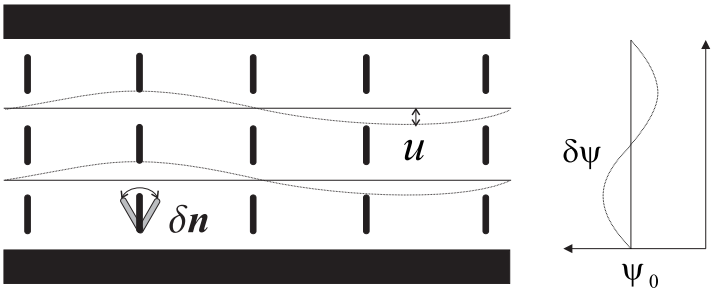

Slika 1 Homeotropna smektična A celica. Prikazane so fluktuacije stopnje smektičnega reda $\delta\psi$, fluktuacije plasti u in direktorske fluktuacije $\delta\mathbf{n}$.

direktor orientiran pravokotno na plošči. Ravnovesno strukturo lahko tedaj zapišeno kot: $\mathbf{n}_{mf} = \mathbf{n}_z = (0,0,1)$, $u_{mf}(\mathbf{r}) = 0$. Hkrati predpostavimo, da je stopnja smektičnega reda v celici konstantna in enaka ravnovesni vrednosti v neomejenem vzorcu: $\psi_{mf} = \psi_0$. Casimirjevo silo povzročajo termične fluktuacije okrog ravnovesja. Hamiltonka fluktuacij se v harmoničnem približku glasi

$$H[\delta\psi, u, \delta\mathbf{n}] = H[\delta\psi] + H[u, \delta\mathbf{n}] \ ,$$

$$H[\delta\psi] = \int \mathrm{d}V \left[-a\delta\psi^2 + \frac{1}{2}C_{\parallel}(\nabla_{\parallel}\delta\psi)^2 + \frac{1}{2}C_{\perp}(\nabla_{\perp}\delta\psi)^2 \right] \ ,$$

$$H[u,\delta\mathbf{n}] = \frac{1}{2}\int \mathrm{d}V \Bigg\{ B\left(\nabla_\parallel u\right)^2 + K_L\left(\nabla_\perp^2 u\right)^2 + D\left(\nabla_\perp u + \delta\mathbf{n}\right)^2 + \\ + K_1\left(\frac{\partial n_x}{\partial x} + \frac{\partial n_y}{\partial y}\right)^2 + K_2\left(\frac{\partial n_x}{\partial y} - \frac{\partial n_y}{\partial x}\right)^2 + K_3\left[\left(\frac{\partial n_x}{\partial z}\right)^2 + \left(\frac{\partial n_y}{\partial z}\right)^2\right]\Bigg\}, \tag{10}$$

kjer smo z $\delta\psi(\mathbf{r}) = \psi - \psi_0$ označili fluktacije stopnje smektičnega reda, z $u(\mathbf{r})$ fluktuacije smektičnih plasti in z $\delta\mathbf{n}(\mathbf{r}) = (n_x, n_y)$ direktorske fluktuacije. Kot vidimo, so fluktuacije smektičnega reda ψ neodvisne od med seboj sklopljenih fluktuacij plasti in direktorja. Za izračun Casimirjeve sile moramo določiti še robne pogoje. Predpostavimo, da sta tako lega smektičnih plasti kot stopnja smektičnega reda na ploščah fiksni: $u(z=0) = u(z=h) = 0$, $\delta\psi(z=0) = \delta\psi(z=h) = 0$. Direktorsko sidranje opišemo z Rapini-Papoularjevim modelom

$$H_S\left[\mathbf{n}\right] = \frac{1}{2}W\int |\delta\mathbf{n}|^2\,\mathrm{d}S\,, \tag{11}$$

kjer parameter W podaja jakost površinskega sidranja.

Fluktuacije stopnje smektičnega reda ψ

Pričnimo z izračunom sile, ki jo povzročajo fluktuacije stopnje smektičnega reda $\delta\psi$. Ker je homeotropna celica v prečnih dimenzijah zelo razsežna, si pomagamo z dvorazsežno Fourierovo transformacijo fluktuirajočega polja, $\delta\psi(\mathbf{r}) = \sum_{\mathbf{q}} \psi_q(z)\exp(i\mathbf{q}\boldsymbol{\rho})$. Hamiltonka se sedaj glasi

$$H[\delta\psi] = \sum_{\mathbf{q}} H_{\mathbf{q}}[\delta\psi] = \frac{1}{2}C_\parallel S\sum_{\mathbf{q}}\int_0^h \mathrm{d}z\left[\left(\xi^{-2} + \frac{C_\perp}{C_\parallel}q^2\right)|\psi_{\mathbf{q}}|^2 + \left|\frac{\partial\psi_{\mathbf{q}}}{\partial z}\right|^2\right], \tag{12}$$

kjer smo vpeljali korelacijsko dolžino fluktuacij $\xi^{-1} = \sqrt{-2a/C_\parallel}$. Ker so fluktuacijski načini z različnimi valovnimi vektorji $\mathbf{q}$ med seboj neodvisni, lahko izračunamo particijsko funkcijo za vsak način posebej

$$Z_{\mathbf{q}}[\delta\psi] = \int_{\psi_{\mathbf{q}}(z=0)=0}^{\psi_{\mathbf{q}}(z=h)=0} \exp\left(-\beta H_{\mathbf{q}}[\delta\psi]\right)\,\mathcal{D}\psi_{\mathbf{q}}(z)\,. \tag{13}$$

Particijska funkcija $Z_{\mathbf{q}}[\delta\psi]$ je analogna kvantnemu propagatorju harmoničnega oscilatorja [168] in jo lahko direktno izračunamo

$$Z_{\mathbf{q}}[\delta\psi] \propto \left[\sinh\left(\sqrt{\xi^{-2} + \frac{C_\perp}{C_\parallel}q^2}\,h\right)\right]^{-1/2}. \tag{14}$$

Prosta energija fluktuacij je sedaj enaka

$$F_{fluc}[\delta\psi] = -k_BT\sum_{\mathbf{q}}\ln Z_{\mathbf{q}}[\delta\psi] = \frac{k_BTS}{4\pi}\int \ln\left[\sinh\left(\sqrt{\xi^{-2} + \frac{C_\perp}{C_\parallel}q^2}\,h\right)\right] q\,\mathrm{d}q\,. \tag{15}$$

Iz celotne proste energije je potrebno izluščiti končen interakcijski prispevek. Z uporabo relacije $\sinh(x) = \exp(x) \times 1/2 \times [1 - \exp(-2x)]$ faktoriziramo prosto energijo

$$F_{fluc}[\delta\psi] = \frac{k_B T S}{4\pi} \frac{C_\parallel}{C_\perp} \int_{\xi^{-1}}^{\infty} \ln\left(\exp(ph) \times \frac{1}{2} \times [1 - \exp(-2ph)]\right) p \, \mathrm{d}p \,, \tag{16}$$

pri čemer smo vpeljali $p^2 = \xi^{-2} + \frac{C_\perp}{C_\parallel} q^2$. Prvi člen v prosti energiji je sorazmeren prostornini vzorca Sh in predstavlja referenčno prosto energijo neomejenega sredstva. Drugi člen ni odvisen od razdalje med ploščama h in zato ne prispeva k interakciji. Zadnji člen, ki gre v limiti $h \to \infty$ proti 0, je iskani interakcijski prispevek

$$F^{int}_{fluc}[\delta\psi] = \frac{k_B T S}{4\pi} \frac{C_\parallel}{C_\perp} \int_{\xi^{-1}}^{\infty} \ln\left(1 - \exp\left(-2ph\right)\right) p \, \mathrm{d}p \,. \tag{17}$$

Casimirjevo silo sedaj dobimo s preprostim odvajanjem po h in ovrednotenjem integrala

$$\mathcal{F}_{Cas}[\delta\psi] = -\frac{k_B T S}{4\pi} \frac{C_\parallel}{C_\perp} \frac{1}{h^3} \sum_{k=1}^{\infty} \frac{\exp(-2hk/\xi)}{k^3} \left(\frac{1}{2} + \frac{h}{\xi} k + \frac{h^2}{\xi^2} k^2\right). \tag{18}$$

Casimirjeva sila zaradi fluktuacij stopnje smektičnega reda je kratkega dosega in v limiti velikih debelin ($h \gg \xi$) upada kot $\exp(-2h/\xi)/h$. Pri majhnih debelinah ($h \ll \xi$) pa se sila spreminja kot $1/h^3$.

Tukaj izpeljan izračun sile predstavlja vzorec po katerem računamo Casimirjevo silo v večini primerov v tej disertaciji. Zato bomo podrobnosti izračunov navajali le, kjer bo nujno potrebno.

Fluktuacije direktorja in smektičnih plasti

Hamiltonka fluktuacij se po Fourierovi transformaciji glasi

$$\begin{aligned} H[u, \delta\mathbf{n}] = \frac{1}{2} S \sum_{\mathbf{q}} \int_0^h \mathrm{d}z \Bigg[& B \left|\frac{\partial u_{\mathbf{q}}}{\partial z}\right|^2 + D q^2 \left|u_{\mathbf{q}}\right|^2 + K_L q^4 \left|u_{\mathbf{q}}\right|^2 \\ & + D\left(\left|n_{1\mathbf{q}}\right|^2 + \left|n_{2\mathbf{q}}\right|^2\right) + iqD\left(u_{\mathbf{q}} n^*_{1\mathbf{q}} - u^*_{\mathbf{q}} n_{1\mathbf{q}}\right) + K_1 q^2 \left|n_{1\mathbf{q}}\right|^2 \\ & + K_2 q^2 \left|n_{2\mathbf{q}}\right|^2 + K_3 \left(\left|\frac{\partial n_{1\mathbf{q}}}{\partial z}\right|^2 + \left|\frac{\partial n_{2\mathbf{q}}}{\partial z}\right|^2\right) \Bigg] . \end{aligned} \tag{19}$$

Pri tem smo izvedli transformacijo direktorskih fluktuacij $\delta\mathbf{n}_{\mathbf{q}} = (n_{x\mathbf{q}}, n_{y\mathbf{q}})$ v $(n_{1\mathbf{q}}, n_{2\mathbf{q}})$, kjer komponenta $n_{1\mathbf{q}}$ predstavlja direktorske fluktuacije vzporedne s $\mathbf{q} = (q_x, q_y)$, in komponenta $n_{2\mathbf{q}}$ fluktuacije pravokotne na $\mathbf{q}$. Površinska energija direktorskih fluktuacij je enaka

$$H_S\left[\mathbf{n}\right] = \frac{1}{2} K_3 S L^{-1} \sum_{\mathbf{q}} \left(\left|n^-_{1\mathbf{q}}\right|^2 + \left|n^+_{1\mathbf{q}}\right|^2 + \left|n^-_{2\mathbf{q}}\right|^2 + \left|n^+_{2\mathbf{q}}\right|^2\right) \,. \tag{20}$$

Vpeljali smo ekstrapolacijsko dolžino sidranja $L = K_3/W$ ter $n^-_{1,2\mathbf{q}} = n_{1,2\mathbf{q}}(z=0)$ in $n^+_{1,2\mathbf{q}} = n_{1,2\mathbf{q}}(z=h)$. Kot vidimo iz hamiltonk, so le fluktuacijski načini $n_{1\mathbf{q}}$ sklopljeni s fluktuacijami plasti $u_\mathbf{q}$, medtem ko načini $n_{2\mathbf{q}}$ predstavljajo čiste direktorske fluktuacije. Particijska funkcija sklopljenih fluktuacij $Z_\mathbf{q}[n_{1\mathbf{q}}, u_\mathbf{q}]$ je analogna kvantnemu propagatorju dveh sklopljenih harmoničnih oscilatorjev, particijska funkcija čistih direktorskih fluktuacij $Z_\mathbf{q}[n_{2\mathbf{q}}]$ pa propagatorju navadnega harmoničnega oscilatorja [168, 169]. Obe particijski funkciji lahko izračunamo analitično in po prej opisanem postopku regularizacije proste energije dobimo Casimirjevo silo

$$\mathcal{F}_{Cas}[u, \delta\mathbf{n}] = \mathcal{F}[n_2; L] + \mathcal{F}_1[n_1, u] + \mathcal{F}_2[n_1, u] + \mathcal{F}_3[n_1, u; L] \,, \tag{21}$$

kjer so

$$\mathcal{F}[n_2; L] = -\frac{k_B T S}{2\pi} \int_0^\infty \frac{\Omega_3 q \,\mathrm{d}q}{\frac{(\Omega_3 + L^{-1})^2}{(\Omega_3 - L^{-1})^2} \exp(2\Omega_3 h) - 1} \,, \tag{22}$$

$$\mathcal{F}_1[n_1, u] = -\frac{k_B T S}{2\pi} \int_0^\infty \frac{\Omega_1 q \,\mathrm{d}q}{\exp(2\Omega_1 h) - 1} \,, \tag{23}$$

$$\mathcal{F}_2[n_1, u] = -\frac{k_B T S}{2\pi} \int_0^\infty \frac{\Omega_2 q \,\mathrm{d}q}{\exp(2\Omega_2 h) - 1} \,, \tag{24}$$

$$\begin{aligned} \mathcal{F}_3[n_1, u; L] \;\; = \;\; & -\frac{k_B T S}{4\pi} \int_0^\infty q \,\mathrm{d}q \left[\frac{\frac{\Omega_1^2 S^2}{1+\cosh(\Omega_1 h)} + \frac{\Omega_2^2 C^2}{1+\cosh(\Omega_2 h)}}{\Omega_1 S^2 A_1^- + \Omega_2 C^2 A_2^- + L^{-1}} \right] \\ & -\frac{k_B T S}{4\pi} \int_0^\infty q \,\mathrm{d}q \left[\frac{\frac{\Omega_1^2 S^2}{1-\cosh(\Omega_1 h)} + \frac{\Omega_2^2 C^2}{1-\cosh(\Omega_2 h)}}{\Omega_1 S^2 A_1^+ + \Omega_2 C^2 A_2^+ + L^{-1}} \right] \,. \end{aligned} \tag{25}$$

Vpeljali smo sledeče oznake

$$\begin{aligned} \Omega_{1,2} = \frac{1}{\sqrt{2}} \frac{1}{\Lambda} \Bigg\{ & 1 + (\rho^2 + \lambda^2) q^2 + \frac{K_L}{K_3} \lambda^2 \Lambda^2 q^4 \\ & \mp \sqrt{\left[1 - (\lambda^2 - \rho^2) q^2 - \frac{K_L}{K_3} \Lambda^2 \lambda^2 q^4 \right]^2 + 4\lambda^2 q^2} \Bigg\}^{1/2} \,, \end{aligned} \tag{26}$$

$$\Omega_3 = \sqrt{\Lambda^{-2} + \frac{K_2}{K_3} q^2} \,, \tag{27}$$

$$C^2 = \frac{1}{2} + \frac{1}{2} \sqrt{\frac{\left[1 + (\rho^2 - \lambda^2) q^2 - \frac{K_L}{K_3} \lambda^2 \Lambda^2 q^4 \right]^2}{\left[1 + (\rho^2 - \lambda^2) q^2 - \frac{K_L}{K_3} \Lambda^2 \lambda^2 q^4 \right]^2 + 4 q^2 \lambda^2}} \,, \tag{28}$$

$$S^2 = 1 - C^2 \,, \tag{29}$$

$$A^\pm_{1,2} = \frac{\cosh(\Omega_{1,2} h) \pm 1}{\sinh(\Omega_{1,2} h)} \tag{30}$$

in korelacijske dolžine $\Lambda = (K_3/D)^{1/2}$, $\lambda = (K_3/B)^{1/2}$ in $\rho = (K_1/D)^{1/2}$.

Casimirjeva sila vsebuje štiri prispevke. Prispevek direktorskih fluktuacij $\mathcal{F}[n_2; L]$ je kratkega dosega in pri velikih debelinah upada kot $\exp(-2h/\Lambda)/h$. Člen $\mathcal{F}_1[n_1, u]$ predstavlja prispevek fluktuacij, kjer so plasti in direktor v fazi. Ta prispevek je dolgega dosega in v limiti velikih razdalj vodi k znani Casimirjevi sili sorazmerni z $1/h^2$ [enačba (8)]. Člen $\mathcal{F}_2[n_1, u]$ predstavlja prispevek fluktuacij, kjer direktor ne sledi plastem. Ta prispevek je kratkega dosega in ima podobne lastnosti kot prispevek čistih direktorskih fluktuacij $\mathcal{F}[n_2; L]$. Zadnji člen, $\mathcal{F}_3[n_1, u; L]$, predstavlja popravek zaradi končne jakosti sidranja direktorja in je enak 0 v limiti neskončno močnega sidranja $W \to \infty$. Obnašanje Casimirjeve sile je prikazano na sliki 2. Primerjamo

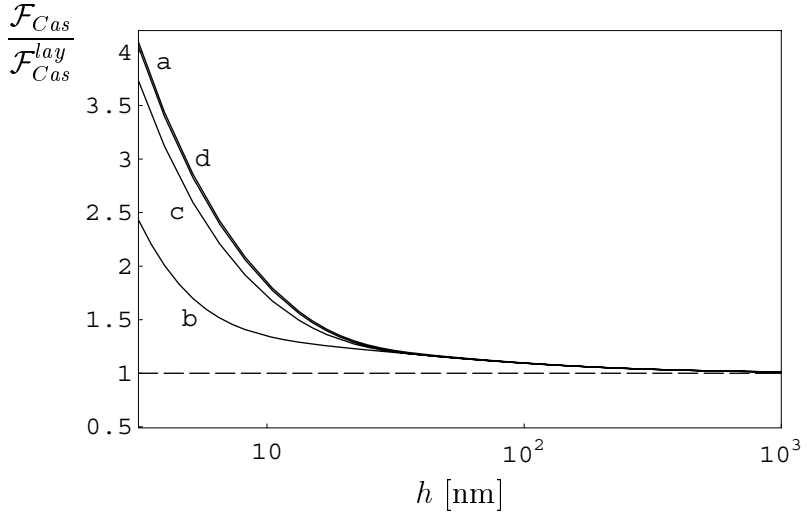

Slika 2 Casimirjeva sila $\mathcal{F}_{Cas}[u, \delta\mathbf{n}]$ v homeotropni smektični A celici v primerjavi z referenčno silo $\mathcal{F}_{Cas}^{lay}$ za različne jakosti direktorskega sidranja: a) $W \to \infty$, b) $W = 10^{-3}$ J/m^2, c) $W = 10^{-4}$ J/m^2, d) $W = 10^{-5}$ J/m^2.

jo z referenčno silo $\mathcal{F}_{Cas}^{lay} = -k_B T S \zeta(2)/16\pi h^2 \sqrt{K_L'/B}$, ki jo dobimo, če upoštevamo le fluktuacije smektičnih plasti in zanemarimo direktorske prostostne stopnje s predpostavko, da je direktor stalno orientiran pravokotno na plasti. Casimirjeva sila $\mathcal{F}_{Cas}[u, \delta\mathbf{n}]$ je občutno večja od referenčne sile $\mathcal{F}_{Cas}^{lay}$ le v tankih celicah debeline največ nekaj korelacijskih dolžin Λ (pri uporabljenih snovnih parametrih je $\Lambda = 10$ nm). V tem območju k sili znatno prispevata tudi člena kratkega dosega $\mathcal{F}[n_2; L]$ in $\mathcal{F}_2[n_1, u]$. Pri večjih debelinah k sili znatno prispeva le člen dolgega dosega $\mathcal{F}_1[n_1, u]$. Le-ta je v limiti $h/\Lambda \gg 1$ točno enak referenčni sili $\mathcal{F}_{Cas}^{lay}$. Končna jakost sidranja v splošnem zmanjša jakost Casimirjeve sile v primerjavi z limitnim primerom fiksnih robnih pogojev. To je najbolj očitno v primeru parametra sidranja $W = 10^{-3}$ J/m^2 ($L = 10$ nm) na sliki 2, kjer je ekstrapolacijska dolžina L primerljiva s karakterističnimi dolžinami v sistemu in je sidranje nekje vmes med močnim in šibkim. Pri ostalih parametrih, kjer je sidranje bodisi močno bodisi šibko, se jakost sile bistveno ne zmanjša.

Vpliv različnih parametrov sklopitve med smektičnimi plastmi in direktorjem D je prikazan na sliki 3. Čim šibkejša je sklopitev D tem večja je Casimirjeva sila.

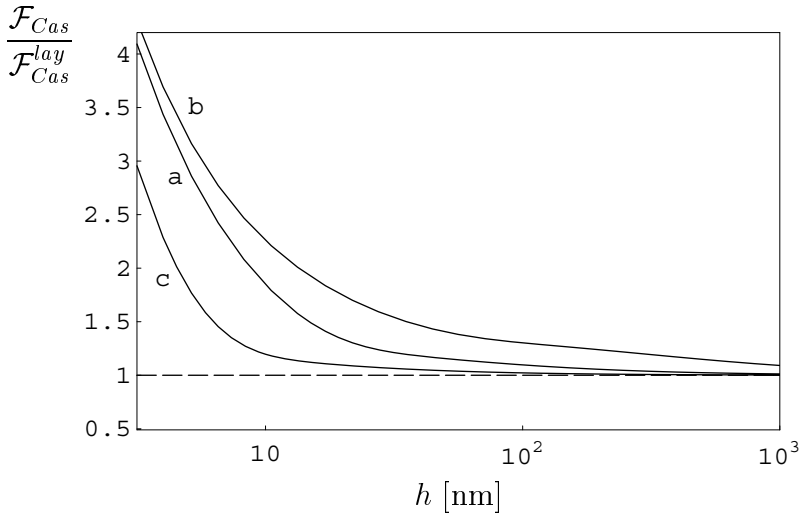

Slika 3 Vpliv različnih jakosti sklopitve med direktorjem in smektičnimi plastmi D na Casimirjevo silo: a) $D = 10^5$ N/m^2, b) $D = 10^4$ N/m^2, c) $D = 10^6$ N/m^2. Predpostavili smo neskončno močno sidranje direktorja ($W \to \infty$).

To je po eni strani posledica povečane korelacijske dolžine Λ in s tem povezanim večjim prispevkom direktorskih členov kratkega dosega. Poleg tega se pri šibkejši sklopitvi poveča tudi velikost člena dolgega dosega $\mathcal{F}_1[n_1, u]$. Tako povečanje jakosti Casimirjeve sile lahko pričakujemo v bližini faznega prehoda iz smektične A faze v smektično C fazo, kjer se sklopitvena konstanta v okviru Landauovega modela spreminja kot $D \propto (T - T_c)$. Bolj podrobno si obnašanje sile v okolici tega faznega prehoda ogledamo v posebnem poglavju.

Prostostoječi smektični A film

Prostostoječi filmi so poseben primer ograjenega sistema, kjer smektika ne omejujeta trdni plošči, ampak prosti površini, ki sta v stiku z zrakom (slika 4). Pripravijo jih tako, da smektik razvlečejo preko luknjice v stekleni ali kovinski ploščici. Smektične plasti se uredijo vzporedno s prosto površino. Debeline filmov lahko znašajo od le nekaj (najmanj dveh) do več tisoč plasti. Prostostoječi filmi so zelo primerni za študij lastnosti tekočih kristalov, saj je razmeroma enostavno doseči homogeno strukturo brez defektov.

Ravnovesna struktura prostostoječega filma je enaka strukturi v homeotropni celici. Razlika se pojavi pri robnih pogojih, saj so v filmu dovoljene tudi fluktuacije

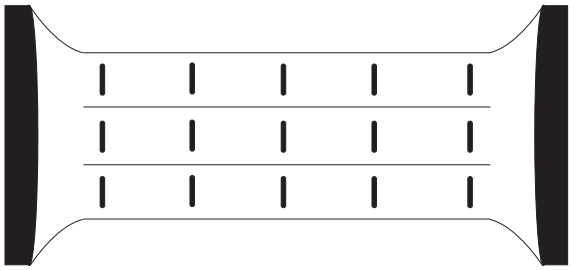

Slika 4 Prostostoječi smektični A film. V prostostoječem filmu je smektični material razvlečen preko luknjice v kovinski ali stekleni plošči. Smektične plasti se uredijo vzporedno s prosto površino. Direktor je v smektičnem A filmu orientiran pravokotno na plasti.

robnih plasti. Površinska hamiltonka se sedaj glasi

$$H_S\left[\mathbf{n},u\right]=\frac{1}{2}W\int\left|\delta\mathbf{n}\right|^2\mathrm{d}S\ +\frac{1}{2}\gamma\int\left(\nabla_\perp u\right)^2\mathrm{d}S\ . \tag{31}$$

Direktorsko sidranje smo znova opisali z Rapini-Papoularjevim modelom. Drugi člen opisuje povečanje površinske energije zaradi zvečanje stične površine med smektikom in zrakom, ki ga podaja površinska napetost γ. S Fourierovo transformacijo dobimo

$$\begin{aligned}H_S\left[\mathbf{n},u\right]=&\frac{1}{2}K_3SL^{-1}\sum_{\mathbf{q}}\left(\left|n^-_{1\mathbf{q}}\right|^2+\left|n^+_{1\mathbf{q}}\right|^2+\left|n^-_{2\mathbf{q}}\right|^2+\left|n^+_{2\mathbf{q}}\right|^2\right)+\\&+\frac{1}{2}K_3S\chi^{-1}\sum_{\mathbf{q}}q^2\left(\left|u^-_{\mathbf{q}}\right|^2+\left|u^+_{\mathbf{q}}\right|^2\right)\ .\end{aligned} \tag{32}$$

Vpeljali smo ekstrapolacijsko dolžino $\chi=K_3/\gamma$ ter $u^-_{\mathbf{q}}=u_{\mathbf{q}}(z=0)$ in $u^+_{\mathbf{q}}=u_{\mathbf{q}}(z=h)$. Ker je snovna hamiltonka $H[u,\delta\mathbf{n}]$ enaka kot v homeotropni celici, lahko na podoben način izračunamo Casimirjevo silo tudi v prostostoječem filmu. Ta se sedaj glasi

$$\mathcal{F}_{Cas}[u,\delta\mathbf{n}]=\mathcal{F}[n_2;L]+\mathcal{F}_1[n_1,u]+\mathcal{F}_2[n_1,u]+\mathcal{F}_3[n_1,u;L,\chi]\ . \tag{33}$$

Prvi trije členi so enaki kot pri homeotropni celici. Spremeni se le zadnji člen $\mathcal{F}_3[n_1,u;L,\chi]$, ki opisuje vpliv direktorskega sidranja in sidranja plasti

$$\begin{aligned}\mathcal{F}_3[n_1,u;L,\chi]=&-\frac{k_BTS}{4\pi}\sum_{i=1,2}\int_0^\infty q\,\mathrm{d}q\Bigg[\Omega_1\Omega_2\lambda^{-2}\Big(\frac{\Omega_1A_2^\mp}{1\pm\cosh(\Omega_1h)}+\frac{\Omega_2A_1^\mp}{1\pm\cosh(\Omega_2h)}\Big)\\&+\chi^{-1}q^2\Big(\frac{\Omega_1^2S^2}{1\pm\cosh(\Omega_1h)}+\frac{\Omega_2^2C^2}{1\pm\cosh(\Omega_2h)}\Big)+L^{-1}\lambda^{-2}\Big(\frac{\Omega_1^2C^2}{1\pm\cosh(\Omega_1h)}\\&+\frac{\Omega_2^2S^2}{1\pm\cosh(\Omega_2h)}\Big)\Bigg]\times\Bigg[\Omega_1\Omega_2\lambda^{-2}A_1^\mp A_2^\mp+\chi^{-1}q^2\Big(\Omega_1S^2A_1^\mp+\Omega_2C^2A_2^\mp\\&+L^{-1}\Big)+L^{-1}\lambda^{-2}\Big(\Omega_1C^2A_1^\mp+\Omega_2S^2A_2^\mp\Big)\Bigg]^{-1}\ .\end{aligned} \tag{34}$$

Ta člen je vsota dveh prispevkov ($i = 1, 2$), ki se razlikujeta le po zamenjavi predznakov ($\pm$) v nekaterih faktorjih. Ker sedaj robni pogoji vsebujejo tudi sidranje plasti, je popravek zaradi končne jakosti površinske interakcije $\mathcal{F}_3[n_1, u; L, \chi]$ dolgega dosega.

Vpliv končne površinske napetosti na Casimirjevo silo v prostostoječih filmih je predstavljen na sliki 5. Prikazana je primerjava med silo v prostostoječem filmu

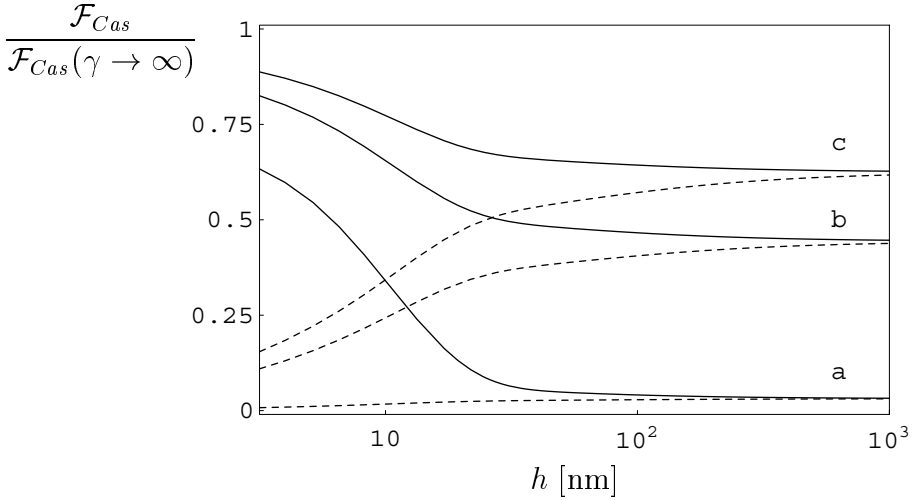

Slika 5 Casimirjeva sila $\mathcal{F}_{Cas}[u, \delta\mathbf{n}]$ v prostostoječem smektičnem filmu v primerjavi s silo v homeotropni celici [$\mathcal{F}_{Cas}(\gamma \to \infty)$]. Uporabili smo sledeče parametre: jakost direktorskega sidranja $W = 10^{-5}$ J/m^2, sklopitveno konstanto med direktorjem in plastmi $D = 10^5$ N/m^2 ter različne površinske napetosti [a) $\gamma = 10^{-2}$ J/m^2, b) $\gamma = 5 \times 10^{-2}$ J/m^2, c) $\gamma = 10^{-1}$ J/m^2]. Prekinjene črte predstavljajo $\mathcal{F}_{Cas}^{lay}(\gamma)$.

in homeotropni celici. Izbrali smo si specifičen parameter direktorskega sidranja $W = 10^{-5}$ J/m^2, vendar to ne vpliva bistveno na dobljene rezultate, ki bi bili podobni tudi pri izbiri kake druge vrednosti W. Kot je vidno s slike 5 se v primeru končne površinske napetosti γ velikost Casimirjeve sile zmanjša. To je napovedal že Mihejev v okviru modela, ki upošteva le fluktuacije smektičnih plasti [128]. Sila zaradi fluktuacij plasti znaša $\mathcal{F}_{Cas}^{lay}(\gamma) = -\frac{k_B T S}{16\pi h^2}\sqrt{\frac{B}{K_L'}}\ \mathrm{Li}_2\left[(\gamma - \sqrt{K_L' B})/(\gamma + \sqrt{K_L' B})\right]^2$ in je na sliki predstavljena s prekinjenimi črtami. V limiti velikih debelin, kjer direktorski prispevki kratkega dosega nimajo vpliva, se naš rezultat ujema z $\mathcal{F}_{Cas}^{lay}(\gamma)$. Pri majhnih debelinah so pomembni tudi prispevki kratkega dosega. Le-ti so v homeotropni celici in prostostoječem filmu podobni, zato se razlika med primerjanima silama pri majhnih debelinah zmanjša.

Casimirjeva sila v rahlo raztegnjeni ali stisnjeni celici

V prejšnjih razdelkih smo obravnavali Casimirjevo silo v sistemih, katerih debelina je točno ustrezala mnogokratniku debeline smektične plasti d_0. Sedaj nas zanima, kaj se zgodi s Casimirjevo silo, če smektično celico nekoliko raztegnemo ali stisnemo (slika 6). Zaradi preprostosti obravnavamo le deformacije smektičnih plasti

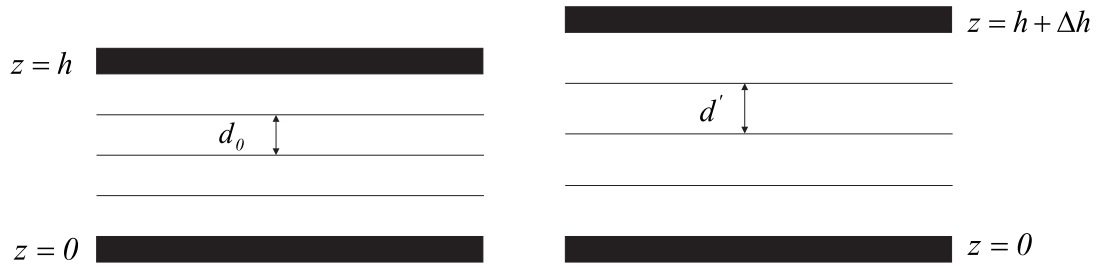

Slika 6 Homeotropna celica, katere debelina je enaka mnogokratniku ravnovesne debeline smektičnih plasti d_0 (levo). Na desni je nekoliko raztegnjena celica. V tem primeru so smektične plasti še vedno ekvidistantne, vendar s povečano periodo d'.

in zanemarimo druge vidike smektične ureditve. Prosta energija deformacij plasti je enaka

$$F_{lay} = \frac{1}{2}\int \left[B\left(\frac{\partial u}{\partial z}\right)^2 + K_L\left(\nabla_\perp^2 u\right)^2 \right] \mathrm{d}V \,. \tag{35}$$

Z minimizacijo proste energije enostavno dobimo ravnovesni profil $u_{mf}(z) = z\Delta h/h$. Pripadajoča prosta energija ravnovesne konfiguracije

$$F_{lay}^{mf} = \frac{1}{2} BS \frac{\Delta h^2}{h} \,, \tag{36}$$

je odvisna od razdalje med ploščama in vodi do sile povprečnega polja

$$\mathcal{F}_{mf} = -\frac{\partial F_{lay}^{mf}}{\partial(\Delta h)} = -BS\frac{\Delta h}{h} \,. \tag{37}$$

Hamiltonko fluktuacij dobimo z razvojem proste energije okrog ravnovesne konfiguracije $u(\mathbf{r}) = u_{mf}(z) + \delta u(\mathbf{r})$,

$$H[\delta u] = \frac{1}{2}\int \left[2B\frac{\Delta h}{h}\frac{\partial(\delta u)}{\partial z} + B\left(\frac{\partial(\delta u)}{\partial z}\right)^2 + K_L\left(\nabla_\perp^2 \delta u\right)^2 \right] \mathrm{d}V \,. \tag{38}$$

S Fourierovo transformacijo $\delta u(\mathbf{r}) = \sum_{\mathbf{q}} \delta u_{\mathbf{q}}(z) \exp(i\mathbf{q}\boldsymbol{\rho})$ hamiltonko prepišemo v

$$H[\delta u] = \sum_{\mathbf{q}} H_{\mathbf{q}} = \frac{1}{2} S \int_0^h \mathrm{d}z \sum_{\mathbf{q}} \Bigg(B\left|\frac{\partial(\delta u_{\mathbf{q}})}{\partial z}\right|^2 + K_L q^4 \left|\delta u_{\mathbf{q}}\right|^2 + \\ + 2B\frac{\Delta h}{h}\frac{\partial(\delta u_{\mathbf{q}})}{\partial z}\,\delta_{\mathbf{q},\mathbf{0}} \Bigg) \,. \tag{39}$$

Prisotnost trdih plošč ne dovoljuje fluktuacij plasti na robu celice, torej je $\delta u_{\mathbf{q}}(z = 0) = \delta u_{\mathbf{q}}(z = h) = 0$. Zadnji člen v hamiltonki lahko z integracijo pretvorimo v površinski člen, ki je zaradi zgoraj opisanih robnih pogojev enak 0. Sedaj ni težko izračunati particijske funkcije

$$Z_{\mathbf{q}} \propto \left[\sinh\left(\sqrt{\frac{K_L}{B}}q^2 h\right)\right]^{-\frac{1}{2}} \tag{40}$$

in pripadajoče Casimirjeve sile

$$\mathcal{F}_{Cas}^{lay} = -\frac{k_B T S}{16\pi h^2}\zeta_R(2)\sqrt{\frac{B}{K_L}}\,. \tag{41}$$

Kot vidimo, je sila v rahlo stisnjeni oziroma raztegnjeni smektični celici povsem enaka kot v nedeformiranem sistemu. Netrivialna ravnovesna struktura tu ni vplivala na Casimirjevo silo.

O vplivu netrivialne ravnovesne strukture na Casimirjevo silo lahko razmišljamo tudi bolj na splošno. Recimo, da lahko neki enorazsežen sistem opišemo s parametrom reda η in kvadratičnim razvojem proste energije po tem parametru:

$$F = \int_{z'}^{z''} \left[a(z)\dot{\eta}^2 + 2b(z)\dot{\eta}\eta + c(z)\eta^2 + 2d(z)\dot{\eta} + 2e(z)\eta\right] \mathrm{d}z\,. \tag{42}$$

Ravnovesni profil parametra urejenosti podaja Euler-Lagrangeva enačba

$$a\ddot{\eta}_{mf} + \dot{a}\dot{\eta}_{mf} + (\dot{b} - c)\eta_{mf} + \dot{d} - e = 0 \tag{43}$$

z robnima pogojema $\eta_{mf}(z') = \eta'$ in $\eta_{mf}(z'') = \eta''$. Če sedaj vpeljemo fluktuacije okrog ravnovesnege profila $\eta(z) = \eta_{mf}(z) + \delta\eta(z)$, dobimo z razvojem proste energije hamiltonko fluktuacij

$$H = \int_{z'}^{z''} \left[a(z)\delta\dot{\eta}^2 + 2b(z)\delta\dot{\eta}\delta\eta + c(z)\delta\eta^2\right] \mathrm{d}z \tag{44}$$

s pripadajočima robnima pogojema $\delta\eta(z') = \delta\eta(z'') = 0$. Kot vidimo ima hamiltonka enako obliko kot prosta energija, le da ne vsebuje več linearnih členov. Poleg tega v hamiltonki ni odvisnosti od ravnovesne konfiguracije η_{mf}. Zaradi tega tudi Casimirjeva sila ni odvisna od ravnovesne konfiguracije. Potrebno je poudariti, da ti zaključki veljajo le za sisteme, katere lahko opišemo s kvadratičnim razvojem proste energije in s fiksnimi robnimi pogoji, ki ne dovoljujejo fluktuacij. Rahlo deformirana smektična celica je le poseben primer, ki demonstrira navedena opažanja.

Casimirjeva sila v bližini prehoda iz smektične A faze v smektično C fazo

Fazni prehod iz smektične A faze v smektično C fazo lahko opišemo z dvorazsežnim parametrom reda $\boldsymbol{\xi} = (\xi_x, \xi_y)$, ki podaja nagib molekul glede na normalo smektičnih

plasti. Obnašanje sistemov v bližini tega prehoda modeliramo s fenomenološkim Landauovim razvojem proste energije

$$f = f_A + \frac{1}{2}\widetilde{a}(T)\left(\xi_x^2+\xi_y^2\right) + \frac{1}{4}b\left(\xi_x^2+\xi_y^2\right)^2 - \widetilde{\Lambda}\left(\xi_x\frac{\partial\xi_y}{\partial z} - \xi_y\frac{\partial\xi_x}{\partial z}\right) + \frac{1}{2}K_1\left(\frac{\partial\xi_x}{\partial x}+\frac{\partial\xi_y}{\partial y}\right)^2 + \frac{1}{2}K_2\left(\frac{\partial\xi_x}{\partial y}-\frac{\partial\xi_y}{\partial x}\right)^2 + \frac{1}{2}\widetilde{K}_3\left[\left(\frac{\partial\xi_x}{\partial z}\right)^2+\left(\frac{\partial\xi_y}{\partial z}\right)^2\right] . \tag{45}$$

Ta model vsebuje tudi opis kiralnih smektikov, torej prehoda iz kiralne smektične A* faze v kiralno smektično C* fazo. Temperaturna odvisnost je vsebovana v koeficientu $\widetilde{a}(T)$, ki vodi fazni prehod, medtem ko ostali koeficienti v razvoju niso odvisni od temperature. Lifšicev člen, $\Lambda\left(\xi_x\frac{\partial\xi_y}{\partial z} - \xi_y\frac{\partial\xi_x}{\partial z}\right)$, opisuje vijačno strukturo kiralne smektične C* faze. Trije elastični členi opisujejo deformacijsko energijo direktorskega polja in so analogni Frankovi elastični energiji v nematikih. V smektični A fazi, kjer so molekule orientirane pravokotno na plasti, je ravnovesna vrednost parametra urejenosti $\boldsymbol{\xi}_0$ enaka 0. V smektični C fazi, kjer je prisoten nagib molekul od normale, pa se velikost parametra reda spreminja kot $|\boldsymbol{\xi}_0| \propto (T_c - T)^{1/2}$.

Z razvojem parametra reda v ravnovesni in fluktuacijski del, $\boldsymbol{\xi} = \boldsymbol{\xi}_0 + \delta\boldsymbol{\xi}$, dobimo hamiltonko fluktuacij

$$h = \frac{1}{2}K_3\left\{\begin{array}{c}\eta^{-2}\left(\delta\xi_{\shortparallel}^2+\delta\xi_{\perp}^2\right)\\ \rho^{-2}\delta\xi_{\shortparallel}^2\end{array}\right\} + \frac{1}{2}K_3\left[\left(\frac{\partial\left(\delta\xi_{\shortparallel}\right)}{\partial z}\right)^2+\left(\frac{\partial\left(\delta\xi_{\perp}\right)}{\partial z}\right)^2\right] + \frac{1}{2}K\left[\left(\frac{\partial\left(\delta\xi_{\shortparallel}\right)}{\partial x}+\frac{\partial\left(\delta\xi_{\perp}\right)}{\partial y}\right)^2+\left(\frac{\partial\left(\delta\xi_{\shortparallel}\right)}{\partial y}-\frac{\partial\left(\delta\xi_{\perp}\right)}{\partial x}\right)^2\right] . \tag{46}$$

V prvem členu zgornja vrstica ustreza smektični A fazi, spodnja pa smektični C fazi. Vpeljali smo korelacijski dolžini fluktuacij: $\eta^{-2} = \alpha(T - T_c)$ in $\rho^{-2} = 2\alpha(T_c - T)$. Spotoma smo izvedli transformacijo parametra reda v rotirajoč sistem, $(\xi_x, \xi_y) \rightarrow (\xi_{\shortparallel}, \xi_{\perp})$, ki sledi vijačni strukturi kiralne C faze. V smektični A fazi sta prisotna dva degenerirana masivna fluktuacijska načina, ki predstavljata nagib molekul od normale. V smektični C fazi pa sta prisotna dva tipa fluktuacij. Masivne amplitudne fluktuacije $\delta\xi_{\shortparallel}$ vplivajo na velikost kota nagiba molekul, medtem ko brezmasne fazne fluktuacije $\delta\xi_{\perp}$ le spremenijo smer nagiba v prostoru.

Homeotropna celica

V homeotropni celici ograjujoči plošči vsiljujeta orientacijo direktorja pravokotno na njuno površino. To opišemo z Rapini-Papoularjevim modelom

$$F_S[\boldsymbol{\xi}] = \frac{1}{2}W_1\int \sin^2(|\boldsymbol{\xi}|)\,\mathrm{d}S_1 + \frac{1}{2}W_2\int \sin^2(|\boldsymbol{\xi}|)\,\mathrm{d}S_2 . \tag{47}$$

Tukaj dopustimo možnost različnih jakosti direktorskega sidranja na eni in drugi površini. Zaradi vsiljenih homeotropnih robnih pogojev je možno v celici smektično A strukturo podhladiti pod temperaturo faznega prehoda v smektično C fazo. Tak sistem je frustriran, saj smektik ne more hkrati zadovoljiti robnih pogojev in tendence po nagibu molekul v smektični C fazi. Zaradi frustracije so fluktuacije direktorja izrazitejše, zato moramo ločeno obravnavati primer normalne homeotropne celice ($T > T_C$) in podhlajene celice ($T < T_C$), čeprav je ravnovesna struktura v obeh enaka. Maksimalna možna temperatura podhladitve T_{max}, kjer pride v celici do prehoda v deformirano smektično C strukturo, je odvisna od debeline celice in jakosti sidranja. Izračunamo jo lahko z minimizacijo celotne proste energije, kar vodi do relacije

$$h_c = \sqrt{2}\rho \operatorname{arccot}\left(\frac{L_1 L_2 - (\sqrt{2}\rho)^2}{\sqrt{2}\rho(L_1 + L_2)}\right) . \tag{48}$$

Temperaturna odvisnost je tu skrita v korelacijski dolžini $\rho = [2\alpha(T_c - T_{max})]^{-1/2}$, medtem ko h_c označuje kritično debelino, pri kateri pride do prehoda. Ekstrapolacijski dolžini sidranja sta definirani kot $\lambda_i = K_3/W_i$. V limiti neskončno močnega sidranja se relacija poenostavi v $h_c = \sqrt{2}\pi\rho$.

Casimirjeva sila nad T_C

Casimirjeva sila zaradi direktorskih fluktuacij v homeotropni celici je enaka

$$\mathcal{F}_{Cas} = -\frac{k_B T S}{\pi}\frac{K_3}{K}\int_{1/\eta}^{\infty} \frac{p^2\,\mathrm{d}p}{\frac{(p+L_1^{-1})(p+L_2^{-1})}{(p-L_1^{-1})(p-L_2^{-1})}\exp(2ph) - 1} . \tag{49}$$

Predstavlja prispevek dveh degeneriranih masivnih fluktuacijskih načinov s končno korelacijsko dolžino η. Ta sila je ekvivalentna prispevku čistih direktorskih fluktuacij v sklopljenem sistemu plasti in direktorja, ki smo ga že obravnavali. Tu se bomo osredotočili le na vpliv različnih robnih pogojev na Casimirjevo silo.

Profil Casimirjeve sile za različne vrednosti parametrov površinskega sidranja je prikazan na sliki 7. Predstavljen je redukcijski količnik R, ki je definiran kot razmerje med silo pri končnih jakostih sidranja in silo v limitnem primeru neskončno močnega sidranja

$$R = \frac{\mathcal{F}_{Cas}(L_1, L_2, h, \eta)}{\mathcal{F}_{Cas}(L_1 = L_2 = 0; h, \eta)} . \tag{50}$$

Sila $\mathcal{F}_{Cas}(L_1 = L_2 = 0; h, \eta)$ je pri tem enaka

$$\mathcal{F}_{Cas}(L_1 = L_2 = 0; h, \eta) = -\frac{k_B T S}{2\pi}\frac{K_3}{K}\frac{1}{h^3}\sum_{k=1}^{\infty}\frac{\exp(-2hk/\eta)}{k^3}\left(\frac{1}{2} + \frac{h}{\eta}k + \frac{h^2}{\eta^2}k^2\right) . \tag{51}$$

Profile na sliki 7 lahko razložimo takole. Casimirjeva sila je v primeru simetričnih robnih pogojev, torej močnega ali šibkega sidranja na obeh ploščah, privlačna. V

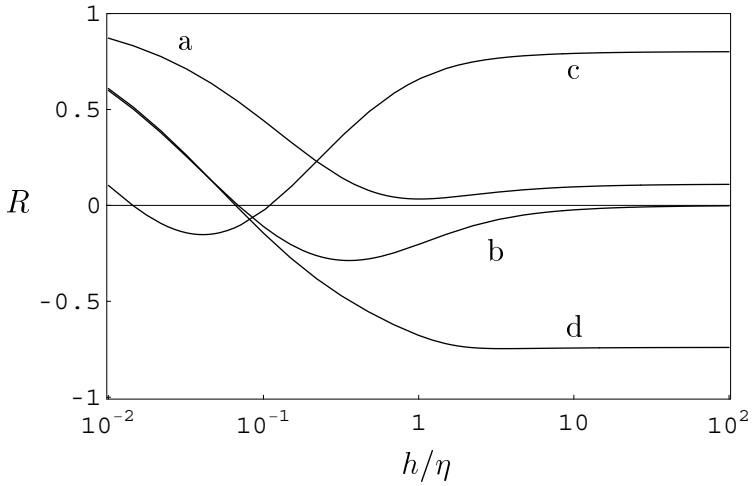

Slika 7 Casimirjeva sila v homeotropni celici pri temperaturi nad T_c. Prikazana je odvisnost redukcijskega količnika R od reducirane debeline celice h/η. Uporabljeni so sledeči parametri sidranja: a) $L_1/\eta = 0.5$, $L_2/\eta = 0.5$; b) $L_1/\eta = 1$, $L_2/\eta = 0.05$; c) $L_1/\eta = 0.1$, $L_2/\eta = 0.01$; d) $L_1/\eta = 10$, $L_2/\eta = 0.05$.

primeru antisimetričnih robnih pogojev, ko je sidranje na eni plošči močno, na drugi pa šibko, Casimirjeva sila spremeni predznak in postane odbojna. Efektivno jakost sidranja določajo razmerja med ekstrapolacijskima dolžinama L_1 in L_2 ter karakterističnimi dolžinami v sistemu, v našem primeru sta to debelina celice h in korelacijska dolžina η. V tankih celicah ($h/\eta < 1$) efektivno jakost sidranja določata razmerji L_1/h in L_2/h. V primeru, da je $L_i/h < 1$, je sidranje na izbrani plošči efektivno močno, medtem ko je v primeru $L_i/h > 1$ sidranje efektivno šibko. V debelejših celicah ($h/\eta > 1$) efektivno jakost sidranja določata razmerji L_1/η in L_2/η, upoštevaje enak princip kot v prvem režimu. Navedene kriterije za določitev efektivne jakosti sidranja obrazložimo z dejstvom, da je sidranje efektivno močno, če je interakcija med tekočim kristalom in površino močnejša od notranjih interakcij v tekočem kristalu. Jakost površinske interakcije nam podajata ekstrapolacijski dolžini L_1 in L_2. Notranjo interakcijo pa opišemo z dvema prispevkoma, kot je razvidno iz hamiltonke (46): jakost "masivnega" prispevka je karakterizirana s korelacijsko dolžino η, medtem ko se elastični prispevek skalira kot h^{-1}. Pri majhnih debelinah h/η je dominanten elastični prispevek, zato efektivno jakost sidranja podaja razmerje L_i/h. Pri velikih h/η prevlada "masivni" prispevek, zato efektivno jakost sidranja merimo s parametroma L_1/η in L_2/η.

Uporabimo sedaj zgornjo argumentacijo za razlago slike 7. Vse dolžine na sliki so skalirane s korelacijsko dolžino η. Parametra L_1/h in L_2/h sta odvisna od reducirane debeline h/η. Zato se v režimu $h/\eta < 1$ s spreminjanjem debeline lahko zamenja predznak sile [slika 7(b)-(d)]. Parametra L_1/η in L_2/η sta fiksna, zato v

režimu $h/\eta > 1$ sila ne spremeni predznaka. Ne smemo pozabiti, da je korelacijska dolžina η odvisna od temperature in da se zato značaj sile lahko spreminja s temperaturo. V limiti velikih debelin ($h/\eta \gg 1$) se redukcijski količnik ustali pri konstantni vrednosti, kar pomeni, da je krajevna odvisnost sile tam enaka $\exp(-2h/\eta)/h$. Saturacijsko vrednost R lahko izračunamo analitično za primer zelo močnega sidranja na obeh ploščah, kjer znaša $R = 1 - 2(L_1/\eta + L_2/\eta)$ [slika 7(c)]. V primeru zelo šibkega sidranja na obeh ploščah pa je enaka $R = 1 - 2(\eta/L_1 + \eta/L_2)$. V antisimetričnem primeru z zelo močnim sidranjem na eni plošči in zelo šibkim na drugi se redukcijski količnik nasiti pri $R = -1 + 2(\eta/L_1 + L_2/\eta)$ [slika 7(d)]. Posebno obnašanje sile pri velikih razdaljah opazimo pri parametrih sidranja $L_i/\eta = 1$, kjer sidranje na ploščah ni niti močno niti šibko. V tem primeru sila upada hitreje, in sicer kot $\exp(-2h/\eta)/h^3$.

Casimirjeva sila v frustriranem sistemu ($T_{max} < T < T_c$)

Casimirjeva sila v frustrirani homeotropni celici je enaka

$$\begin{aligned}\mathcal{F}_{Cas} = &- \frac{k_B T S}{\pi}\frac{K_3}{K}\Bigg[\int_0^\infty \frac{p^2\,\mathrm{d}p}{\frac{(p+L_1^{-1})(p+L_2^{-1})}{(p-L_1^{-1})(p-L_2^{-1})}\exp(2ph)-1} \\ &+ \frac{1}{2}\int_0^{(\sqrt{2}\rho)^{-1}} \frac{(L_1^{-1}L_2^{-1}-p^2)\cot(ph) - p(L_1^{-1}+L_2^{-1})}{(L_1^{-1}L_2^{-1}-p^2) + p(L_1^{-1}+L_2^{-1})\cot(ph)}\,p^2\,\mathrm{d}p\Bigg]\,.\end{aligned} \tag{52}$$

Bolj ilustrativen izraz dobimo v limiti neskončno močnega sidranja ($L_1 = 0$, $L_2 = 0$)

$$\mathcal{F}_{Cas}(L_1 = 0, L_2 = 0) = -\frac{k_B T S}{4\pi}\frac{K_3}{K}\left[\frac{\zeta(3)}{h^3} + 2\int_0^{(\sqrt{2}\rho)^{-1}} \cot(ph)p^2\,\mathrm{d}p\right]\,. \tag{53}$$

Prvi člen v sili je tipičen Casimirjev prispevek dolgega dosega, značilen za direktorske fluktuacije v nematiku. Drugi člen je pri majhnih debelinah h/ρ privlačen in približno enakega velikostnega reda kot prvi člen. Z večanjem debeline drugi člen postane odbojen in končno logaritemsko divergira pri prehodu v deformirano smektično C strukturo.

Temperaturna odvisnost Casimirjeve sile v homeotropni celici je prikazana na sliki 8. Pri temperaturah nad T_c je sila podana z enačbo (49). Glede na parametre sidranja je sila v tem območju lahko privlačna ali odbojna. S podhladitvijo sistema sila najprej doseže lokalni minimum, nato pa pride do odbojne divergence sile pri prehodu v deformirano smektično C strukturo. Čim močnejše je sidranje na ploščah, tem nižja je temperatura do katere lahko podhladimo smektično A strukturo, in izrazitejši je lokalni minimum. Naj omenimo, da je obnašanje frustriranega smektičnega sistema analogno obnašanju Casimirjeve sile v frustrirani nematski Fréedericksovi celici [121].

V frustrirani homeotropni celici dobimo poleg že opisanih prispevkov h Casimirjevi sili še dodaten prispevek, ki je posledica dejstva, da je pri temperaturi $T < T_c$

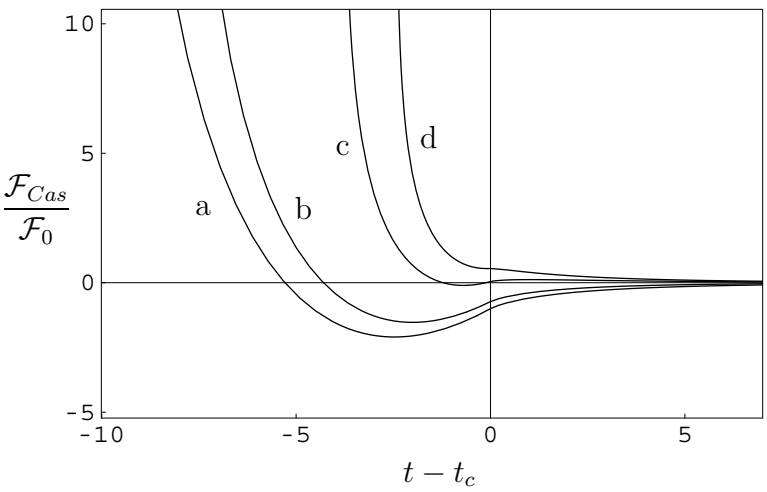

Slika 8 Temperaturni profil Casimirjeve sile v homeotropni celici. Vpeljali smo reducirano temperaturo $t = \alpha h^2 T/K_3$. Amplituda sile je podana v naravni enoti $\mathcal{F}_0 = k_B T S K_3 \zeta_R(3)/4\pi K h^3$. Uporabljeni so sledeči parametri sidranja: a) $L_1/h = 0$, $L_2/h = 0$; b) $L_1/h = 0.1$, $L_2/h = 0.01$; c) $L_1/h = 1$, $L_2/h = 0.05$; d) $L_1/h = 10$, $L_2/h = 0.05$.

referenčna konfiguracija tekočega kristala izven plošč v smektični C fazi, medtem ko je med ploščama še vedno struktura smektika A. Ta prispevek je divergenten in ga z našo metodo nismo uspeli regularizirati. Vendar za praktične namene to ni ključno, saj ta prispevek ni odvisen od razdalje med ploščama in ga z eksperimentalnimi aparaturami (AFM, SFA), ki merijo razliko sil pri različnih debelinah, ne bi zaznali. Nadalje je v frustrirani homeotropni celici prisotna tudi sila povprečnega polja, ki je posledica razlik prostih energij med smektično A fazo in referenčno strukturo izven plošč, ki je v smektični C fazi. Sila povprečnega polja je enaka

$$\mathcal{F}_{mf} = (f_C - f_A)S = -\frac{1}{4}\frac{\alpha^2}{b}(T_c - T)^2 S \ , \tag{54}$$

kjer sta f_C in f_A gostoti prostih energij smektične C oziroma smektične A faze. Sila povprečnega polja je precej močnejša od Casimirjeve sile, vendar je neodvisna od razdalje med ploščama h, zato ne bi ovirala eksperimentalne detekcije Casimirjeve sile.

Prostostoječi filmi

V prostostoječih filmih je smektični material omejen s prostima površinama, ki sta v stiku z zrakom. V našem preprostem modelu predpostavimo, da zaželena orientacija direktorja na prostih površinah sovpada z ravnovesno orientacijo direktorja v notranjosti filma. Vpeljemo torej neke vrste efektivno notranje sidranje. Ravnovesna struktura filma je v takem modelu vedno homogena. Zaradi simetričnih robnih pogojev je Casimirjeva sila v prostostoječih filmih vedno privlačna.

V smektičnem A filmu je sila identična kot v homeotropni celici, le da sta ekstrapolacijski dolžini L_1 in L_2 na obeh površinah enaki:

$$\mathcal{F}_{Cas} = -\frac{k_B T S}{\pi}\frac{K_3}{K}\int_{1/\eta}^{\infty}\frac{p^2\,\mathrm{d}p}{\frac{(p+L^{-1})^2}{(p-L^{-1})^2}\exp(2ph)-1}\,. \tag{55}$$

To je tipična Casimirjeva sila kratkega dosega za masivne fluktuacijske načine s korelacijsko dolžino η.

V smektičnem C filmu so molekule nagnjene glede na normalo plasti. V našem modelu površinsko sidranje opišemo z

$$F_S[\boldsymbol{\xi}] = \frac{1}{2}K_3\sum_{i=1,2}\left[L_{\shortparallel}^{-1}\int\sin^2(\xi_{\shortparallel}-\xi_{\shortparallel 0})\,\mathrm{d}S_i + L_{\perp}^{-1}\int\sin^2(\xi_{\perp})\,\mathrm{d}S_i\right]\,, \tag{56}$$

kjer je $\xi_{\shortparallel 0}$ ravnovesna vrednost nagiba molekul. V splošnem uvedemo različni jakosti sidranja za amplitudne fluktuacije $\delta\xi_{\shortparallel}$ in fazne fluktuacije $\delta\xi_{\perp}$. Casimirjeva sila je v takem sistemu enaka

$$\mathcal{F}_{Cas} = -\frac{k_B T S}{2\pi}\frac{K_3}{K}\left[\int_{1/\rho}^{\infty}\frac{r^2\,\mathrm{d}r}{\frac{(r+L_{\shortparallel}^{-1})^2}{(r-L_{\shortparallel}^{-1})^2}\exp(2rh)-1} + \int_{0}^{\infty}\frac{r^2\,\mathrm{d}r}{\frac{(r+L_{\perp}^{-1})^2}{(r-L_{\perp}^{-1})^2}\exp(2rh)-1}\right]\,. \tag{57}$$

Prvi člen predstavlja prispevek masivnih amplitudnih fluktuacij s korelacijsko dolžino ρ, ki je kratkega dosega. Drugi člen pa je prispevek brezmasnih faznih fluktuacij in je dolgega dosega.

Temperaturni profil Casimirjeve sile v prostostoječem filmu je predstavljen na sliki 9. Predpostavili smo, da je sidranje neskončno močno: $L = 0$ v smektičnem A filmu ter $L_{\shortparallel} = 0$ in $L_{\perp} = 0$ v smektičnem C filmu. Casimirjeva sila doseže maksimalno amplitudo pri strukturnem prehodu iz smektičnega A filma v smektični C film ($T = T_c$). Pri zviševanju ali nižanju temperature se jakost sile zmanjša. V smektičnem A filmu sta prisotna dva degenerirana masivna fluktuacijska načina, katerih amplituda z oddaljevanjem od prehoda hitro upada. V smektičnem C filmu pa je prispevek brezmasnih faznih fluktuacij skoraj neodvisen od temperature, medtem ko prispevek masivnih amplitudnih fluktuacij naglo upada z nižanjem temperature. Zato je profil Casimirjeve sile nesimetričen. Ob strukturnem prehodu Casimirjeva sila v prostostoječem filmu ne divergira. To je posledica preprostega modela sidranja, v katerem se površinski red vedno ujema z ureditvijo v notranjosti filma in ne pride do frustracije. Povečana jakost sile pri prehodu je posledica divergence korelacijskih dolžin pri temperaturi $T = T_c$. Uporaba bolj realističnih robnih pogojev s končno jakostjo sidranja ne bi bistveno spremenila temperaturnega profila, ampak bi zgolj zmanjšala amplitudo sile.

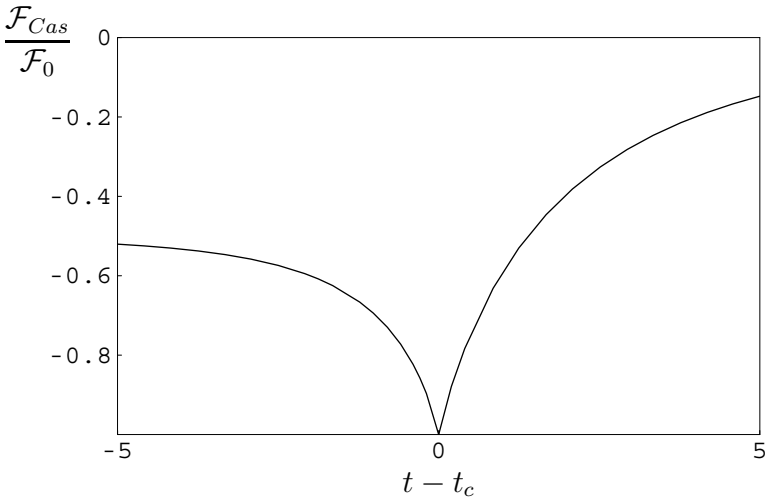

Slika 9 Temperaturni profil Casimirjeve sile v prostostoječem smektičnem filmu. Vpeljali smo reducirano temperaturo $t = \alpha h^2 T/K_3$. Amplituda sile je podana v naravni enoti $\mathcal{F}_0 = k_B T S K_3 \zeta_R(3)/4\pi K h^3$. Predpostavili smo, da je sidranje neskončno močno: $L = 0$ v smektičnem A filmu ter $L_{\shortparallel} = 0$ in $L_{\perp} = 0$ v smektičnem C filmu.

Casimirjeva sila v prostostoječem smektičnem A filmu s povečanim površinskim redom

V bližini faznega prehoda iz smektične A faze v smektično C fazo se pogosto zgodi, da so molekule v robnih plasteh prostostoječega filma nagnjene, medtem ko je notranjost filma še v smektični A fazi [164]. Tak sistem modeliramo tako, da v robnem pogoju za velikost nagiba $\boldsymbol{\xi}$ predpišemo neko neničelno vrednost ξ_S (slika 10). Ob

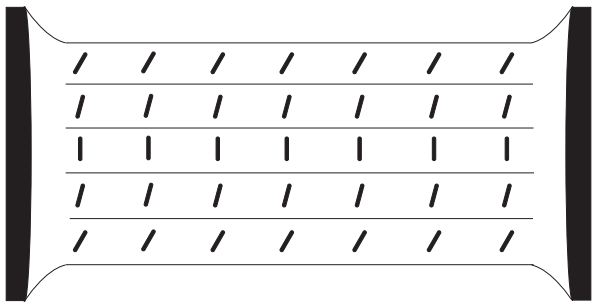

Slika 10 Prostostoječi smektični A film s povečanim površinskim redom. Molekule v robnih plasteh so nagnjene, medtem ko je v notranjosti filma še vedno v smektična A struktura.

predpostavki, da je površinski nagib molekul majhen, lahko v okviru kvadratičnega razvoja proste energije določimo ravnovesni profil nagiba molekul v filmu

$$\xi_{\shortparallel}^{mf}(z) = \xi_S \frac{\cosh(z/\eta)}{\cosh(h/2\eta)} \,. \tag{58}$$

Posledica te nehomogene ravnovesne ureditve je prisotnost sile povprečnega polja

$$\mathcal{F}_{mf} = -\frac{\partial F_{mf}}{\partial h} = -\frac{K_3 S \xi_S^2}{2\eta^2 \cosh^2(h/2\eta)} \ . \tag{59}$$

Sila povprečnega polja je privlačna in kratkega dosega.

Hamiltonko fluktuacij dobimo z razvojem proste energije okrog ravnovesja ($\xi_{\shortparallel} = \xi_{\shortparallel}^{mf} + \delta\xi_{\shortparallel}$, $\xi_{\perp} = \delta\xi_{\perp}$)

$$\begin{aligned} h = \frac{1}{2} K_3 \eta^{-2} \left(2\xi_{\shortparallel}^{mf} \delta\xi_{\shortparallel} + \delta\xi_{\shortparallel}^2 + \delta\xi_{\perp}^2 \right) + \frac{1}{2} K_3 \Bigg[\left(\frac{\partial(\delta\xi_{\shortparallel})}{\partial z} \right)^2 + 2 \frac{\partial \xi_{\shortparallel}^{mf}}{\partial z} \frac{\partial(\delta\xi_{\shortparallel})}{\partial z} \\ + \left(\frac{\partial(\delta\xi_{\perp})}{\partial z} \right)^2 \Bigg] + \frac{1}{2} K \left[\left(\frac{\partial(\delta\xi_{\shortparallel})}{\partial x} + \frac{\partial(\delta\xi_{\perp})}{\partial y} \right)^2 + \left(\frac{\partial(\delta\xi_{\shortparallel})}{\partial y} - \frac{\partial(\delta\xi_{\perp})}{\partial x} \right)^2 \right] \ . \end{aligned} \tag{60}$$

V hamiltonki nastopata dva člena, ki sta odvisna od ravnovesne konfiguracije $\xi_{\shortparallel}^{mf}$, vendar ju je možno prevesti v površinski prispevek. Če predpostavimo fiksne robne pogoje, ki ne dopuščajo fluktuacij na površini filma, sta ta člena enaka 0 in ne prispevata k hamiltonki. V tem primeru je hamiltonka enaka hamiltonki fluktuacij v homogenem smektičnem A filmu. Zato je tudi Casimirjeva sila v filmu s povečanim površinskim redom enaka kot v homogenem filmu. To je torej še en primer sistema z netrivialno ravnovesno strukturo, ki pa se ne odraža v Casimirjevi sili. Ponovno poudarimo, da to velja za sisteme, ki jih lahko opišemo s kvadratičnim razvojem proste energije in s fiksnimi robnimi pogoji.

Nehomogeni sistemi

Sistemi z netrivialno ravnovesno ureditvijo predstavljajo posebno poglavje v teoriji Casimirjeve interakcije in so bili dosedaj le redko obravnavani [120, 129, 180]. Glavni problem v teh sistemih je regularizacija divergentne proste energije fluktuacij, ki je ni vedno možno izvesti analitično. V predhodnih razdelkih smo že srečali dva primera sistemov z netrivialno ravnovesno strukturo – rahlo deformirano smektično celico in prostostoječi film s povečanim površinskim redom. V obeh teh primerih se je ravnovesna struktura odražala v dodatnih členih v hamiltonki fluktuacij, ki pa jih je bilo možno ob predpostavki fiksnih robnih pogojev izločiti. Zato netrivialna ureditev ni vplivala na Casimirjevo silo. V tem razdelku obravnavamo dva primera sistemov, kjer se nehomogenost ravnovesne ureditve odraža v krajevni odvisnosti snovnih konstant. V tem primeru je vpliv nehomogenosti na Casimirjevo silo bistven.

Casimirjeva sila v bližini prehoda iz smektične v nematsko fazo

V dosedaj obravnavanih sistemih smo predpostavljali, da je ravnovesna stopnja smektičnega reda ψ homogena po celotnem vzorcu. Vendar v bližini faznega pre-

hoda iz smektične v nematsko fazo ta predpostavka postane vprašljiva, saj ograjujoče površine pogosto vsiljujejo večjo stopnjo pozicijske ureditve od lastne, kakršna je v notranjosti vzorca.

Obravnavajmo primer homeotropne smektične A celice, kjer ograjujoči plošči vsiljujeta stopnjo pozicijskega reda $\tilde{\psi}_S$ (slika 11). Profil pozicijske ureditve približno

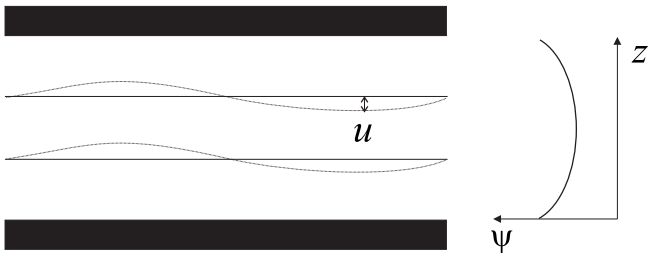

Slika 11 Homeotropna smektična A celica s povečanim površinskim pozicijskim redom ψ. Profil pozicijskega reda je prikazan shematično na desni. Obravnavamo Casimirjevo silo, ki jo povzročajo fluktuacije smektičnih plasti u.

opišemo z

$$\psi(z) = \tilde{\psi}_S \frac{\cosh(z/\xi)}{\cosh(h/2\xi)} \,, \tag{61}$$

kjer je ξ smektična korelacijska dolžina. Zaradi preprostejšega opisa smo za koordinate ograjujočih plošč vzeli $z = \pm h/2$. Sedaj želimo izračunati Casimirjevo silo zaradi fluktuacij smektičnih plasti, ki jih opišemo s hamiltonko

$$H = \frac{1}{2} \int \left[B \left(\frac{\partial u}{\partial z} \right)^2 + K_L \left(\nabla_\perp^2 u \right)^2 \right] \mathrm{d}V \,. \tag{62}$$

Elastični konstanti B in K_L sta sorazmerni s kvadratom pozicijskega reda ψ in ju lahko zapišemo kot

$$B = B_S \frac{\cosh^2(z/\xi)}{\cosh^2(h/2\xi)} \,, \qquad K_L = K_S \frac{\cosh^2(z/\xi)}{\cosh^2(h/2\xi)} \,. \tag{63}$$

Imamo torej opravka s hamiltonko fluktuacij smektičnih plasti, kjer so elastične konstante odvisne od kraja. S Fourierovo transformacijo fluktuirajočega polja u se hamiltonka pretvori v

$$H_{\mathbf{q}}[u] = \frac{1}{2} S K_S \int_{-h/2}^{h/2} \left[\lambda^{-2} \frac{\cosh^2(z/\xi)}{\cosh^2(h/2\xi)} \left| \frac{\partial u_{\mathbf{q}}}{\partial z} \right|^2 + \frac{\cosh^2(z/\xi)}{\cosh^2(h/2\xi)} q^4 \left| u_{\mathbf{q}} \right|^2 \right] \mathrm{d}z \,, \tag{64}$$

kjer smo vpeljali karakteristično dolžino $\lambda = \sqrt{K_S/B_S}$. Ob predpostavki fiksnih robnih pogojev, $u(z = \pm h/2) = 0$, lahko ovrednotimo particijsko funkcijo fluktuacij, ki se glasi

$$Z_{\mathbf{q}}[u] \propto [\sinh(\sqrt{\lambda^2 q^4 + \xi^{-2}}\, h)]^{-\frac{1}{2}} \,. \tag{65}$$

Po običajni regularizaciji proste energije fluktuacij dobimo Casimirjevo silo

$$\mathcal{F}_{Cas} = -\frac{k_B T S}{2\pi\xi} \int_0^\infty \frac{\sqrt{1+\xi^2\lambda^2 q^4}}{\exp\left(2h\sqrt{1+\xi^2\lambda^2 q^4}/\xi\right) - 1}\, q\, \mathrm{d}q \; . \tag{66}$$

Tega integrala ni možno izračunati analitično, lahko pa izpeljemo obnašanje sile v limitah velikih in majhnih debelin celice. V limiti majhnih debelin ($h/\xi \to 0$) je sila enaka

$$\mathcal{F}_{Cas}\left(h/\xi \to 0\right) = -\frac{k_B T S \zeta_R(2)}{16\pi\lambda h^2} \; . \tag{67}$$

To je znan izraz za Casimirjevo silo, ki jo povzročajo fluktuacije plasti, v homogenih smektičnih sistemih. V limiti majhnih debelin je namreč profil pozicijskega reda ψ praktično konstanten, zato vpliva nehomogenosti na silo ni. V limiti velikih debelin ($h/\xi \to \infty$) je sila enaka

$$\mathcal{F}_{Cas}\left(h/\xi \to \infty\right) = -\frac{k_B T S}{8\sqrt{\pi}\xi^2\lambda} \frac{\exp\left(-2h/\xi\right)}{\sqrt{h/\xi}} \; . \tag{68}$$

To je zelo zanimiv rezultat, saj fluktuacije smektičnih plasti, ki jih opišemo z elastično hamiltonko, zaradi krajevno odvisnih elastičnih konstant povzročajo Casimirjevo silo kratkega dosega. Le-ta upada kot $\exp(-2h/\xi)/\sqrt{h/\xi}$. Tak eksponentni upad Casimirjeve sile pri velikih debelinah je sicer značilen za masivne fluktuacijske načine. Zato lahko sklepamo, da ima nehomogenost v takem sistemu vlogo efektivne mase fluktuacij. Numerično izračunan profil Casimirjeve sile za širši razpon debelin je prikazan na sliki 12.

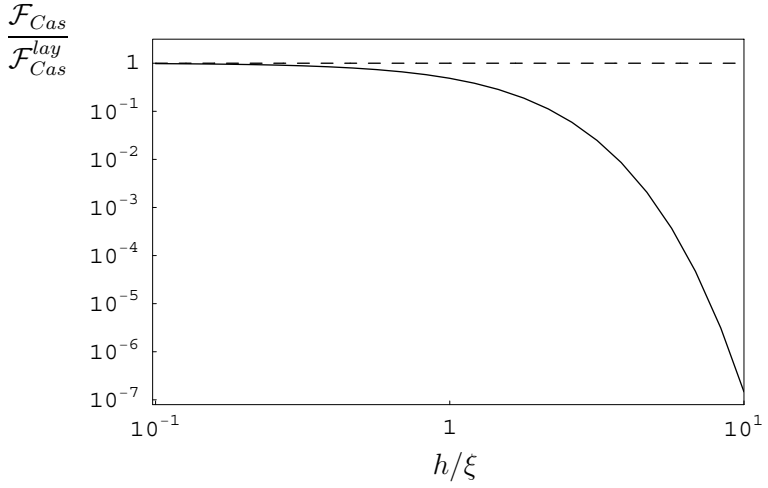

Slika 12 Profil Casimirjeve sile v homeotropni smektični A celici z nehomogenim pozicijski redom. Silo skaliramo s Casimirjevo silo v homogeni smektični celici $\mathcal{F}_{Cas}^{lay} = -k_B T S \zeta_R(2)/16\pi\lambda h^2$. Pri majhnih debelinah je $\mathcal{F}_{Cas}$ enaka $\mathcal{F}_{Cas}^{lay}$. Pri velikih debelinah pa upada hitreje, in sicer kot $\exp(-2h/\xi)/\sqrt{h/\xi}$.

Casimirjeva sila v predsmektični nematski celici

Tudi če je tekoči kristal v nematski fazi, je v ograjenih sistemih vedno prisotna delna površinsko vsiljena pozicijska urejenost. Izvor tega reda je v preprostem dejstvu, da molekule ne morejo prodreti v trde robove, zato je vedno prisotna vsaj ena plast pozicijsko urejenih molekul ob površini. Orientacijske direktorske fluktuacije so sklopljene s smektičnim redom, zato se prisotnost predsmektične pozicijske ureditve odraža v povečani energiji direktorskih fluktuacijskih načinov oziroma njihovi "masi".

Obravnavamo Casimirjevo silo v homeotropni nematski celici s površinsko vsiljenim smektičnim redom (slika 13). Ravnovesni profil stopnje pozicijske ureditve

Slika 13 Homeotropna nematska celica s površinsko vsiljenim predsmektičnim redom ψ. Profil pozicijskega reda je shematsko prikazan na desni. Obravnavamo Casimirjevo silo, ki jo povzročajo direktorske fluktuacije $\delta\mathbf{n}$.

opišemo z

$$\psi_{mf}(z) = \psi_S \frac{\cosh(z/\xi)}{\cosh(h/2\xi)} \,. \tag{69}$$

Nematska direktorska prosta energija se v enokonstantnem približku glasi

$$f = \frac{1}{2} D(\delta\mathbf{n})^2 + \frac{1}{2} K \left[(\nabla \cdot \mathbf{n})^2 + (\nabla \times \mathbf{n})^2 \right] \,. \tag{70}$$

Sklopitvena konstanta med (pred)smektičnimi plastmi in direktorjem D je sorazmerna s kvadratom stopnje pozicijskega reda ψ. V običajnih nematikih brez smektičnega reda je konstanta D enaka 0. Hamiltonka direktorskih fluktuacij, $\delta\mathbf{n} = (n_x, n_y)$, je enaka

$$\begin{aligned} H = \frac{1}{2} K \int \Bigg[& \Lambda^{-2}(z) \left(n_x^2 + n_y^2 \right) + \left(\frac{\partial n_x}{\partial x} + \frac{\partial n_y}{\partial y} \right)^2 + \left(\frac{\partial n_y}{\partial x} - \frac{\partial n_x}{\partial y} \right)^2 \\ & + \left(\frac{\partial n_x}{\partial z} \right)^2 + \left(\frac{\partial n_y}{\partial z} \right)^2 \Bigg] \mathrm{d}V \,. \end{aligned} \tag{71}$$

Vpeljali smo krajevno odvisno korelacijsko dolžino $\Lambda^{-2}(z) = D(z)/K$. V splošnem ne moremo izračunati particijske funkcije fluktuacij, zato aproksimiramo odvisnost $D(z)$ s paraboličnim profilom

$$D(z) = D_S \frac{(z/\xi)^2}{(h/2\xi)^2} \,. \tag{72}$$

V tem primeru je particijska funkcija direktorskih fluktuacij enaka

$$Z_{\mathbf{q}}[n_{\mathbf{q}}] \propto \frac{1}{\sqrt{2k}} \Bigg[-\frac{1}{2}x_0 \left(A+\frac{1}{2}\right) \frac{M[\frac{1}{2}A+\frac{5}{4},\frac{3}{2},\frac{1}{8}x_0^2]}{M[\frac{1}{2}A+\frac{1}{4},\frac{1}{2},\frac{1}{8}x_0^2]} + \frac{2}{x_0} + \\ + \frac{1}{2}x_0 \left(\frac{1}{3}A+\frac{1}{2}\right) \frac{M[\frac{1}{2}A+\frac{7}{4},\frac{5}{2},\frac{1}{8}x_0^2]}{M[\frac{1}{2}A+\frac{3}{4},\frac{3}{2},\frac{1}{8}x_0^2]} \Bigg]^{1/2} , \tag{73}$$

kjer je $M[a,b,z]$ Kummrova konfluentna hipergeometrijska funkcija [181]. Vpeljali smo sledeče parametre

$$\alpha = \frac{\xi^2 C_\perp q_0^2 \psi_S^2}{K} , \quad A = \frac{h\xi}{4\sqrt{\alpha}}\, q^2 , \quad x_0 = \sqrt{\frac{4h\sqrt{\alpha}}{\xi}} , \quad k = \sqrt{\frac{h}{4\xi\sqrt{\alpha}}} . \tag{74}$$

Prosta energija fluktuacij je sedaj podana z

$$F_{fluc} = \frac{k_B T S}{2\pi} \int_0^\infty \ln(Z_{\mathbf{q}}[n_{\mathbf{q}}]) q \, \mathrm{d}q , \tag{75}$$

pri čemer smo upoštevali, da sta v sistemu prisotna dva degenerirana direktorska fluktuacijska načina. Proste energije fluktuacij žal ni možno regularizirati analitično. Zato uporabimo sledečo proceduro. Najprej izračunamo odvod proste energije $\partial F_{fluc}/\partial h$, s čimer se znebimo prispevkov neodvisnih od debeline celice h, ki ne prispevajo k interakciji. Nadalje upoštevamo dejstvo, da mora iti v limiti velikih debelin h interakcijski del proste energije proti 0. Zato za različne vrednosti valovnega vektorja $\mathbf{q}$ izračunamo odvod $\partial F_{fluc}/\partial h$ pri velikih h. S tem dobimo referenčno vrednost, ki jo je potrebno odšteti od celotnega odvoda, da nam ostane le interakcijski del oziroma sila. Vrednost odvoda $\partial F_{fluc}/\partial h$ pa pri velikih h ni povsem konstantna, kot bi pričakovali, ampak se z večanjem debeline rahlo spreminja. Zato naša numerična procedura regularizacije proste energije ni povsem natančna. Dobljeni rezultati so zato omejeni na majhne debeline celic, kjer je interakcijski prispevek velik in je negotovost zaradi ne povsem točne regularizacije razmeroma majhna.

Casimirjeva sila v homeotropni nematski celici s predsmektičnim redom je prikazana na sliki 14. Primerjamo jo z običajno nematsko direktorsko silo, ki je prisotna v sistemih brez smektičnega reda. Redukcijski količnik R_1 je definiran kot

$$R_1 = \frac{\mathcal{F}_{Cas}(\alpha)}{\mathcal{F}_{Cas}^{nem}} , \tag{76}$$

kjer je $\mathcal{F}_{Cas}^{nem} = k_B T S \zeta_R(3)/4\pi h^3$. Različne vrednosti parametra α opisujejo različne stopnje površinsko vsiljenega smektičnega reda. Pri zelo majhnih debelinah je sila v predsmektični nematski celici enaka kot v običajnem nematiku. To je v skladu z znanimi rezultati za homogene sisteme z masivnimi fluktuacijskimi načini. Pri večjih

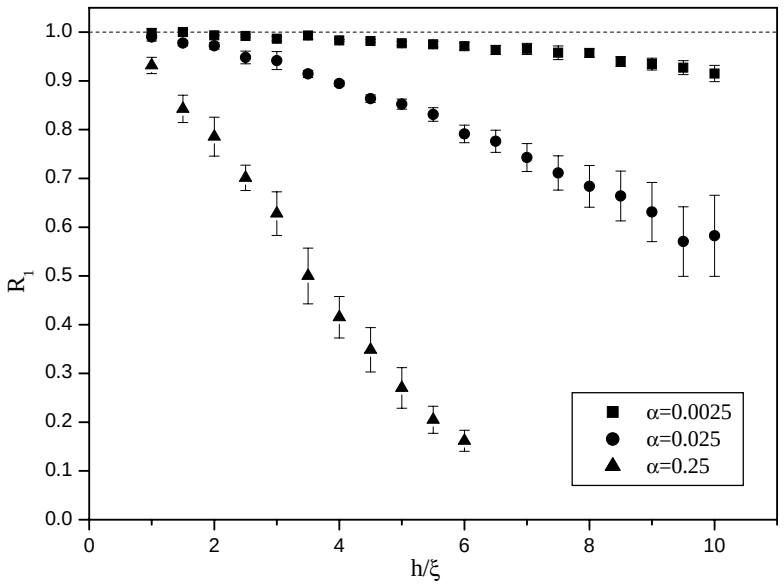

Slika 14 Casimirjeva sila v predsmektičnem nematskem sistemu v primerjavi s tipično Casimirjevo silo v običajnem nematiku, ki je sorazmerna z $1/h^3$. Različne vrednosti parametra α opisujejo različne stopnje površinsko vsiljenega pozicijskega reda ψ_S. Na grafih je označena negotovost zaradi približne numerične regularizacije.

debelinah sila v predsmektičnem sistemu upada hitreje kot $1/h^3$. To je pričakovano, saj so direktorske fluktuacije zaradi prisotnosti smektičnega reda masivne. Čim večja je stopnja površinsko vsiljenega reda, tem večja je masa fluktuacij in tem hitreje upada sila.

Problem Casimirjeve sile v predsmektični nematski celici še ni dokončno rešen. Predvsem bo potrebno poiskati boljšo metodo za regularizacijo proste energije fluktuacij. Kljub temu pa lahko napovemo, da zaradi vedno prisotnega površinskega pozicijskega reda v realnih sistemih ne moremo pričakovati standardne nematske direktorske Casimirjeve sile, sorazmerne z $1/h^3$.

Zaključek

V tem delu smo se ukvarjali z različnimi vidiki Casimirjevega pojava v smektičnih tekočekristalnih sistemih. Najprej smo obravnavali Casimirjevo silo v dveh smektičnih A sistemih s planarno geometrijo – v homeotropni celici in prostostoječem smektičnem filmu. Predpostavili smo, da je ravnovesna ureditev smektika homogena. Izračunali smo silo, ki jo povzročajo termične fluktuacije pozicijskega in orientacijskega reda v smektikih. Pri tem smo upoštevali sklopitev med pozicijsko in orientacijsko ureditvijo. Ugotovili smo, da fluktuacije stopnje smektičnega reda rezultirajo v privlačni Casimirjevi sili kratkega dosega, medtem ko sklopljene fluktuacije

direktorja in smektičnih plasti povzročajo interakcijo dolgega dosega. Izkazalo se je, da je vpliv direktorskih prostostnih stopenj pomemben pri majhnih debelinah sistemov. Pri velikih debelinah pa je možno Casimirjevo silo zadovoljivo opisati s poenostavljenim modelom, ki upošteva le fluktuacije smektičnih plasti, pri čemer predpostavimo, da je direktor stalno orientiran pravokotno na plasti. S predstavljenimi rezultati smo podali celovito sliko Casimirjevega pojava v planarnih smektičnih A sistemih s homogeno ravnovesno strukturo.

Nadalje smo obravnavali obnašanje Casimirjeve sile v bližini faznega prehoda iz smektične A faze v smektično C fazo. Z uporabljenim modelom smo zaobjeli tako kiralne kot tudi običajne smektične faze. Posebej zanimiv je primer frustrirane homeotropne celice, v kateri je smektična A struktura stabilizirana z robnimi pogoji in jo zato lahko podhladimo pod temperaturo faznega prehoda v smektično C fazo. V takem sistemu so direktorske fluktuacije še posebej izrazite, kar se odraža tudi na obnašanju Casimirjeve sile. Pri strukturnem prehodu v deformirano smektično C strukturo Casimirjeva sila logaritemsko divergira. Podrobno smo analizirali vpliv robnih pogojev na Casimirjevo silo, ki jo povzročajo masivne direktorske fluktuacije s končno korelacijsko dolžino v smektični A homeotropni celici. Ugotovili smo, da efektivno jakost sidranja v tankih celicah določa razmerje med ekstrapolacijsko dolžino sidranja in debelino celice, medtem ko v debelejših celicah efektivno jakost sidranja določa razmerje med ekstrapolacijsko dolžino sidranja in korelacijsko dolžino fluktuacij. V primeru simetričnih robnih pogojev, to je močnega ali šibkega sidranja na obeh površinah, je Casimirjeva sila privlačna. V primeru antisimetričnih robnih pogojev, to je močnega sidranja na eni ter šibkega sidranja na drugi površini, pa je Casimirjeva sila odbojna.

Posebno pozornost smo v disertaciji posvetili sistemom z netrivialno ravnovesno strukturo. Najprej smo obravnavali dva sistema, rahlo deformirano smektično celico in prostostoječi film s povečanim površinskim redom, kjer nehomogenost ravnovesne ureditve ni vplivala na Casimirjevo silo. Prišli smo do zaključka, da v sistemih, ki jih lahko opišemo s kvadratičnim razvojem proste energije in fiksnimi robnimi pogoji, nehomogena ravnovesna ureditev ne vpliva na hamiltonko fluktuacij in zato tudi ne na Casimirjevo silo. Nazadnje smo obravnavali dva sistema, kjer se je netrivialna ravnovesna struktura odražala v krajevni odvisnosti snovnih konstant. V homeotropni smektični celici s povečanim površinskim pozicijskim redom smo ugotovili, da je zaradi nehomogenosti ureditve Casimirjeva sila kratkega dosega. Nehomogenost se je torej odrazila kot neka efektivna masa fluktuirajočega polja. Nadalje smo raziskali vpliv površinsko vsiljenega predsmektičnega reda na Casimirjevo silo v homeotropni nematski celici. Izkazalo se je, da Casimirjeva sila v takem sistemu upada občutno hitreje kot običajna direktorska sila v nematikih.

Glavni izziv na področju teorije Casimirjevega pojava v tekočih kristalih bodo v prihodnosti prav gotovo predstavljali sistemi z netrivialno ravnovesno ureditvijo. V tej disertaciji smo podali rešitve le za nekaj posebnih primerov. Za obravnavo

bolj splošnih sistemov bo najbrž potrebno razviti popolnejše in splošnejše metode za izračun ter regularizacijo proste energije fluktuacij. Ker je v realnih ograjenih sistemih nehomogenost ravnovesne tekočekristalne ureditve skoraj vedno prisotna, so ta vprašanja zelo relevantna. Glavni problem tega raziskovalnega področja po našem mnenju predstavlja dejstvo, da obstoj Casimirjeve sile v tekočekristalnih sistemih še ni bil eksperimentalno potrjen. Verjamemo, da bi takšna potrditev stimulirala nadaljni razvoj tega področja, kot se je to zgodilo v primeru elektromagnetnega Casimirjevega pojava.

Izjava

Izjavljam, da sem v disertaciji predstavil rezultate lastnega znanstvenoraziskovalnega dela.

V Ljubljani, 5. 1. 2007. Boštjan Markun